EXPRESSION, SOLUBILISATION, PURIFICATION AND CHARACTERISATION OF RECOMBINANT BLUETONGUE VIRUS VIRAL PROTEIN 7

by

BONNIE LEIGH RUSSELL

submitted in accordance with the requirements for the degree of

MASTER OF SCIENCE

in the subject

LIFE SCIENCES

at the

UNIVERSITY OF SOUTH AFRICA

SUPERVISOR: PROF S GILDENHUYS

2018 JUNE

UNISA | college of agriculture and environmental sciences

Declaration

Name: Bonnie Leigh Russell

Student number: 50520881

Degree: Master of Life Sciences

I, **Bonnie Leigh Russell** hereby declare that the dissertation, which I hereby submit for the degree of **Master of Life Science** at the University of South Africa, is my own work and has not previously been submitted by me for a degree at this or any other institution.

I declare that the dissertation does not contain any written work presented by other persons whether written, pictures, graphs or data or any other information without acknowledging the source.

I declare that where words from a written source have been used the words have been paraphrased and referenced and where exact words from a source have been used the words have been placed inside quotation marks and referenced.

I declare that I have not copied and pasted any information from the Internet, without specifically acknowledging the source and have inserted appropriate references to these sources in the reference section of the dissertation.

I declare that during my study I adhered to the Research Ethics Policy of the University of South Africa, received ethics approval for the duration of my study prior to the commencement of data gathering, and have not acted outside the approval conditions.

I declare that the content of my dissertation has been submitted through an electronic plagiarism detection program before the final submission for examination.

Student signature: _____ Date: 13/06/2018

Abstract

Bluetongue virus belongs to the *Orbivirus* genus from the *Reoviridae* family. It infects predominantly domestic and wild ruminants and is economically significant worldwide. Bluetongue virus VP7 forms the intercepting layer between the outer capsid (VP2 and VP5) and VP3 which surrounds the genomic material. BL21(DE3), NiCo21(DE3), C43(DE3) pLysS and KRX *Escherichia coli* cells were transformed with a pET28a plasmid with the cDNA sequence encoding Bluetongue virus VP7. Expression of Bluetongue virus VP7 was tested at post induction temperatures between 16˚C and 37 ˚C, at inducer concentrations between 0.1 mM and 1.0 mM isopropyl-β-D-thiogalactopyranoside in BL21(DE3), NiCo21(DE3) and C43(DE3) pLysS cells and 0.05 % and 0.15 % rhamnose for KRX cells, in two types of growth media (LB and 2xYT) and post-induction growth times between two and 16 hours. Under all conditions tested; Bluetongue virus VP7 expression was found to be predominantly in the insoluble fraction (pellet). BL21(DE3) and NiCo21(DE3) cells were chosen and grown for five hours post induction, induced with 0.1 mM isopropyl-β-D-thiogalactopyranoside and grown at a post-induction temperature of 37 ˚C. Bluetongue virus VP7 in bacterial cell inclusion bodies was solubilised using urea and a freeze-thaw step. Solubilisation was tested with urea concentrations between 2 M and 8 M, with solubilisation efficiency not increasing past 5 M urea. Solubilized Bluetongue virus VP7 was purified using nickel-affinity chromatography. Purified Bluetongue virus VP7 was then probed with far-UV circular dichroism and intrinsic fluorescence in several buffer conditions including different urea and guanidinium chloride concentrations as well as in the presence of glycerol and sodium chloride. Guanidinium chloride was able to cause Bluetongue virus VP7 unfolding, and the unfolding transition had 94 % and 89 % reversibility at 218 nm and 222 nm respectively. Bluetongue virus VP7 was shown to contain a native-like structure in 20 % glycerol and in up to 8 M urea and was found to be stable till at least 55 ˚C, even in the presence of 5 M urea. Glycerol and sodium chloride influenced the conformation of the protein resulting in different unfolding transitions. Thermal unfolding of Bluetongue virus VP7 was found to be irreversible.

Keywords

Bluetongue virus, *Escherichia coli,* far-UV circular dichroism, fluorescence, inclusion bodies, polyhistidine-tagged purification, protein expression, protein solubilisation, protein stability, VP7.

Research outputs

1. Poster presentation:

   SASM 2018 Conference
   Solubilisation and purification of recombinant Bluetongue virus VP7 expressed in a bacterial system.
   Russell, BL and Gildenhuys, S
   Nominated in the Top 4 by The ISME Journal, Multidisciplinary Journal of Microbial Ecology.

2. Peer-reviewed published journal article:

   Analysis of Conserved, Computationally Predicted Epitope Regions for VP5 and VP7 across 3 Orbiviruses.
   Russell, BL, Gildenhuys, S and Parbhoo, N.
   2018.
   Bioinformatics and Biology Insights. Volume 12. Pages 1-12.
   DOI: 10.1177/ 1177932218755348.

3. Peer-reviewed published journal article:

   Solubilisation and purification of recombinant bluetongue virus VP7 expressed in a bacterial system.
   Russell, BL and Gildenhuys, S.
   2018.
   Protein Expression and Purification. Volume 147. Pages 85-93.
   DOI: 10.1016/j.pep.2018.03.006.

Dedication

I dedicate this to my mother, who is the strongest person I know. She is the inspiration in my fight for knowledge. She keeps me on route to my goal of alleviating suffering, even if it is just for one soul.

Acknowledgements

My parents, Lindsay and Anthony for always supporting me and sharing in my fascination and excitement.

My siblings, Amy and Nicholas for playing a huge role in shaping the person I am today, and Amy specifically for proofreading, the long talks and continuous support.

My sister-in-law, Tracy for encouraging my early fascination in science. Warren for helping with the beautiful diagrams in this document as well as the endless support, and constant reminders to take it one day at a time.

The Evans's for being my second family.

My fellow students Samuel and Tonny for the competition, encouragement and support.

Zara, Kenny, Skye, Ogden, Dinky and Faith for making the bad days good.

Dr. Nishal Parbhoo for his patience in training a novice scientist.

Prof Samantha Gildenhuys for recognising my potential and always being able to push me to my limits but never over the edge. For all the guidance, support and responsibility given to me throughout the study and the opportunity to work in her lab.

The National Research Foundation (South African) and the University of South Africa for financial support.

And last but certainly not least, Jason who he himself does not understand the magnitude of the role he played in making this possible.

Table of Contents

List of Figures

List of Tables

Abbreviations

A_{280}	absorbance at 280 nm
A_{340}	absorbance at 340 nm
a.u.	arbitrary units
BTV	Bluetongue virus
CD	circular dichroism
Da	Dalton
DEAE	diethylaminoethyl
DNase	deoxyribonuclease
DSC	differential scanning calorimetry
dsRNA	double-stranded ribonucleic acid
ε	molar extinction coefficient
E. coli	*Escherichia coli*
EDTA	ethylenediaminetetra-acetic acid
ELISA	enzyme-linked immunosorbent assay
ExPASy	Expert Protein Analysis System
Far-UV CD	far-ultraviolet circular dichroism
Gdm-Cl	guanidinium chloride
GST	Glutathione *S*-transferase
HT voltage	the voltage applied to the circular dichroism photomultiplier tube
IMAC	immobilized metal-affinity chromatography
IPTG	isopropyl-β-D-thiogalactopyranoside
ISVP	infectious subviral particles
kDa	kilodalton
LB	Luria Bertani
λ_{max}	fluorescence emission wavelength maximum
µM	micromolar
mdeg	millidegrees
ml	millilitre
M	molar
Ni	nickel

NSP	non-structural protein
OBP	Onderstepoort Biological Products
OD_{600}	optical density at 600 nm
PDB	Protein Data Bank
pI	isoelectric point
rpm	revolutions per minute
SDS	sodium dodecyl sulfate
SDS-PAGE	sodium dodecyl sulfate-polyacrylamide gel electrophoresis
SEC	size exclusion chromatography
SE-HPLC	size exclusion-high performance liquid chromatography
ssRNA	single-stranded ribonucleic acid
TEMED	N, N, N', N'-tetramethylethylenediamine
[Θ]	mean residual ellipticity
V	volts
VP	viral protein
w/v	weight per volume

The IUPAC-IUBMB three and one letter codes for amino acids were used.

List of Buffers

Lysis buffer: 50 mM sodium phosphate dibasic, pH 7.5 with 0.02 % (w/v) sodium azide, 0.02 mg/ml DNase I, 2 mM magnesium chloride and 0.02 mg/ml lysozyme.

Wash buffer A: 20 mM Tris-HCl, pH 7.8 with 300 mM sodium chloride, 1 mM EDTA, 1 % (w/v) Triton X-100, 1 M Urea.

Wash buffer B: 50 mM sodium phosphate dibasic, pH 8 with 250 mM sodium chloride and 0.02 % (w/v) sodium azide.

Freezing buffer: 50 mM sodium phosphate dibasic, pH 7.5 with 500 mM sodium chloride and 0.02 % (w/v) sodium azide.

Equilibration buffer A: 50 mM sodium phosphate dibasic, pH 9 with 5 M urea, 20 mM sodium chloride, 1 mM EDTA and 0.02 % (w/v) sodium azide.

Equilibration buffer B: 20 mM Tris-HCl, pH 9 with 5 M urea, 20 mM sodium chloride, 1 mM EDTA and 0.02 % (w/v) sodium azide.

Equilibration buffer C: 50 mM sodium phosphate dibasic, pH 8 with 5 M urea, 500 mM sodium chloride and 0.02 % (w/v) sodium azide.

Equilibration buffer D: 50 mM sodium phosphate dibasic, pH 7.4 with 5 M urea, 500 mM sodium chloride, 0.02 % (w/v) sodium azide and either 0 mM or 50 mM imidazole.

Elution buffer A: 50 mM sodium phosphate dibasic, pH 5.5 with 5 M urea, 20 mM sodium chloride, 1 mM EDTA and 0.02 % (w/v) sodium azide.

Elution buffer B: 20 mM Tris-HCl, pH 7 with 5 M urea, 20 mM sodium chloride, 1 mM EDTA, and 0.02 % (w/v) sodium azide.

Elution buffer C: 50 mM sodium phosphate dibasic, pH 8.0 with 5 M urea, 500 mM sodium chloride, 0.02 % (w/v) sodium azide and 250 mM imidazole.

Elution buffer D: 50 mM sodium phosphate dibasic, pH7.4 with 5 M urea, 500 mM sodium chloride, 0.02 % (w/v) sodium azide and 500 mM imidazole.

Primary buffer: 50 mM sodium phosphate dibasic, pH 6 with 0.02 % (w/v) sodium azide.

SDS-PAGE sample buffer: 0.5 M Tris-HCl, pH 6.8 with 10 % (w/v) glycerol, 2 % (w/v) SDS, 5 % (w/v) β-mercaptoethanol and 0.05 % (w/v) bromophenol blue.

SDS-PAGE running buffer: 0.5 M Tris, pH 8.3 with 7.2 % (w/v) glycine and 0.5 % SDS (w/v)

BioRad native PAGE sample buffer: 62.5 mM Tris-HCl, pH 6.8 with 40 % (w/v) glycerol and 0.01 % (w/v) bromophenol blue.

BioRad native PAGE running buffer: 25 mM Tris, pH 8.3 with 192 mM glycine.

1. Introduction.

1.1 Bluetongue virus.

Bluetongue virus belongs to the genus *Orbivirus* from the family *Reoviridae* as indicated by Viral Zone, a viral database (Hulo *et al*., 2011). The family *Reoviridae* has twelve types of dsRNA viruses which are all multi-segmented, and infect a large range of hosts including insects, reptiles, fish, crustaceans, mammals (including *Homo sapiens*), plants and fungi (Howerth *et al*., 1988; MacLachlan, 1994; Mertens *et al*., 2004). Bluetongue virus is particularly important economically, not only because of livestock fatalities, but also the indirect loss due to banning the movement of livestock because of the potential spread of infection to susceptible areas (Alexander *et al*., 1996).

Before the 1940's Bluetongue virus was believed to occur only within Southern Africa, but in 1943 the first comprehensively documented occurrence of Bluetongue virus outside of Africa occurred in Cyprus (Gambles, 1949). The reliance on the anthropoid vector at first meant Bluetongue virus occurred exclusively in the tropic and temperate areas (Gorman, 1990), but climate change has resulted in the midges migrating out of these areas (Mellor and Wittmann, 2002; Enserink, 2006). This has resulted in Bluetongue virus being present on every continent excluding Antarctica (MacLachlan *et al*., 2009). Periodically, pandemic outbreaks of Bluetongue virus, now commonly occur throughout the world (Patel and Roy, 2014). Outbreaks are seen to be seasonal, and mainly in areas that promote proliferation of the vector, such as a hot, humid climate, which also provides the required environment for larvae development (e.g. stagnant water and cattle dung) (Spreull, 1905; Ward, 1994).

The poorer and marginal farmers suffer from high mortality rates and many wool industries have been crippled due to outbreaks in susceptible areas (Pathak *et al*., 2008). Biosecurity is fundamental to the prevention of accidental spreading of the Bluetongue virus to vulnerable and susceptible areas (Waage and Mumford, 2008; Noad and Roy, 2009). Bluetongue virus affects many domestic and wild ruminants (Bekker *et al*., 1934; Howell, 1966). It has also been found in buffalo, camels, deer and other Artiodactyla (Erasmus, 1975; Howerth *et al*., 1988) and has even been found in some African carnivores (Alexander *et al*., 1994).

One of the biggest challenges faced with Bluetongue virus is that it is not immunologically simple, as it has multiple serotypes. A serotype is a serologically distinguishable strain of a microorganism. That is, through examination of blood serum for antibodies the strains are distinguishable from one another as they elicit a different immune response.

Through the use of serum neutralization tests, 24 serotypes of Bluetongue virus have been known for decades (Huismans *et al*., 1987b) and subsequently a 25th (Chaignat *et al*., 2009), 26th (Maan *et al*., 2011) and 27th (Jenckel *et al*., 2015) serotype have been discovered. The great number of serotypes significantly complicates the ability to treat, diagnose and vaccinate animals against Bluetongue virus. Viral protein 2 (VP2) and viral protein 5 (VP5) are the greatest contributors to serotype determination as together they form the exposed surface of the virion (Huismans and Erasmus., 1981).

1.2 Structure of Bluetongue virus.

All *Reoviridae* viruses are dsRNA viruses that appear to have a similar capsid organization that is made up of more than one protein layer, each having a core that contains the viral genome (Hulo *et al*., 2011). The Bluetongue virion is 80nm in diameter with a distinctive structure of an outer and inner capsid (Verwoerd *et al*., 1972; Prasad *et al*., 1992; Grimes *et al*., 1998), which can be seen in Figure 1.1. The viral particle contains seven structural proteins named VP1 through 7, four non-structural proteins named NS1 through 4 and 10 dsRNA molecules that are enclosed within the core (Verwoerd *et al*., 1972; Huismans, 1979). Viral proteins 1, 4 and 6 are considered minor proteins as they have a much lower concentration compared to the major viral proteins 2, 3, 5 and 7 (Verwoerd *et al*., 1972). The inner capsid core is comprised of a lattice of VP7 trimers that coats a layer of VP3 monomers (Grimes *et al*., 1998) along with VP1, VP4 and VP6 (Figure 1.1). VP2 trimer spikes surrounding VP5 trimers (Figure 1.1) make up the outer capsid (Huismans and Erasmus, 1981; Hyatt and Eaton, 1988; Zhang *et al*., 2016).

VP2 has the highest sequence variability and is, therefore, the principal determinant of serotype antigens, and VP5 to a lesser degree is also involved in serotype determination (Huismans and Erasmus, 1981). VP7 is important structurally as it is the bridge between the VP2-VP5 capsid layer and VP3, which surrounds the genome. The core contains multiple solvent channels and the outer capsid has intrinsic instability and can easily be made to dissociate by proteolysis and mildly acidic conditions, a characteristic vital to viral replication as it allows core release which then activates the transcription machinery within the core to start replication of the viral RNA (Verwoerd *et al*., 1972; Patel and Roy, 2014).

VP2 is imperative to host cell attachment and VP5 has been found to be able to penetrate the host cell membrane (Huismans *et al*., 1987c; Hassan, 1999; Hassan *et al*., 2001; Forzan *et al*., 2007) which is vital for viral replication within the mammalian host.

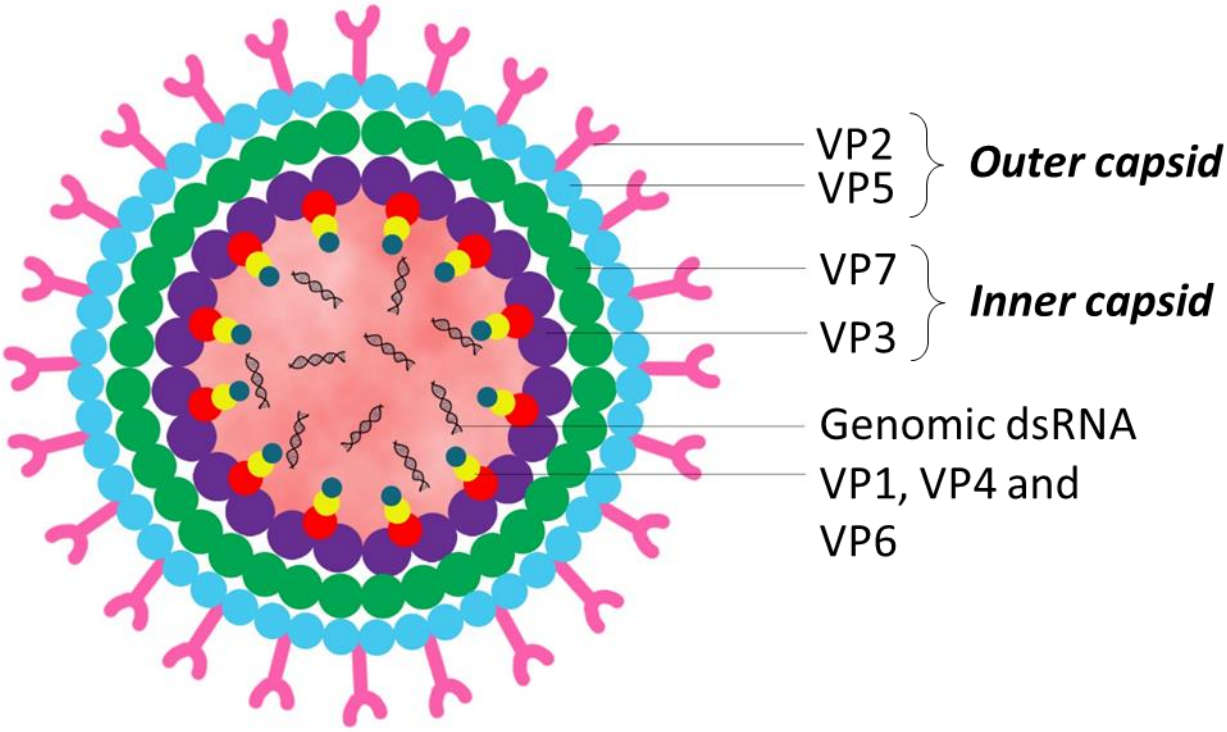

Figure 1.1. Structure of Bluetongue virion.

Diagrammatic representation of the structural organization of the viral proteins that construct the Bluetongue virion. Shown are proteins VP1 through 7. Figure constructed by the author based on information obtained from Verwoerd et al. (1972); Huismans (1979); Patel and Roy (2014).

1.3 Mode of infection and replication cycle of Bluetongue virus.

Culicoides midges are responsible for the transmission of Bluetongue virus (Du Toit, 1944). Of over a thousand species of *Culicoides,* only a small percentage have been connected to contracting and transmitting Bluetongue virus (Mellor, 1990). It has been seen that even individual midges within a single species show a variation of susceptibility to infection (Jones and Foster, 1978).

Culicoides midges become infected through ingestion of a viraemic blood meal when feeding (Du Toit, 1944). The female midges are responsible for Bluetongue virus transmission as they feed on blood meals, whereas, the male's diet consists of only plant juices (Birley and Boorman, 1982). Specific molecular details of replication after attachment to *Culicoides* midge's cells is unknown, however, more is known on the viral pathway through the midge from infection to transmission. Once ingested Bluetongue virus enters the mid-gut cells, infecting them and thus replicating within them (Megahed, 1956; Chamberlain and Sudia, 1961; Jennings and Mellor, 1988). Progeny viruses enter the haemocoel, which is the primary body cavity of most invertebrates that contains its circulatory fluid, via the basement lamina. From the haemocoel, secondary infection occurs (Bowne and Jones, 1966; Chandler *et al*., 1985).

Secondary infection results in the virus replicating in other targeted tissues most significantly being the salivary glands. Once sufficient replication has occurred in the salivary glands, the infected midges can transmit the disease to susceptible animals. The cycle from infection of the midge to its ability to transmit the virus to the animals it feeds on is approximately 15 days and varies mainly due to temperature (Chandler *et al*., 1985; Mellor, 1990). Infected *Culicoides* midges predominantly remain infected for life (Mellor, 1990). Foster and Jones (1979) discovered a two-phase replication cycle with a large increase in viral titre occurring at three to four days, which they attributed to the progeny virus leaving the gut wall and a second large viral titre increase at 10 to14 days which they attributed to secondary target organ infection. The lag in viral titre before three days is presumably because of the viral attachment and penetration within the midge gut wall cells.

Culicoides midge cells have been shown to become infected by full Bluetongue virions (VP2 and VP5 mediated pathway), by core particles that have had the outer capsid layer removed, and by ISVPs, which are infectious subviral particles that are produced by the digestion of full Bluetongue virions with chymotrypsin and trypsin (Mertens *et al*., 1987). With ISVPs showing the highest infectability (Mertens *et al*., 1987). For core particles and ISVPs, it appears that Bluetongue virus VP7 has the ability to attach and penetrate the *Culicoides* host cells (Xu *et al*., 1997; Tan *et al*., 2001).

It has long since been believed that digestive enzymes in the midge gut could result in modification of the viral particle. The digestive enzyme profile of *Culicoides* midges themselves is unknown, but it has been discovered that many other groups of haematophagous insects secrete, into the gut, an assortment of proteases, most commonly including chymotrypsin and trypsin (Akov, 1972; Briegel and Lea, 1975). This is further supported by the RGD motif present in Bluetongue virus VP7 forming the attachment to midge's cells during infection (Tan *et al*., 2001).

The Bluetongue virus replication cycle alternates between *Culicoides* midges and mammalian hosts. Bluetongue virus is non-contagious and cannot be transmitted by contact with or between animals (Hutcheon, 1902; Spreull, 1905). For mammalian hosts, *Culicoides* transfer the virus through their saliva while feeding, and thus the virus is able to enter the mammalian bloodstream (Du Toit, 1944; Barratt-Boyes and MacLachlan, 1994). In addition to transmission via midges, it has been seen that in certain specific serotypes, trans-placental transmission can occur with subsequent foetal infection (Gibbs *et al*., 1979). Studies have also shown that when the bull is viraemic, transmission of the virus can occur via its semen (Bowen and Howard, 1984; Howard *et al*., 1985).

The primary infection after viral entry occurs mainly in endothelial cells and phagocytes, found within the lymph nodes close to the location where the *Culicoides* midge has fed (Barratt-Boyes and MacLachlan, 1994). Adhesion to the host cell is possible because VP2 has the ability to attach to the cell membrane's glycoproteins (seen in Figure 1.2) (Huismans *et al*., 1987c; Mertens *et al*., 1987; Hassan, 1999; Du *et al*., 2014). After attachment, internalization of the virus is facilitated by the host cell's calthrin-mediated endocytosis machinery (Eaton and Crameri, 1989; Forzan *et al*., 2007). VP5 pierces the host cell endosome and facilitates the delivery of the viral core into host cytosol (Huismans *et al*., 1987c; Mertens *et al*., 1987; Hassan, 1999; Hassan *et al*., 2001; Forzan *et al*., 2007; Du *et al*., 2014). The lower pH inside the endosome causes the release of VP2 first and then in the late endosome, the pH drops even lower which causes VP5 to bind and penetrate the endosome membrane and facilitate the core's translocation into the cytoplasm (Forzan *et al*., 2007; Zhang *et al*., 2016).

The genome is retained within the core which helps to prevent an innate immune response being activated (Mohl and Roy, 2014). The core holds all the essential components needed for transcription of the ten genome segments to produce ten viral single-stranded (positive sense) RNA molecules, which are then later extruded from the core (Van Dijk and Huismans, 1982). Host cell ribosomes then translate the RNA molecules, generating VP1 to VP7 and NS1 to NS4 (Mertens *et al*., 1984; Ratinier *et al*., 2011). Positive sense ssRNAs also acts as the template for negative sense ssRNA that together makes up the viral genome dsRNA (Verwoerd and Huismans, 1972).

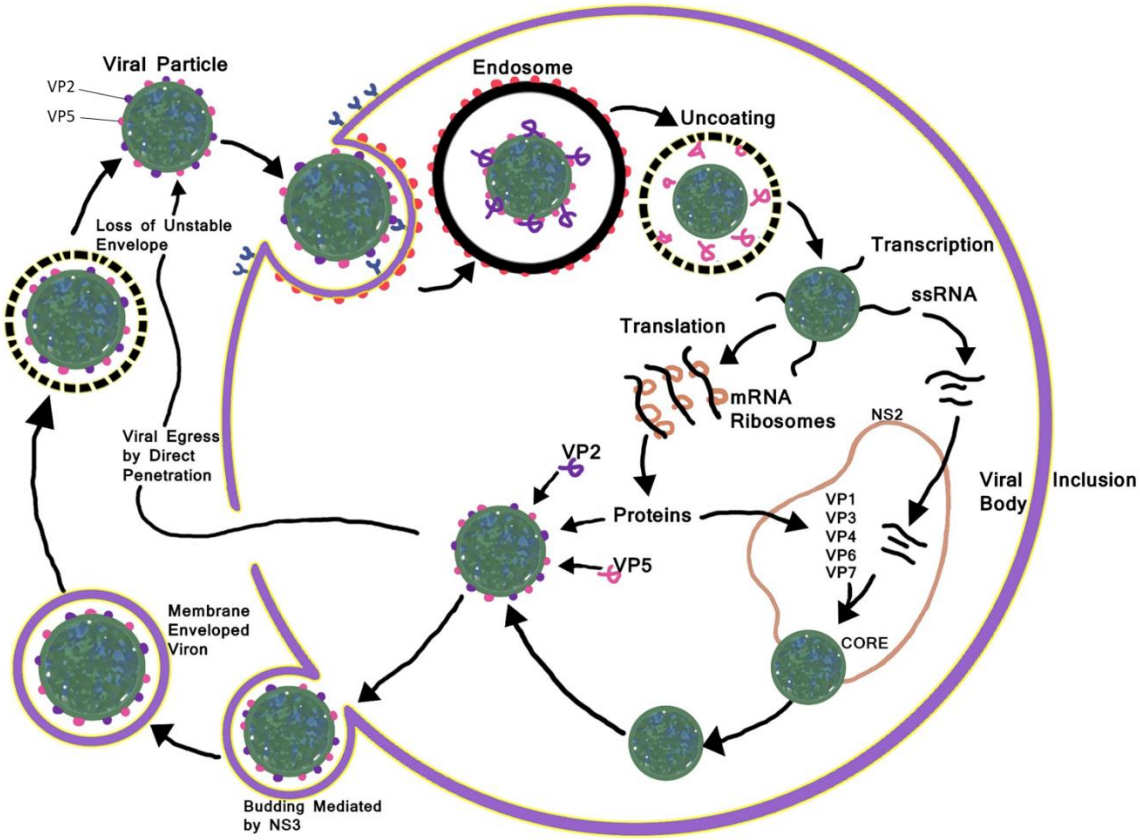

Figure 1.2. Replication of Bluetongue virus.

Represents Bluetongue virus replication following the steps of cell entry, replication, assembly and release. It utilizes inclusion bodies in order to assemble the proteins required to form its core, but the addition of the final viral protein layer occurs in the cytoplasm before viral maturation and release. Figure constructed by author based on information obtained from Van Dijk and Huismans (1982); Mertens et al. (1987a); Hyatt et al. (1989); Hassan (1999); Hassan et al. (2001); Wirblich et al. (2006); Forzan et al. (2007); Zhang et al. (2016).

Within viral inclusion bodies formed by NS2 in the host cell cytoplasm (Eaton *et al*., 1987; Kar *et al*., 2007), the core particles are assembled. After core particles are excised from the viral inclusion bodies, VP2 and VP5 are attached, signifying the maturation of the viral particles (Kar *et al*., 2007).

Complete Bluetongue virus particles then leave the host cell by two main methods, namely NS3 mediated budding, which usually occurs in the early stages of viral infection, or by penetration through the host cell membrane, which causes irreparable damage to the host cell and results in the lysis (Hyatt *et al*., 1989; Wirblich *et al*., 2006). Lysis in *Culicoides* cells rarely occurs (Mellor, 1990). Lysis of host cells during late stage replication of the virus results in many of the symptoms commonly seen in Bluetongue virus infection.

1.4 Bluetongue virus symptoms and infection.

Common signs and symptoms include depression, fever, nasal discharge and crusting, drooling saliva, facial oedema, an excess of blood in coronary bands and general muscle weakness which often leads to lameness (Spreull, 1905; Moulton, 1961; Erasmus, 1975). Common lesions of Bluetongue virus include haemorrhage and ulcers in the mouth and gastrointestinal tract, muscle atrophy (due to necrosis), oedema of the lungs as well as pericardial, pleural and abdominal discharge (Spreull, 1905; Moulton, 1961; MacLachlan *et al*., 2009). Laboured breathing is seen in animals where severe pulmonary oedema has occurred (Moulton, 1961; Erasmus, 1975). Animals that develop prolonged illness suffer acute muscle atrophy and weakness, fatigue, generalized oedema and torticollis (animals head permanently tilted to one side due to muscle spasms) (Erasmus, 1975; Verwoerd and Erasmus, 2004).

The virus then enters the bloodstream causing primary viraemia and quickly spreads to secondary tissues (Barratt-Boyes and MacLachlan, 1994; Sanchez-Corden *et al*., 2010). The virus replicates most frequently in vascular endothelial cells, macrophages and lymphocytes (Barratt-Boyes and MacLachlan, 1994; MacLachlan *et al*., 2009; Drew *et al*., 2010a, Drew *et al*., 2010b).

At the molecular level, the symptoms seen result from various processes within the animal's body that are activated by the viral infection. One example is that during infection the p38 MAP kinase gets activated, which causes the permeability of the animal's vascular system to increase (Chiang *et al*., 2006; Drew *et al*., 2010b). There is also an increased production of TNF alpha, IL-1, IL-8, IL-6, IFN-1, cylooxygenase-2, prostacyclin and thromboxane which are all responsible for the extreme inflammatory response (MacLachlan and Thompson, 1985; DeMaula *et al*., 2001). The excessive inflammatory response results in oedema and damage to tissue seen in a Bluetongue virus infection.

There is a four to eight day delay before symptoms appear and viraemia duration varies between species and even within different breeds within each species. It persists for 14 to 54 days in sheep (Koumbati *et al*., 1999), 19 to 54 days in goats (Barzilai and Tadmor, 1971) and 60 to 100 days in cattle (Sellers and Taylor, 1980).

Bluetongue virus produces variable signs and symptoms in different species and breeds, with numerous species not showing any at all (Hutcheon, 1902; Spreull, 1905; Gard, 1984; MacLachlan, 1994). Viraemia occurs in sheep, who generally develop the most severe symptoms. The disease is rarely symptomatic in cattle, goats or wild ruminants (Gard, 1984; Maclachlan, 1994). The ability of the virus to infect animals without causing them to become symptomatic creates the opportunity of the asymptomatic or less severely affected animals to provide a reservoir for the disease, which enables it to spread to more susceptible species and breeds while remaining undetected in the animals that do not show typical signs of infection (Hourrigan and Klingsporn, 1975).

As there is currently no treatment for Bluetongue virus available, other than symptomatic treatment, there is an urgent need for effective vaccines and fast diagnosis of infected animals. (Li *et al*., 2009; Amin *et al*., 2016).

1.5 Diagnosis and vaccines.

Effective, reliable and fast diagnostic tools are very important in controlling Bluetongue virus. There are various serological and virological procedures for diagnosis. Serological methods include agar gel, immunodiffusion and competitive ELISA, whereas virological methods include virus isolation and reverse transcription polymerase chain reaction (RT-PCR) (Afshar *et al*., 1987; Drolet *et al*., 1990; Vandenbussche *et al*., 2008). Several enzyme immunoassays have been created to distinguish between many Bluetongue virus serotype specific antibodies. The Bluetongue virus VP7 protein is the favourite for the development of group-specific serological assays because of it having a high sequence similarity between all serotypes (Kowalik and Li, 1991).

Many different kinds of vaccines have been created for Bluetongue virus including antigen, inactivated and live attenuated viral vaccines (Alexander *et al*., 1951; Parker *et al*., 1975; Campbell, 1985; Hunter and Modumo, 2001; Savini *et al*., 2008). There are however two major problems with the current vaccines in use. Firstly that it is not currently possible to distinguish between a vaccinated animal and an infected one, which is important for the ability to move livestock (DIVA-Differentiating infected from vaccinated animals). Secondly, Bluetongue virus is not immunologically simple, as it exists in 27 serotypes that are distinct from each other and the vaccines given are serotype specific.

That is, they only provide immune protection against a specific serotype (Huismans *et al*., 1987b; Chaignat *et al*., 2009). VP2 and VP5 are the major antigenic proteins and inducers of the production of neutralizing antibodies (Huismans *et al*., 1987a). However, they are also highly variable (Huismans *et al*., 1987a; Iwata *et al*., 1992; Russell *et al*., 2018) and therefore the root cause of the lack of cross neutralization seen between serotypes. (Huismans and Erasmus, 1981; Appleton and Letchworth, 1983).

To try overcome this a cocktail of attenuated virus strains is usually administered, but a vaccine containing all 27 serotypes is not commercially viable (Noad and Roy, 2009). There is also the issue that genome segment re-assortment between different serotypes can occur, so the more you increase the number of serotypes in each single vaccination, the greater the chance of generating novel progeny strain, for which there is no vaccine available (Cowley and Gorman, 1989; Mertens *et al*., 1984; Batten *et al*., 2008). The vaccine currently used in South Africa is an Onderstepoort Biological product, a live attenuated polyvalent vaccine that administers a cocktail of 15 serotypes over three doses in 9 weeks (Dungu *et al*., 2004; Coetzee *et al*., 2012).

Several of the problems that have been encountered with the currently available vaccines are thought to be able to be overcome by the development of protein-based vaccines (Huismans *et al*., 1987b; Roy, 1990; Roy *et al*., 1992; Stewart *et al*., 2013; Thuenemann *et al*., 2013). Promising protein-based vaccines include subunit vaccines (Huismans *et al*., 1987b) that contain either solitary proteins or combinations of proteins. However, subunit vaccines have proved to be expensive to develop. One of the most promising approaches for future vaccines is the production of a composite of VP2, VP5, VP7 and VP3 into a virus-like particle (Roy, 1990), which contains no virus nucleic acids, so is, therefore, able to initiate a similar immune response but is unable to replicate. This allows for vaccinated animals to be distinguishable from infected animals, as animals that have received the vaccine will not display the viral nucleic acids (French *et al*., 1990; Loudon *et al*., 1991; Roy *et al*., 1992).

The main aim of a vaccine is to induce the same long lasting level of protection that infection would incur without suffering from the actual disease. Studies have shown that Bluetongue virus VP7 is able to induce an antibody response that is at least partially protective, suggesting that sections of VP7 are accessible on the viral surface (Lewis and Grubman, 1990; Martin *et al*., 2015). Bluetongue virus VP7 is recognised to induce a T-cell immune response, namely, it is able to activate $CD8^+$ and $CD4^+$ cells (Kowalik and Li, 1991; Rojas *et al*., 2011). Bluetongue virus VP7 is also the major serogroup-reactive antigen (Huismans and Erasmus, 1981; Gumm and Newman, 1982) and therefore, is an excellent candidate for cross-serotype protection.

This is significant as VP5 and VP2 are known to induce a B cell immune response and therefore by combining a mixture of recombinant viral proteins within a vaccine you are potentially activating both B cell and T cell immune responses, which are known to provide stronger and longer lasting immune protection than vaccinations that just activate the B cells (Brooks *et al*., 2016; Linterman and Hill, 2016).

1.6 The Bluetongue virus VP7 protein.

Bluetongue virus VP7 is encoded by Bluetongue virus genome segment seven and contains 349 amino acids, which is 1154-1156 base pairs (Caspar *et al*., 1962; Pathak *et al*., 2008). Bluetongue virus VP7 has a reported molecular mass of 38 kDa (Basak *et al*., 1992; Grimes *et al*., 1995) and contains 9 tyrosine (Tyr), 5 tryptophan (Trp) and 14 phenylalanine (Phe) amino acids (Grimes *et al*., 1995; Gasteiger *et al*., 2005; Russell *et al*., 2018). The VP7 trimer has a length of 85Å and a width of 65Å (Grimes *et al*., 1995). As seen in Figure 1.3, a monomeric subunit contains two distinct domains. One domain is smaller as it is composed of approximately one-third of the polypeptide residues (residues 121 to 149) and forms a beta-sheet. The second domain is bigger and consists of the residues 1 to 120 and 250 to 349 and forms alpha-helices that contain long extending loops (Grimes *et al*., 1995).

The domains are twisted around a 3-fold axis so one monomer's alpha-helical domain lines up with the beta-sheet domain of a neighbouring subunit as seen in Figure 1.3 (Grimes *et al*., 1995). Each viral particle contains 780 replicates of the VP7 protein, which arranges into 260 trimers with a T=13 quasi-equivalent lattice (Caspar *et al*., 1962; Grimes *et al*., 1997). The Bluetongue virus VP7 used for structural determination by Grimes *et al.* (1995) was expressed using a baculovirus system, based on methods described by Oldfield *et al.* (1990) who used *Spodoptera frugiperda* cells which were transfected with pAcYM1 baculovirus transfer vector containing the Bluetongue virus VP7 gene sequence. Infected *Spodoptera frugiperda* cells were grown in monolayers at 28˚C for 3 days, before extraction and purification using Q-Sepharose column and sodium chloride as the eluting agent (Basak *et al*., 1992). Expression of recombinant proteins in a baculovirus system is a common method, but the culture of insects that is required is expensive and difficult to work with, it is, therefore, a lot cheaper and easier to work with prokaryotic systems (Marino, 1989; Dater *et al*., 1993).

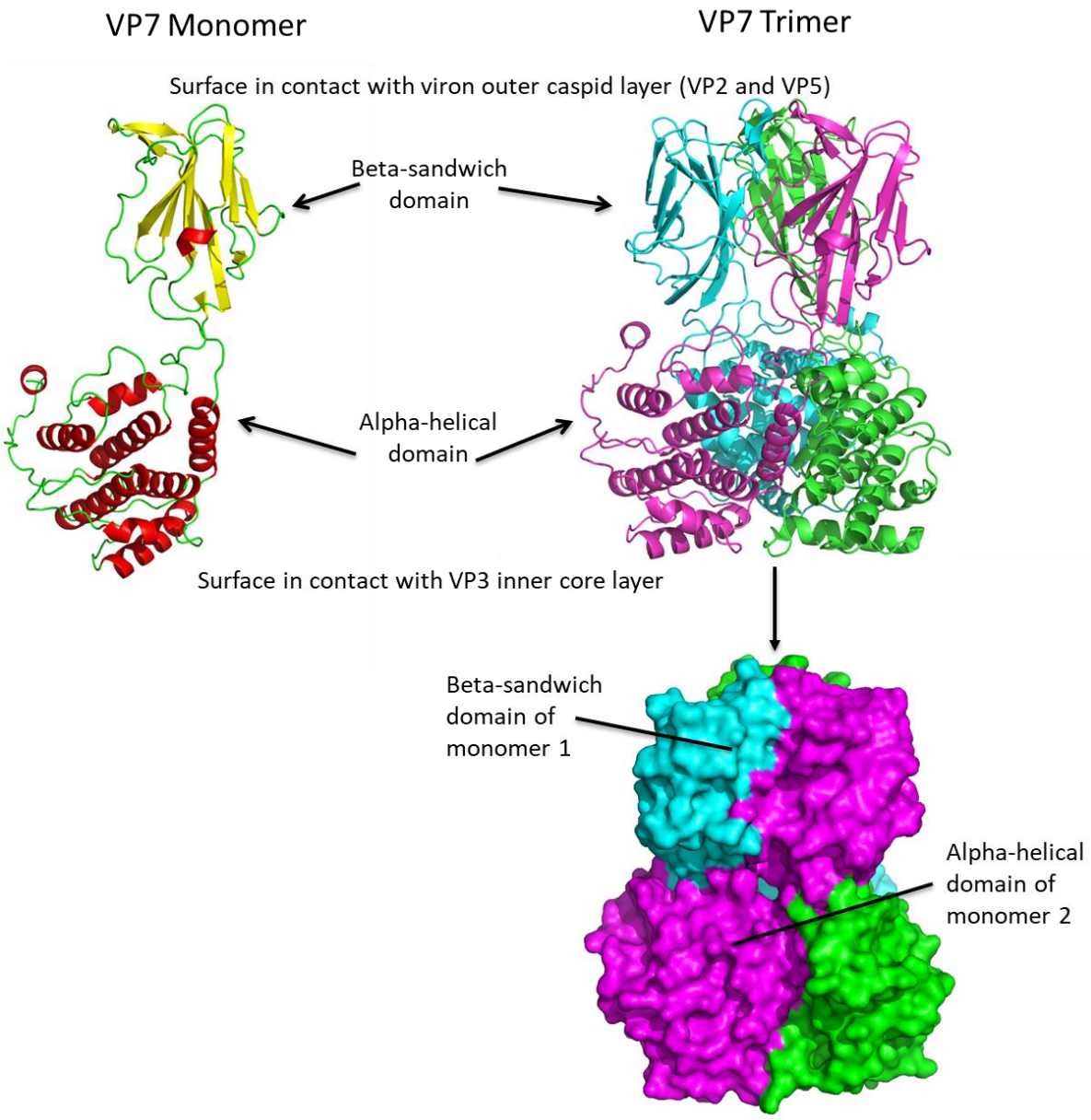

Figure 1.3. Bluetongue virus VP7 structure.

Diagram showing Bluetongue virus VP7 monomer and trimer conformations. The two domains found in a VP7 molecule are labelled beta-sandwich and alpha-helical respectfully. The surfaces in contact with the other protein layers found within a Bluetongue viral particle are also labelled. Trimer with surface covering is shown to indicate how the domains from monomer subunits interact. The structure was acquired from the protein data bank (1BVP) and viewed with PyMOL Molecular Graphics System (1.3rl Edu), Schrödinger, LLC.

1.7 Bacterial protein expression systems and inclusion body formation.

Recombinant proteins have been expressed in various systems including mammalian, insect, yeast, plant, bacterial and in vitro translation systems (Itakura *et al*., 1977; Hitzeman *et al*., 1981; Wirth *et al*., 1988; Marino, 1989). One of the most common prokaryotes used as an expression system is *Escherichia coli* (Marino, 1989; Terpe, 2006).

The advantage of *Escherichia coli* is its ability to produce large quantities of the desired protein for a low price (Datar *et al*., 1993), as *Escherichia coli* cultures do not require very strict sterile conditions, expensive media and extensive growth maintenance like mammalian and insect cells (Verwoerd *et al*., 1979; Marston, 1986; Marino, 1989; Martyn *et al*., 1991). The *Escherichia coli* cells also have a much faster growth rate than mammalian cells and therefore this shortens the total time needed for an expressed protein to be utilised (Marino, 1989).

Escherichia coli importantly possesses inducible promoters, prokaryotic ribosome binding sites (with initiation codon and Shine-Dalgarno sequence) and a transcription terminator, which all help make translation and transcription of the desired protein possible (Itakura *et al*., 1977; Marino, 1989; Makrides, 1996).

Plasmids are commonly found in bacterial cells and consist of small double-stranded circular DNA molecules that are naturally taken up by bacteria, often allowing them to incur antibiotic resistance as the plasmids frequently hold genes for antibiotic resistance (Lederberg, 1952; Stanisich, 1988; Gogarten and Townsend, 2005). Plasmids replicate independently of the host genome and can transfer genes horizontally (Gogarten and Townsend, 2005). The plasmid can be genetically modified to contain a foreign gene insert that is then expressed by the bacteria transcription and translation machinery when induced. This is achieved by cutting the plasmid at specific restriction sites, which results in single-stranded overhangs which are then duplicated on the gene insert so that the gene insert can bind to the plasmid. The plasmid DNA contains a promoter, which is upstream of the target gene, and repressor that binds the operator and prevents the expression of RNA polymerase until the addition of an inducer. When the plasmid is induced the repressor is removed allowing RNA polymerase to be expressed, resulting in expression of the desired gene. Finally, the plasmid contains a gene that gives it resistance to an antibiotic which is important as this acts a selectable marker.

Expression in bacterial cells has two main disadvantages, firstly that they are unable to perform as extensive posttranslational modifications as eukaryotic cells which can be critical for correct production of certain proteins and secondly, in bacterial cells recombinant proteins are frequently overexpressed in insoluble inclusion bodies (Marston, 1986; Hockney, 1994; Makrides, 1996). However, inclusion bodies are able to form in mammalian, yeast and insect cells (Palmer and Wingfield, 2004). Studies into inclusion body formation in bacterial cells found that the aggregation of the expressed protein is strongly dependent on expression conditions, including temperature, inducer concentration, post induction growth time and bacterial cell line (Hockney, 1994; Makrides, 1996; Calamai *et al*., 2005; Terpe, 2006).

Despite extensive studies little is understood about inclusion body structure or formation (Villaverde and Carrio, 2003). Regulatory mechanisms in the crowded cellular environment try to balance a number of different processes for peptides and proteins including folding, prevention of aggregation, protein transport and proteolysis (Dobson, 2003). Several studies suggest that aggregation of protein occurs from protein folding intermediates produced in the process of folding (Gupta *et al*., 1998; Smith and Hall, 2001). This follows the thought that the process of protein aggregation is reliant on the primary sequence of the expressed protein and the physiological and chemical interactions the sequence creates (Chiti *et al*., 2003; Dubay *et al*., 2004).

Also important is the phenomenon of protein macromolecular crowding in *Escherichia coli's* cytoplasm, which increases the likelihood of incorrect protein folding and often occurs in long post induction growth times and high inducer concentrations and temperatures (Van den Berg *et al*., 1999; Van den Berg *et al*., 2000).

The metabolic burden on bacterial cells also plays a significant role in inclusion body formation. Metabolic burden is the use of host cell's energy and raw materials for the transcription and translation of foreign DNA into protein, and it is often linked to causing a stress response in the cells, which causes a serious disruption in host cell metabolism (Bentley and Kompala, 1990; Rahmen *et al*., 2015). Maintenance of a plasmid often places strain on bacterial cells, particularly when the foreign protein is greatly expressed (Bailey, 1993; Hoffmann and Rinas, 2004).

The appearance of numerous target proteins in bacterial inclusion bodies resulted in research being conducted into the utilization of protein found in the inclusion bodies by solubilisation of the protein and subsequent retention of native protein or the refolding into active native protein (Przybycien *et al*., 1994; Jevsevar *et al.*, 2005; Umetsu *et al*., 2005; Ami *et al*., 2006; Doglia *et al*., 2008).

1.8 Solubilisation of recombinant protein expressed in insoluble bacterial inclusion bodies.

Although the exact structural formation of inclusion bodies is not yet known they are said to be made up of a sponge-like organization containing structural amyloid-like fibres and a protein filled matrix (Carrio *et al*., 2005; Morell, 2008; Wang, 2009; Walther *et al*., 2013). Little is understood about inclusion body structure or the process of solubilisation, however, Walther *et al.* (2013) discovered that the inclusion body size shrinks during solubilisation and pore-like structures appear in the structural inclusion body, through which the proteins diffuse out of and become soluble.

Therefore, the difference seen in the degree of solubilisation of protein from inclusion bodies with different solubilisation methods is directly linked to the methods ability to create these pores in the inclusion body structure. The effectiveness of protein solubilisation is also said to be dependent on the concentration of solubilizing agents, pressure, temperature, and the level of dissolved oxygen during the experiment (Walther *et al*., 2013).

Solubilisation can occur through various methods including using detergents (Puri *et al*., 1992; Kurucz *et al*., 1995), arginine (Tsumoto *et al*., 2004; Umetsu *et al*., 2005) as well as extreme pH values (Iwakura *et al*., 1992) but most commonly, a high concentration of denaturants or strong ionic detergents is used (Tsumoto *et al*., 2003).

However, this has a disadvantage, as the high denaturant concentrations have been known to cause permanent structural damage to the proteins found within the inclusion body. Therefore, it is more advantageous to use milder solubilisation conditions that disrupt the inclusion body structure but not the protein structure within (Kurucz *et al*., 1995; Tsumoto *et al*., 2004). That being said, the solubilisation of each individual protein is said to be unique as it has been found that the recombinant protein itself, as well as the expression conditions, influence the inclusion bodies structure and porosity (Margreiter *et al*., 2008).

Some advantages to using proteins found in inclusion bodies include the fact that there are less other bacterial cell proteins in comparison to the proteins that have been expressed in the soluble fraction in a cell. Other proteins present in inclusion bodies are largely just proteins from the bacterial cell wall, meaning that the proteins found in inclusion bodies are more likely to be protected from proteolytic degradation. The inclusion bodies help guard the cell against the potential toxicity of the recombinant protein. The lower amount of bacterial cell protein expression found in inclusion bodies in comparison to the soluble fraction helps simplify further purification steps.

1.9 Purification of recombinant proteins using liquid chromatographic techniques.

Using liquid chromatography to purify recombinant protein exploits characteristics that the target protein contains to separate it from a mixture of proteins. Chromatography generally consists of a fixed matrix with which the proteins interact, and different buffers that cause the desired interaction. Three of the most common chromatography techniques are affinity, size exclusion and ion-exchange. Affinity chromatography bases separation of proteins on the specificity of interactions between a ligand and receptor. Commonly a "tag" is added to a protein that allows it to bind specifically to a matrix. Frequently used tags include histidine residues, glutathione *S*-transferase (GST) and S peptide (Kimple *et al*., 2015).

Size exclusion chromatography exploits the different sizes of proteins within a mixture and is influenced by the proteins molecular mass, with heavier molecules eluting first and lighter ones eluting last as smaller proteins are able to interact to a greater extent with the pores that the matrix contains, due to their smaller size (Lathe, 1956; Porath and Flodin, 1959; Hjerten, 1964). Ion-exchange exploits the ability of a protein to be either negatively or positively charged depending on the pH of the buffer it is in (Eckweiler *et al*., 1921; Giddings, 1965). For this study, two forms of liquid chromatography are important, namely ion-exchange chromatography and affinity chromatography.

1.9.1 Ion-exchange chromatography.

Ion-exchange chromatography utilises the ability of oppositely charged molecules to be attracted to one another (Adams and Holmes, 1935, Myers *et al*., 1941; Boyd *et al*., 1947; Peterson and Sober, 1956; Chang *et al*., 1976) and the reversible reaction that can occur between charged molecules and an oppositely charged matrix (Adams and Holmes, 1935) and consists of a mobile and stationary phase. In terms of protein purification, the mobile phase is the mixture of molecules and the stationary phase is the fixed insoluble matrix within the resin that contains charged groups (Giddings, 1965).

Proteins are amphoteric, that is they can react with either a base or an acid as they can either receive or donate hydrogen ions (Eckweiler *et al*., 1921). This is predominantly due to the presence of an N-terminal amine group, a C-terminal carboxyl group and ionisable side chain groups of amino acid residues, which creates the ability to manipulate the protein's net surface charge by manipulating the pH and ionic strength of the buffer it is in, creating either a positive, negative or no net charge on the protein's surface. The isoelectric point (pI) for a protein is the pH value where the protein doesn't contain a charge, therefore the pI is also the isoionic point (Lampson and Tytell, 1965).

At a pH greater than its pI, a protein will reversibly bind a resin carrying a positive charge and at a pH less than its pI, the protein will reversibly bind a resin carrying a negative charge (Lampson and Tytell, 1965). A protein's net surface charge is dependent on the protein's composition, as each protein is made up of a different combination of amino acids. The theory is that the protein will obtain a unique charge, as well as charge distribution and will, therefore, be eluted separately during purification when conditions on the column for binding and elution are changed (Tanford, 1961; Tanford, 1962; Himmelhoch, 1971).

Bound proteins are eluted off the column by either a change in pH or an increase in ionic strength. (Karlsson *et al*., 1998). For pH elution the net charge of the molecule changes as the pH of the buffer does, causing it to lose the net charge that is creating its ability to bind to the column, thus causing its elution off the column. An ionic strength elution is commonly achieved with the use of sodium chloride. When sodium chloride is added the sodium and chloride ions compete with bound molecules for the charges on the surface of the medium (Karlsson *et al*., 1998). Proteins with lower net charge are eluted first as the ionic strength begins to increase and proteins with higher net charge require higher ionic strengths in order to be eluted. Ion-exchange chromatography is popular as it has a large application base, a high resolving power, high binding capacity, is easy to manipulate to conditions required and has a relatively low cost.

1.9.2 Immobilized metal affinity chromatography.

Immobilized metal affinity chromatography (IMAC) is an affinity method presented in 1975 by Porath *et al.* (1975). IMAC utilizes the ability to fuse a protein to small molecules linked to a solid support (Hochuli *et al*., 1987). It is a form of protein purification that exploits specific binding between molecules. A specific ligand is coupled with a support molecule within a resin so that a mixture of proteins can be filtered through and those with the ligand affinity bind the resin. The non-affinity molecules in the original sample can then be washed off and the bound molecule can be isolated. The molecules with ligand affinity are then eluted from the column by reversing the binding by changing the conditions within the column and thereby purifying it out of its original sample. Ligand affinity is often added to the protein by the addition of an affinity tag, which is a sequence that has a binding affinity to the IMAC resin. Polyhistidine is the most frequently used tag (Yip *et al.,* 1989).

The amino acid histidine is capable of forming complexes with the nickel (Ni^{2+}), and additional histidines increase the protein's affinity for it (Yip *et al.,* 1989; Hutchens and Yip, 1990). Histidine interacts strongly with immobilized metal ions due to the histidine having imidazole rings that have the ability to donate electrons which readily form bonds with the immobilized transition metals.

Application of affinity tag purification allows for the execution of general purification protocol for all tagged proteins as the purification is not dependent on the protein's properties, such as size and charge, which creates extra testing work for other chromatography methods. That being said it is vulnerable to different behaviours of proteins such as aggregation and correct protein folding, hiding the tag and preventing binding (Lichty *et al*., 2005).

Affinity tag chromatography, and specifically polyhistidine tagged purification, has several advantages including the ease at which the tag can be added in the vector to the protein, the high expression of the tagged protein, little need for removal of the tag as its small size enables the protein to stay functional and the mild elution conditions help preserve the protein's natural structure and function (Crowe, 1994; Terpe, 2003; Lichty *et al*., 2005).

The efficacy of purification of proteins containing a polyhistidine tag was increased by the invention of nickel-nitrilotriacetic acid (Ni^{2+}-NTA) matrices (Hochuli *et al*., 1987). Nickel-nitrilotriacetic acid (Ni^{2+}-NTA) and CO^{2+}-carboxymethylaspartate are matrices that chelate the transition metals via four different coordination sites, whilst still allowing for two of the transition metals coordination sites to be free to interact reversibly with histidine residues. This results in a more stable matrix and therefore higher elution product purity (Hochuli *et al*., 1987; Chaga *et al*., 1999) in comparison to iminodiacetic acid (IDA), a matrix that chelates the transition metals through three different coordination sites (Porath *et al*., 1975). This, however, results in a loosely bound metal ion and therefore a greater amount of metal leaching during purification.

Histidine-tagged affinity chromatography is among the most cost effective affinity tag purifications possible, taking into account resin, buffers and elution methods (Lichty *et al*., 2005). Although histidine residues occur reasonably seldom, cellular proteins do occasionally contain enough adjacent histidine residues to enable them to bind the IMAC matrix and be co-eluted with the target protein, decreasing the purity of the purification product (Schmitt *et al*., 1993). However bacterial cells contain fewer proteins than mammalian cells that contain histidines, and therefore purification using nickel affinity resin is easier using bacterial cells rather than mammalian cells (Bornhorst and Falke, 2000).

1.10 Previous expression and purification of Bluetongue virus VP7.

Expression of Bluetongue virus VP7 has been possible in multiple different systems including bacterial (Wang *et al*., 1994), yeast (Martyn *et al*., 1991), mammalian (Marin-Lopez and Ortego, 2016) and insectoid systems (Oldfield *et al*., 1990). Some of the significant studies that have expressed Bluetongue virus VP7 include two studies that used insect cells infected by genetically modified baculovirus namely Oldfield *et al.* (1990) who used DEAE-Sephacel purification.

Bluetongue virus VP7 eluted off at 200 mM sodium chloride in a 10 mM Tris-HCl buffer, pH 7.5 and a yield of 100 mg/litre of cell culture of soluble Bluetongue virus VP7 protein was reported and Hosamani *et al*. (2011) who purified with histidine-tagged purification using a ProBond purification system (Invitrogen), which uses a sodium phosphate buffer with sodium chloride at pH 8 and obtaining 1.87 mg/7x10^6 cells of protein in four days.

Also significant, French and Roy (1990) expressed core-like particles (VP7 and VP3) in insect cells using baculovirus infection and achieved a yield of 30 mg/litre of cells (1.5 x 10^9 cells) after lysing cells and purification using a discontinuous sucrose gradient. Core-like particles are formed when VP3 and VP7 are expressed together in an expression system and the proteins naturally form the viral core particle scaffolding without the presence of the genomic dsRNA or other viral proteins.

High-level expression of soluble protein in bacterial cells has been challenging as high expression often leads to the protein being found predominantly in insoluble inclusion bodies (Verwoerd *et al*., 1979, Marston, 1986; Martyn *et al*., 1991; Wang *et al*., 1994). Wu *et al*. (2015) used BL21(DE3) *Escherichia coli* cells and reported a yield of 0.8 mg/ml and 1.0 mg/ml of insoluble Bluetongue virus VP7 after gel cutting and GST tagged purification respectfully. Other studies that have expressed Bluetongue virus VP7 in bacterial cells include Wang *et al*. (1994) who obtained insoluble protein and purified using preparative SDS-PAGE as defined by Hager and Burgess (1980) and Sudheerbabu *et al.* (2016) that expressed only the upper domain of Bluetongue virus VP7, also in the insoluble fraction, and purified using a chloroform wash. Pathak *et al.* (2008) expressed truncated Bluetongue virus VP7 in prokaryotic cells *(Escherichia coli* BL21) and purified using histidine-tagged affinity chromatography, with a sodium phosphate buffer containing urea and sodium chloride at a pH of 7.8, and eluted with imidazole.

Martyn *et al.* (1991) used in vitro transcription/translation system and a yeast expression system, using sonication to extract Bluetongue virus VP7 from yeast cells. Finally, Bouet-Cararo *et al.* (2014) used mammalian hamster ovary cells (CHO-CAR) but no further expression details were given. Protein expression in insect and mammalian cells have not been able to consistently produce high quantities of soluble protein, and bacterial cells have consistently produced predominantly insoluble protein.

The main focus of previous expression and purification protocols for Bluetongue virus VP7 has been the characterisation of the purified protein's antigenicity and construction of viral-like particles (French and Roy, 1990; Oldfield *et al*., 1990; Wang *et al*., 1994; Pathak *et al*., 2008; Bouet-Cararo *et al*., 2014; Wu *et al*., 2015).

1.11 Spectroscopic determination of protein characteristics.

Spectroscopy works on the principle that every molecule absorbs, transmits or reflects light (electromagnetic radiation) over a particular wavelength range. Absorbance spectroscopy studies the relationship between particles and electromagnetic radiation. Therefore, a spectrophotometer measures the number of photons that are absorbed as the light passes through a given sample solution. The absorption of light is measured as a function of its wavelength (Lakowicz, 1999).

The peptide groups of the protein main chains and aromatic side chains of tyrosine, tryptophan and phenylalanine absorb light in the far-UV range (wavelengths between 180–230 nm) but the aromatic side chains also absorb light in the near-UV range which contained wavelengths between 240–300 nm. Disulfide bonds (between two cysteine residues) also show an absorbance reading near a wavelength of 260 nm. The maxima of protein absorption is found between 275 nm and 280 nm and is produced predominantly by tryptophan and tyrosine. The absorbance of phenylalanine and cysteine disulfide bonds also contribute to the reading in this wavelength range, but only to a very small extent (Schmid, 2001).

The secondary structure of a protein defines the localized polypeptide chain fold that results from hydrogen bonds and it includes characteristic structures such as alpha-helices and beta-strands or sheets. A protein's secondary structure can be determined by producing a far-UV circular dichroism spectrum for the protein of interest. Circular dichroism (CD) is able to quantify the variance between absorption coefficients for left and right circulatory polarized light of molecules that contain one or more light-absorbing groups known as chiral chromophores (Ranjbar and Gill, 2009). The spectrum produced by a protein is caused by absorption by disulfide groups, aromatic side chains, and the peptide backbone (Woody, 1995). Circular dichroism is measured over a range of wavelengths and is used to deduce the protein's secondary and tertiary structure as well as protein conformational changes due to environmental variables (Ranjbar and Gill, 2009).

In the far-UV region (180-250 nm) the signal is principally produced by the peptide backbone. Distinct CD spectra are a result of the peptide backbone adopting various secondary structures (Woody, 1995). Therefore, the shape of the curve produced by this wavelength range produces a description of the protein's secondary structure.

The maxima positive and negative points are especially important as they provide information about the specific protein being studied (Ranjbar and Gill, 2009). Proteins that contain alpha-helices display troughs at 208 nm and 222 nm, and a more positive peak near 190 nm, on the other hand, beta-strands display a characteristic minima at 218 nm and a positive band at 196 nm and random coils display a positive band at 212 nm and a minima at 195 nm (Ranjbar and Gill, 2009).

Absorption in the far-UV region (180-250 nm) is particularly vulnerable to interference from other components such as the buffer, solvents and reagents (Kelly and Price, 2000). Phosphate, borate and Tris are safe buffers to use, but even they should be kept to low concentrations. Chloride ions absorb strongly below 195 nm, and therefore should be kept to a minimum in buffers, instead, fluoride and sulfate can be used to maintain ionic strength (Kelly and Price, 2000).

The tertiary structure of a protein defines the three-dimensional folding of the polypeptide and can be probed using fluorescence. The tertiary structure is held in its specific formation by electrostatic attractions between oppositely charged ionic groups, by weak van der Waal forces, by hydrogen bonds and by hydrophobic interactions. In certain proteins, disulfide bridges are essential for the tertiary structure formation.

Fluorescence studies a protein's tertiary structure by using the energy emitted from light in the electromagnetic spectrum to excite electrons from ground state to an excited state (Schmid, 2001). Fluorescence is, therefore, the emission that results from an electron returning from its excited state to its ground state (Lakowicz, 1999). The energy loss that occurs between excitation and emission causes a shift in the spectrum into the longer wavelengths, which is known as bathochromic (red) shift of the emission spectra and is due to a phenomenon called Stokes' Shift (Lakowicz, 1999). In proteins, the intrinsic (naturally occurring) fluorophores are the aromatic amino acids tryptophan, tyrosine and phenylalanine. The fluorescence produced by most proteins is mainly the result of tryptophan, this is because native tyrosine and phenylalanine emission is transferred to tryptophan (Lakowicz, 1999).

Tryptophan (Trp) fluorescence can be selectively excited at 295 nm, which avoids excitation of tyrosine. Hydrophobic environments (where Trp is concealed within the centre of the protein), results in Trp having a high quantum yield and therefore a high fluorescence intensity and a λ_{max} around 335 nm (Lakowicz, 1999). Hydrophilic environments (where Trp is exposed to the aqueous solution surrounding the protein) results in the quantum yield declining and therefore a decrease in fluorescence intensity and a λ_{max} around 355 nm.

Therefore, it can be seen that for Trp residues, there is strong Stokes' Shift which varies depending on the solvent present, meaning that the maximum emission wavelength and fluorescence intensity of a Trp molecule will fluctuate depending on the environment it is in (Lakowicz, 1999). Fluorescence is a valuable probe as it is robust, highly sensitive and non-invasive (Ladokhin *et al*., 2000). The high sensitivity of intrinsic fluorescence allows for micro-molar concentration of protein to be used, minimizing the sample used (Eftink, 1994).

Tryptophan residues are a valuable intrinsic probe as most proteins contain very few of them, and the indole ring they contain is sensitive to their environment (Eftink, 1994). Spectroscopic analysis of proteins can also be valuable to study changes in protein structure in different environments including buffer conditions, denaturant concentration and changes in temperature.

1.12 Thermodynamic protein stability studies.

The main contributors to protein stability are the hydrogen bonds that form the secondary, tertiary and quaternary structures, as well as, van der Walls forces, hydrophobic interactions and disulfide bridges that contribute to the tertiary and quaternary structure and lastly, the protein's interaction with its solvent environment (Kauzmann, 1959). In order to denature a protein, which means to unfold or deactivate a protein, these bonds and interactions need to be disrupted. The Gibbs free energy of a molecule is the usable energy of said molecule and is responsible for the spontaneity of the reactions possible by the molecule.

The Gibbs free energy (ΔG) difference between the folded state (G_F) and unfolded state (G_U) can be used to express the thermodynamic stability of a protein. Gibbs free energy of a molecule is influenced by the enthalpy and entropy of the system. The enthalpy is the internal energy of a system, and entropy is a measure of disorder within a system. Change in Gibbs free energy is calculated by subtracting the product of the change in entropy and temperature ($T\Delta S$) from the change in enthalpy (ΔH). When ΔG is negative the reaction is said to be spontaneous. When the protein is folded the entropy of the system is low as the protein structure allows only a few conformations for the protein to move in. The enthalpy of the system is however also low, but proteins spontaneously fold into their lowest energy form and therefore the folded state is more favourable, that being said, the folded state of a protein is only marginally more stable than the fully unfolded state (Privalov, 1979).

Thermodynamic reactions can also be seen in terms of an equilibrium reaction. The equilibrium constant (K) of said reaction is, therefore, the amount of product, in our case unfolded protein, divided by the amount of reagent, in our case folded protein. When the equilibrium constant (K) is greater than one, the product reaction is favoured, in other words, the unfolding reaction is favoured, if the equilibrium constant (K) is less than one the reagent is favoured, in this case, the folded protein.

When the temperature is increased, the entropy of the system increases, making ΔG more negative and therefore favouring the unfolding of the protein as G_U is greater than G_F. Enthalpy is also temperature dependent and increases with an increase in temperature, but to a lesser extent then entropy (Schellman, 1987).

Chemical denaturants similarly cause disruption to the bonds and interactions that maintain secondary, tertiary and quaternary structures as well as the protein's interactions with their environments (Timasheff, 1993). Therefore chemical denaturants are also able to increase the entropy of the system, favouring the unfolding reaction.

Protein unfolding can either be reversible or irreversible, with the reversible reaction having the equilibrium constant (*K*) balancing the unfolded and folded protein percentages. Irreversible reactions have an unfolding rate constant that results in the formation of a final form, which is then unable to refold back to native form. Common causes of the irreversible unfolding of proteins include aggregation, autolysis and chemical alteration of residues (Privalov, 1982; Ahern and Klibanov, 1987). In order to obtain the parameters that are required to determine the function of protein stability, the protein unfolding has to be fully reversible, which is often not the case in thermal unfolding (Privalov, 1979).

Two common techniques used in the analyses of protein thermodynamics are spectral techniques and differential scanning calorimetry (DSC). Fluorescence and circular dichroism can monitor alterations in secondary and tertiary structure whereas DSC measures the difference in heat capacity between a protein sample and a reference sample.

For spectroscopic analysis of protein stability the peptide backbone and the aromatic amino acids Phe, Tyr and Trp (protein chromophores) are used to probe protein structural changes. Thermodynamic stability of a protein can be evaluated by consistently increasing the temperature of a protein sample and monitoring changes in protein structure using spectroscopy. The spectroscopic techniques of circular dichroism and fluorescence have been described in detail in section 1.11. However, notably, as tryptophan fluorescence signals (including signal intensity, emission maximum, quantum yield, fluorescence anisotropy and rotational correlation time to name a few) are subject to change depending on the protein's environment. This allows these parameters to assist in monitoring structural changes, including unfolding (Eftink and Ghiron, 1981; Gryczynski *et al*., 1988a; Eftink, 1994). However, it must be noted that a temperature dependent relationship is seen with the quantum yield of the indole chromophore. This phenomenon known as thermal quenching has been seen to occur in intrinsic tryptophan fluorescence which can result in a decrease in fluorescence intensity (quantum yield) with an increase in temperature without structural changes occurring (Demchenko, 1986). Similarly, circular dichroism spectra give details of the protein's structure and therefore is able to monitor structural changes caused by changes in the protein's environment (Righetti and Verzola, 2001).

On the other hand differential scanning calorimetry measures thermal events that occur in a protein that is being heated. Differential scanning calorimetry (DSC) directly measures the transition energy of the sample analysed (Watson *et al*., 1964). This is done by measuring the difference in energy needed to increase the temperature of a protein and a reference sample by the same amount. DSC can, therefore, monitor thermal events that accompany protein unfolding by measuring the energy released or absorbed.

Enthalpy of denaturation can be determined from DSC experimental data. DSC measures the excess heat capacity at a constant pressure (Cp_{ex}) of a protein in relation to a reference sample as a function of temperature. The protein stability function ($\Delta G(T)$) is determined using the melting temperature, (T_m), enthalpy, ($\Delta H(T_m)$) and heat capacity increment (ΔC_p) (Privalov, 1979).

The unfolding of a protein is an endothermic event, due to the hydration of side chains that are concealed in the protein's hydrophobic core, that become exposed to the hydrophilic solvent upon denaturation (Privalow, 1980; Sturtevant, 1987; Bruylants *et al*., 2005). Thus a greater amount of energy is needed to heat the protein sample compared to the reference sample and this additional energy is additional heat capacity above the normal heat capacity of the protein (Privalov, 1980; Atkins and de Paula, 2006).

The denaturation of a protein appears as a peak in a DSC thermo analytical curve, the top of the peak, where the excess heat capacity is maximal, is the transition midpoint T_m. The integral of the area under the denaturation peak is the enthalpy of denaturation (ΔH_m), which reflects the amount of secondary structure the protein contains (Watson *et al*., 1964; Tanford, 1970; Privalov, 1980; Koshiyama *et al*., 1981; Spink, 2008). The shift in the baseline between pre and post transition area is the difference in heat capacity (ΔC_p) from the native to denatured protein. In general, the heat capacity of a denatured protein is higher than the heat capacity of the folded protein (Edsall, 1935; Privalov, 1980; Privalov, 1988; Robertson and Murphy, 1997).

With (ΔH_m), and (ΔC_p) it is possible to calculate Gibbs free energy ($\Delta G(T)$) and entropy ($\Delta S(T)$) of denaturation at the temperature (T) of interest. Protein stability, in general, is measured by the ΔG of denaturation, with a stable protein having a high and positive ΔG. As with spectral studies of unfolding, it is important for the unfolding to be fully reversible in order to obtain all these values.

1.13 Aims and objectives.

Viral proteins are increasing in importance as they are vital to improvements in the vaccine, treatment and diagnostic development. Therefore, an economical and reliable expression protocol for full-length Bluetongue virus VP7 is desirable.

The aim of this project is to optimize overexpression of full-length Bluetongue virus VP7 using a bacterial expression system and to optimize the purification of said Bluetongue virus VP7 so that studies into its structure and stability can be undertaken using spectroscopy techniques.

The objectives of this study are threefold. The first is to test protein expression conditions including growth medium, post-induction temperature, inducer concentration and post-induction time of a bacterial expression system, consisting of a GenScript® constructed pET28a plasmid containing cDNA of polyhistidine-tagged Bluetongue virus VP7 gene sequence transformed into BL21(DE3), NiCo21(DE3), C43(DE3) pLysS and KRX *Escherichia coli* bacterial cells.

Secondly, is to purify Bluetongue virusVP7 protein using affinity tag chromatography. And lastly, when purified Bluetongue virus VP7 is obtained, the characterization of the secondary and tertiary structure using far-UV CD, fluorescence and clear native-PAGE. Conformational stability of Bluetongue virus VP7 will be determined by increasing temperature or denaturant concentration and monitoring protein behaviour using spectroscopic probes (fluorescence and far-UV CD) and differential scanning calorimetry.

2. Materials and Methods.

2.1 Materials.

A pET28a plasmid was procured from GenScript® and was generated by inserting the codon optimized cDNA, which encodes the Bluetongue virus VP7 consensus sequence (Russell *et al*., 2018), segment between the Ndel and Xhol restriction sites and the recombinant plasmid supplied to Prof. Samantha Gildenhuys. Confirmation of gene insert in the plasmid was performed by GenScript® via sequencing alignment and restriction digests. Kanamycin and isopropyl-β-D-thiogalactoside were obtained from Melford (Ipswich, United Kingdom). DNase I was obtained from Roche Diagnostics (Mannheim, Germany). SDS-PAGE protein molecular mass marker was obtained from Thermo Scientific (Massachusetts, United States). DEAE-Sepharose and histidine affinity nickel cross-linked agarose resins were obtained from GE Healthcare Life Sciences (Uppsala, Sweden) and Macherey-Nagel (Duren, Germany). Ultra-pure urea and Bradford reagent was obtained from Sigma-Aldrich (St. Louis, MO USA), and any additional chemicals were of analytical grade.

2.2 Transformation of competent cells and production of glycerol stocks.

Competent *Escherichia coli* BL21(DE3), NiCo21(DE3), C43(DE3) pLysS and KRX cells were transformed with the pET28a plasmid containing DNA encoding Bluetongue virus viral protein 7 (VP7).

Competent *Escherichia coli* BL21(DE3), NiCo21(DE3), C43(DE3) pLysS and KRX cells were thawed on ice for 15 minutes. Then 3 µl of pET28a plasmid DNA (100 ng.µl^{-1}) was added to 100 µl of competent cell mixture and placed on ice for 30 minutes. The BL21(DE3), NiCo21(DE3), C43(DE3) pLysS and KRX cells were then heated at 42 °C for 45 seconds, using a heating block, and then rapidly transferred to ice for two minutes.

Then 500 µl of SOC outgrowth media was mixed into the cell mixture followed by an incubation of 90 minutes at 37 °C with 230 rpm shaking. All cells were plated, using the spread plate technique, on LB-agar plates supplemented with 30 µg/ml kanamycin and for the C43(DE3) pLysS cells, an additional 30 µg/ml chloramphenicol was used. Agar plates were then incubated at 37 °C for 12-16 hours. Single colonies were taken from each cell line and added into 20 ml of sterile, fresh LB and grown for 12-16 hours, after which a 1:50 dilution was added to fresh LB and grown to mid-log. Glycerol stocks were then created by adding equal volumes of 30 % autoclaved glycerol and cell culture. The glycerol-cell mixture was frozen at -80 °C until needed.

2.3 Induction study.

BL21(DE3), NiCo21(DE3) and C43(DE3) pLysS contain the λDE3 lysogen, which contains the gene for T7 RNA polymerase controlled by a lac UVS promoter, which is inducible by IPTG (Studier and Moffatt, 1986). In addition, the pET28a plasmid is inducible by IPTG as it contains a lac UV5 promoter upstream from the target gene, as well as the repressor *lacI* gene and has kanamycin antibiotic resistance, which acts as a selectable marker. The system controlling gene expression in this plasmid involves the T7 promoter, from the bacteriophage T7 which is not acknowledged by bacterial mRNA polymerase. Instead, the activity of the T7 promoter is regulated by the lac UV5 promoter, which is situated upstream from the gene of interest (Sorenson and Mortensen, 2005).

The plasmid contains the *LacI* gene which encodes the LacI repressor, which allows for its production. The LacI repressor blocks the expression of T7 RNA polymerase by binding to the lac operator. IPTG binds to the LacI repressor, resulting in structural changes that cause the lac operator to be released. This frees the lac UV5 promoter and therefore allows transcription of T7 RNA polymerase to occur (Sorenson and Mortensen, 2005). The expressed T7 RNA polymerase interacts with the T7 promoter, that is situated upstream of the target gene within the plasmid, in this case, the gene coding for Bluetongue virus VP7, which is then translated into the Bluetongue virus VP7 protein and overexpression occurs. KRX cells contain a copy of T7 RNA polymerase modulated by a rhamnose promoter (rhaP$_{BAD}$), not the UV5 promoter. Rhamnose is able to induce the expression of the T7 RNA polymerase, which is then able to transcribe the target gene, in our case the Bluetongue virus VP7 gene.

Glycerol stocks (50 µl) of all *Escherichia coli* cell lines containing the pET28a plasmid (with the consensus Bluetongue virus VP7 encoding sequence insert) were added to 20 ml sterile, fresh LB media inoculated with 30 µg/ml kanamycin for all cell lines and an additional 30 µg/ml chloramphenicol for C43(DE3) pLysS cells.

All cell lines were grown for 12-16 hours at 37 ˚C with 230 rpm shaking, before being inoculated into fresh LB media to a dilution of 1:50, containing kanamycin (30 µg/ml) for all cell lines and an additional 30 µg/ml chloramphenicol for C43(DE3) pLysS cells. Cells were grown to an OD_{600} of between 0.5 and 0.8 at 37 ˚C with 230 rpm shaking, before being induced with IPTG concentrations of 0.1 mM and 1.0 mM IPTG for BL21(DE3), NiCo21(DE3) and C43(DE3) pLysS cells and 0.1 mM IPTG with 0.05 %, 0.1 % and 0.15 % rhamnose for KRX cells. All cells were grown at different post-induction temperatures between 16 ˚C and 37 ˚C, as well as at various post induction times from two to 16 hours.

BL21(DE3) cells and NiCo21(DE3) cells were grown in two growth mediums, namely Luria-Bertani medium (1.0 % (w/v) tryptone, 0.5 % (w/v) yeast extract, 0.5 % (w/v) sodium chloride) and 2xYT medium (1.6 % (w/v) tryptone, 1.0 % (w/v) yeast extract, 0.5 % (w/v) sodium chloride). Induction was performed when the cell culture produced a reading between 0.5 and 0.8 computed using optical density readings with an Implen P330 NanoPhotometer (München, Germany), at wavelength of 600 nm.

After induction, whole cell samples were collected by centrifugation of 1 ml of cell culture for five minutes at 12,100 x g. The whole cell pellet obtained from this centrifugation was then resuspended in 400 µl. Primary buffer. To analyse the extent of soluble protein expression, the soluble (supernatant) and insoluble (pellet) fractions were separated by taking 5 ml of cell culture and centrifuging it at 3000 x g for 15 minutes at 4 ˚C and then resuspending it in 700 µl of Lysis buffer and this mixture was rotated at 22 ˚C for 20 minutes. The cell mixture was then sonicated with a Qsonica Q700 sonicator (Newtown, USA) at 35 amperes for five, 10 second rounds (pulsed at two seconds on, one second off) and placed on ice for two minutes in between each cycle for BL21(DE3), NiCo21(DE3) and KRX cells and at 60 amperes for five, 10 second (pulsed at two seconds on, one second off) for C43(DE3) pLysS. The sonicated cell mixture was then centrifuged for 20 minutes at 12,100 x g at 4 ˚C before removing the supernatant. The pellet was then re-suspended in 700 µl Primary buffer. Sonication and centrifugation were repeated for samples taken at various time intervals between two and 16 hours post induction, depending on the cell line. Whole cells, supernatant (soluble fraction) and pellet (insoluble fraction) samples were investigated using SDS-PAGE (see section 2.7.1).

2.4 Isolation of inclusion bodies.

BL21(DE3) and NiCo21(DE3) whole cell samples were defrosted and prepared for separation of soluble (supernatant) and insoluble (pellet) fractions as described in section 2.3, with volumes altered proportionately.

As presented in Russell and Gildenhuys (2018), the pellet containing, Bluetongue virus VP7, was collected after sonication and centrifugation of whole cell samples and then placed in 50 ml of Wash buffer A. The detergent Triton X-100 was used as it facilitates the removal of bacterial cell membrane proteins and other cellular debris (Lilie *et al*., 1998; De Bernardez, 1998; Georgiou and Valax, 1999). EDTA was added to prevent the air oxidation of cysteines (Kaur *et al*., 2017). To isolate the bacterial cell inclusion bodies the pellet was washed twice in Wash buffer A and centrifuged at 12,100 x g for 16 minutes.

This was followed by resuspending the pellet twice in 50 ml of Wash buffer B and centrifuging at 12,100 x g for 10 minutes to remove the Triton X-100 as it can interfere with further solubilisation and purification. The resulting pellet was used for further solubilisation and purification.

2.5 Solubilisation of inclusion bodies containing Bluetongue virus VP7.

To solubilise the inclusion bodies containing Bluetongue virus VP7, a method of freezing the inclusion bodies in the presence of urea was used as presented in Russell and Gildenhuys (2018). All urea used was prepared as described by Pace (1986) using the necessary buffer for the solvent. Urea stock solutions were filtered with a 0.4 µm filter after having the pH adjusted as needed. Stock solution concentration of 10 M was confirmed using an Atago R5000 refractometer (Tokyo, Japan). The stock solution produced was frozen at -20 ˚C and defrosted on the day needed, stock solutions were used within five days of being made.

Seven urea concentrations were evaluated, namely 2 M, 3 M, 4 M, 5 M, 6 M, 7 M and 8 M urea in the Freezing buffer. The urea suspended inclusion bodies were frozen at -20 ˚C for 16 hours and defrosted at 22 ˚C before being centrifuged at 12,100 x g for 15 minutes. The degree of protein solubilisation was analysed by SDS-PAGE (section 2.7.1). For solubilisation of protein samples for ion-exchange chromatography the inclusion bodies were frozen with the same Freezing buffer, but with only 20 mM sodium chloride, as the higher concentration of sodium chloride would interfere with protein binding to the column.

2.6 Purification of solubilized Bluetongue virus VP7.

2.6.1 Anion-exchange chromatography.

In anion-exchange chromatography, the binding ions on the proteins have a negative charge and the immobilized functional groups in the resin have a positive charge (Adams and Holmes, 1935). The isoelectric point for Bluetongue virus VP7 is predicted to be pH 7.07 by ProtParam tool on the ExPASy proteomics server (Gasteiger *et al*., 2005).

Purification by anion-exchange chromatography of solubilized Bluetongue virus VP7 from BL21(DE3) cells was performed using a DEAE-Sepharose (GE Healthcare Life Science, Uppsala, Sweden) with one of two buffers. Firstly the column was pre-equilibrated with five column volumes of Equilibration buffer A. The sample of solubilized protein from 250 ml of cell culture was diluted with Equilibration buffer A and a pH of 9 was confirmed before being applied to the column. Next, eight column volumes of Equilibration buffer A were used to wash the column, to wash away any unbound protein.

Bound protein was eluted off the column using five isocratic column volumes of Elution buffer A, followed by a linear salt gradient (seven column volumes) from 20 mM to 1 M sodium chloride. The gradient was produced by mixing the Elution buffer A with 1 M sodium chloride.

Secondly, Equilibration buffer B was used to equilibrate the DEAE-Sepharose column. The sample of solubilized protein from one litre of cell culture was diluted with Equilibration buffer B and a pH of 9 was confirmed before it was applied to the column.

Five column volumes of Equilibration buffer B were washed through the column, to wash away unbound protein. Bound protein was eluted off the column using five column volumes of Elution buffer B, followed by a linear salt gradient (seven column volumes) from 20 mM to 1 M sodium chloride. The gradient was produced by mixing Elution buffer B with 1 M sodium chloride.

All urea used was prepared as described in section 2.5. Anion-exchange chromatography was coordinated using an ÄKTAprime system with PrimeView 5.31 software (GE Healthcare Life Sciences, Uppsala, Sweden). Bluetongue virus VP7 was detected using SDS-PAGE (section 2.7.1) analysis of fractions with high 280 nm readings.

2.6.2 Nickel-IMAC chromatography.

Solubilized protein from BL21(DE3) and NiCo21(DE3) *Escherichia coli* inclusion bodies were loaded onto two different nickel cross-linked agarose resins, namely Macherey-Nagel Protino® Ni-NTA agarose (Duren, Germany) and GE Healthcare Histrap high performance (Uppsala, Sweden).

All urea used was prepared as described in section 2.5. Macherey-Nagel Protino® Ni-NTA columns were equilibrated with 10 column volumes of Equilibration buffer C. The addition of salt (up to 500 mM sodium chloride) was added to reduce nonspecific hydrophobic protein interactions with the nickel affinity resin (Bornhorst and Falke, 2000). The protein sample consisting of the solubilised protein was loaded onto the column. The column was then washed with 10 column volumes of the Equilibration buffer C.

The protein was eluted using a linear gradient (six column volumes) from 0 to 250 mM imidazole followed by five isocratic column volumes of Elution buffer C. The gradient was produced by mixing the Equilibration buffer C with Elution buffer C. All buffers were filtered using a 0.2 µm filter before use.

GE Healthcare Histrap high performance columns were equilibrated with 10 column volumes of Equilibration buffer D. The solubilized protein sample was loaded onto the column. The column was then washed with 10 column volumes of the Equilibration buffer D.

The protein was eluted off by using a linear gradient (six column volumes) from either no initial imidazole or 50 mM initial imidazole to 500 mM imidazole, followed by five isocratic column volumes of Elution buffer D. The gradient was produced by mixing the Equilibration buffer D with Elution buffer D. All buffers were filtered using a 0.2 µm filter before use.

Nickel-affinity chromatography was conducted using a BioRad NGC™ Chromatography system with a computer loaded with ChromLab software (Hercules, USA). Bluetongue virus VP7 was detected using SDS-PAGE (section 2.7.1) analysis of fractions with high 280 nm absorbance readings. Fractions that were found to contain Bluetongue virus VP7 were then combined and concentrated using a Merck Millipore Amicon® Stirred cell and Ultracel® membrane (Darmstadt, Germany).

Dialysis of concentrated protein samples was performed using three buffer changes, four, six and 16 hours apart, respectfully. Dialysis was performed at approximately 16 ˚C with a buffer volume 10 times the sample size volume. Dialysis of concentrated Bluetongue virus VP7 was performed into the Primary buffer with the addition of 20 mM sodium chloride, 20 % glycerol and 5 M ultra-pure urea. A pH value of 6 was used as Bluetongue virus VP7 isoelectric point is predicted as pH 7.07. Using a buffer with a pH value of at least one point above or below the protein's pI can help in the reduction of protein aggregation as the proteins then contain net charges that help to repel individual proteins from one another (Gitlin, 2006).

2.7 Gel electrophoresis of proteins.

2.7.1 SDS-PAGE.

SDS-PAGE was used to visualise solubility and purity of Bluetongue virus VP7. SDS-PAGE uses electrophoresis to separate proteins (Laemmli, 1970) based on their molecular mass. A 15 % separating gel and 4 % stacking gel was used in a BioRad Mini-PROTEIN Electrophoresis Cell (Hercules, USA). The protein samples were diluted two-fold with SDS-PAGE sample buffer. Protein in the SDS-PAGE sample buffer was boiled for 5 minutes. The gel was run in an SDS-PAGE running buffer at 160 volts for approximately 1 hour.

The molecular mass marker used contained a mixture of seven proteins: β-galactosidase (116 kDa), bovine serum albumin (66.2 kDa), ovalbumin (45 kDa), lactate dehydrogenase (35 kDa), restriction endonuclease Bsp98I (25 kDa), β-lactoglobulin (18.4 kDa) and lysozyme (14.4 kDa). Each gel was then stained with 0.05 % R250 Coomassie Brilliant blue, 10 % acetic acid and 50 % methanol for an hour, and then de-stained with 5 % ethanol and 7 % acetic acid solution overnight. A BioRad, Universal Hood III (Hercules, USA) gel imaging system was used.

2.7.2 Clear native PAGE.

Clear native PAGE samples are prepared in a non-reducing, non-denaturing sample buffer and the proteins separated based on molecular mass, structure and charge. Pre-cast BioRad Mini Protein TGX Protein Gels with premixed BioRad native PAGE sample and BioRad native PAGE running buffer was used. A BioRad Mini-Protein Electrophoresis Cell was used (Hercules, USA). Bluetongue virus VP7 was analysed in a number of different buffers.

Samples were left in BioRad native PAGE sample buffer, and their respective additives, for one hour before loading. Samples of Bluetongue virus VP7 in 2 % SDS, 5 M urea and 5 M with 2 % SDS were boiled at approximately 100 ˚C, for 8 minutes before being loaded. Samples were boiled to assess the ability of high temperatures to denature Bluetongue virus VP7. The gels were run in BioRad native-PAGE running buffer at 120 volts for approximately two hours. Each gel was then stained with 0.05 % R250 Coomassie Brilliant blue, 10 % acetic acid and 50 % methanol for an hour, and then de-stained with 5 % ethanol and 7 % acetic acid solution overnight. A BioRad, Universal Hood III (Hercules, USA) gel imaging system was used.

2.8 Spectroscopic studies.

2.8.1 Spectroscopy for protein concentration determination.

2.8.1.1 Absorbance spectrometry

Protein concentration can be calculated from absorbance spectroscopy using the Beer-Lambert law:

$$A = \varepsilon_{\lambda} cl \quad (1)$$

where A is the absorbance at the respective wavelength, ε_{λ} is the molar extinction coefficient of the absorber at wavelength λ (L. mol^{-1}. cm^{-1}), c is the concentration of the absorber (mol. L^{-1}) and l is the path length of the cuvette (cm). To calculate the molar extinction coefficient ε of a protein the number of tryptophan, tyrosine and cysteine disulfide bonds are obtained and used in the following equation described by Perkins (1986):

$$\varepsilon_{280}\ M^{-1}.\ cm^{-1} = [5550 \times (\Sigma \text{Trp residues})] + [1340 \times (\Sigma \text{Tyr residues})] + [150 \times (\text{Cys residues})] \quad (2)$$

The molar extinction coefficient for Bluetongue virus VP7 was determined to be 40910 $M^{-1}.cm^{-1}$ using formula 2 with Bluetongue virus VP7 containing 5 Trp, 9 Tyr and 3 Cys residues.

Protein concentration was determined prior to other spectroscopic techniques using an Applied Photophysics Chirascan Plus (Leatherhead, United Kingdom) with Photophysics Pro-Data software. A quartz cuvette with a path length of 10 mm was used. A bandwidth of 1 mm was used and a measurement was recorded for every 1 nm between 360 nm and 220 nm. For every sample, three spectra repeats were recorded and averaged. All spectra had buffer contributions subtracted.

2.8.1.2 Bradford assay

For confirmation of protein concentration of purified protein samples, a Bradford assay (Bradford, 1976) was performed using bovine serum albumin as a standard. Colour change was monitored at 595 nm for a number of bovine serum albumin standards of known concentrations using an Implen P330 NanoPhotometer (München, Germany). The concentration of the purified Bluetongue virus VP7 was determined by comparison to the standards of which the concentration is known.

2.8.2 Far-UV circular dichroism.

Far-UV Circular Dichroism spectra were recorded using an Applied Photophysics Chirascan Plus (Leatherhead, United Kingdom) with Photophysics Pro-Data software. Wavelengths between 250 nm to 190 nm were evaluated at 22 ˚C using a 1 mm quartz cuvette with a step size between measurements of 1 nm, bandwidth of 1 nm and scan speed of 2 nm per second. A quartz cuvette was used as quartz does not absorb light in the wavelength range being studied (Kelly and Price, 2000).

Spectra values collected were converted to mean residue ellipticity with the formula:

$$[\theta] = 100 \text{ (signal)}/ \text{Cnl} \quad (3)$$

where C is the concentration of protein in mM, n is the number of amino acid residues and l is the path length in cm. For every sample, three spectra repeats were recorded and averaged. All spectra had buffer contributions subtracted.

2.8.3 Intrinsic fluorescence.

Fluorescence spectra were collected at 22 ˚C, using an Applied Photophysics Chirascan Plus (Leatherhead, United Kingdom) with Photophysics Pro-Data software and a 10 mm quartz cuvette, a bandwidth of 1 mm, step size of 1 nm and wavelength range 500 nm and 275 nm, with excitation wavelength set at 295 nm. For every sample, three spectra repeats were recorded and averaged. All spectra had buffer contributions subtracted.

Bluetongue virus VP7, as mentioned in the introduction, contains 5 tryptophan residues, namely Trp119, Trp141, Trp188, Trp255 and Trp 278. The positioning of tryptophan residues can be seen in Figure 2.1, showing that residue Trp278 is completely buried in the folded protein and therefore not represented on the diagram, and Trp225 is predominantly buried. Trp119, Trp141 and Trp188 are all predominantly exposed in the folded protein.

2.8.4 Protein unfolding.

Heat and denaturants such as urea and guanidinium chloride are capable of unfolding native proteins (Schmid, 2001). Therefore a protein's stability can be tested by subjecting it to the different conditions and measuring the fluorescence spectra. More specifically the intensity and wavelength emission maxima of tryptophan for each desired condition as well as the far-UV circular dichroism spectrum for the presence or absence of characteristic secondary structure measurements (Kelly and Price, 2000). Far-UV CD and fluorescence were used to monitor the stability of the protein by displaying how the secondary and tertiary structure changes in response to changes in buffer conditions.

Far-UV circular dichroism and fluorescence spectra were obtained as described in section 2.8.2 and 2.8.3 while increasing the temperature of the protein sample from 20 ˚C to 90 ˚C. The temperature was maintained by a PCS.3 Single Cell Peltier Temperature Controller, with a circulating chiller unit that is programmed by the Chirascan's Pro-Data software (Leatherhead, United Kingdom).

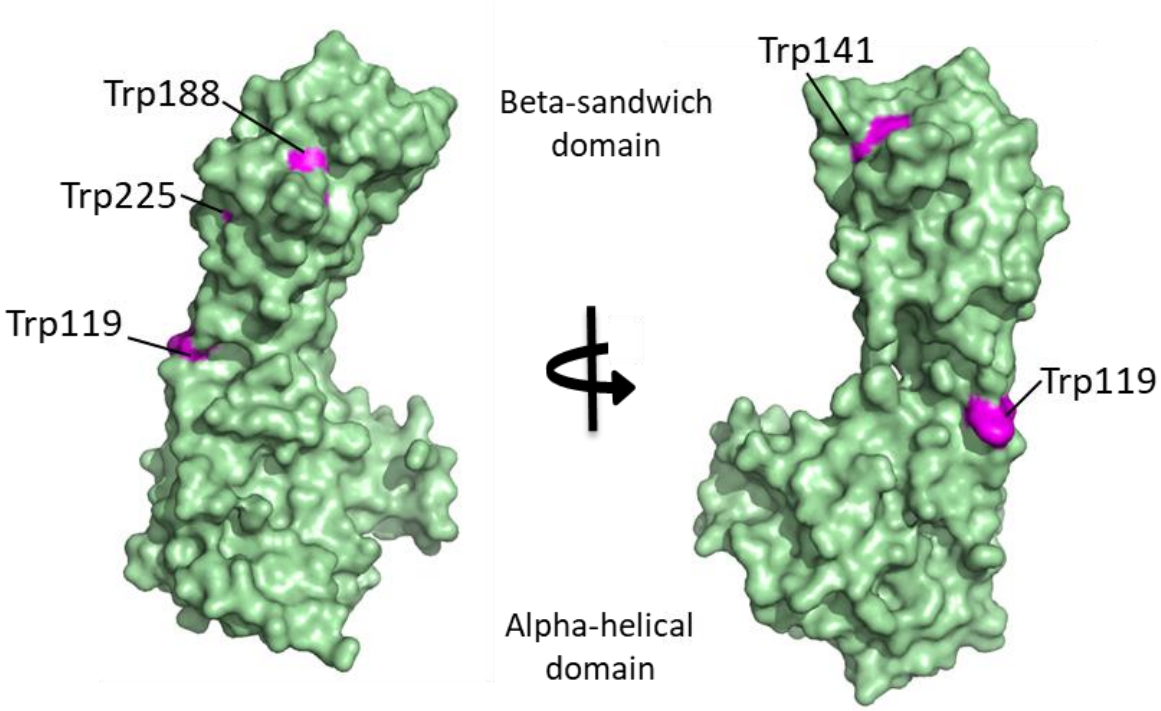

Figure 2.1. Tryptophan residues in Bluetongue virus VP7.

Diagram showing Bluetongue virus VP7 monomer depicting positioning of tryptophan residues, showing surface exposure. Tryptophan residues are highlighted in pink and are numbered with their corresponding residue number. Trp278 is completely buried in the folded protein and is therefore not represented on the diagram. Two orientations of the protein are shown with the two domains found in a Bluetongue virus VP7 molecule labelled beta-sandwich and alpha-helical on the diagram to help orientate the protein. The structure was obtained from the protein data bank (1BVP) and viewed with PyMOL Molecular Graphics System (1.3rl Edu), Schrödinger, LLC.

A spectrum was recorded every two degrees between 20 ˚C and 90 ˚C. A final spectrum was recorded when the protein sample was cooled to 20 ˚C after being heated to 90 ˚C. For far-UV CD the spectrum was recorded between 250 nm and 210 nm, and for fluorescence, the spectrum was recorded between 500 nm and 280 nm.

Bluetongue virus VP7 was tested in the presence of urea and guanidinium chloride. All urea used was prepared as described in section 2.5. Guanidinium chloride was prepared as described by Pace (1986) using the necessary buffer as the solvent. pH was adjusted as needed before being filtered with a 0.4 µm filter. Stock solution concentrations were confirmed using an Atago R5000 Refractometer (Tokyo, Japan), using refractive indices described by Pace (1986) and Nozaki (1972). Stock solutions were used within a week of being made. Samples were prepared in buffers containing the desired denaturant concentration, by addition of denaturant stock solutions, for at least three hours. For guanidinium chloride refolding studies were undertaken by diluting the protein back down from 6 M to 1 M by the addition of Primary buffer at a rate of a decrease of 1 M each time. Protein samples were allowed to fold for one hour before spectra were recorded. Spectra were recorded at 22 ˚C as described in section 2.8.2 and 2.8.3.

2.9 Differential scanning calorimetry.

Thermal stability of the protein was evaluated using a TA Instruments Nano Differential scanning calorimeter (New Castle, Delaware) with DSCRun software version 4.4.25. Data collected was analysed using NanoAnalyze version 3.7.5. Thermal stability is expressed as T_m (peak temperature, in ˚C or K) and is an approximation of the temperature at which 50 % of the proteins in the sample are denatured.

A buffer to buffer reaction (Primary buffer with 5 M urea) was recorded first (buffer in sample and reference cell) to produce a baseline for subtraction. Next, the protein sample containing Bluetongue virus VP7 was loaded into the sample cell with buffer (Primary buffer with 5 M urea) in the reference cell. All samples were degassed for approximately 10 minutes before use. Thermograms were collected as the protein was heated from 10 ˚C to 100 ˚C with a scan speed of 1 ˚C/min. Thermal stability is expressed as T_m (peak temperature, in ˚C or K) and is closely related to the temperature of denaturation.

3. Results.

3.1 BL21(DE3) Cells.

BL21(DE3) is a derivative of *Escherichia coli* BL21 that has a chromosomal DE3 prophage that is able to express T7 RNA polymerase. BL21(DE3) was tested first as it is one of the most extensively used *Escherichia coli* strains to check basic protein expression in *Escherichia coli* (Joseph *et al*., 2015).

3.1.1 Expression.

Protein expression in BL21(DE3) cells was evaluated using four variables, namely (1) post induction time (Figure 3.1A), (2) cell growth medium (Figure 3.1B), (3) post induction temperature (Figure 3.1C) and (4) Inducer concentration (Figure 3.1D).

Soluble (supernatant) and insoluble (pellet) fractions were visualised using SDS-PAGE (see section 2.7.1). Each protein's mass was determined by comparing the protein's migratory distance to the distance travelled by proteins of known molecular mass, under the same conditions. A mass of 41 kDa was obtained, which is consistent with the size of 38 kDa for Bluetongue virus VP7 (Basak *et al*., 1992; Grimes *et al*., 1995) with both a C and N terminal polyhistidine tag and a thrombin cleavage site. This would place the protein between the sizes of ovalbumin (45 kDa) and lactate dehydrogenase (35 kDa) in the protein marker (Figure 3.1E).

When post induction time was evaluated (Figure 3.1A), a large increase in expression of Bluetongue virus VP7 was seen between two and three hours, a gradual increase between three and four hours and four and five hours and a large increase between five hours and 16 hours. The large increase between two and three hours can be attributed to there being low cell numbers at two hours compared to three hours. The larger increase between five and 16 hours could at least in part be attributed to larger cell numbers produced over the increased growing time, as even though the cells would reach stationary phase within this time frame, cell growth and death are still occurring and seeing as the media creates a closed system, the protein becomes more concentrated. This is supported by the increase in all expressed bacterial proteins in the sample. Very little Bluetongue virus VP7 appears to be expressed in soluble form (seen in the supernatant fraction), and no apparent increase in soluble Bluetongue virus VP7 expression occurs over time.

When cell growth medium was evaluated, two compositions were used, namely Luria-Bertani (LB) medium and 2xYT medium (Figure 3.1B). The medium types were assessed as Luria-Bertani medium is the most commonly used growth medium for bacterial cells (Bertani *et al*., 1951) and 2xYT media is richer in the metabolites needed by bacterial cells, and therefore is known to increase protein and cell yields (Miller, 1972; Lessard, 2013).

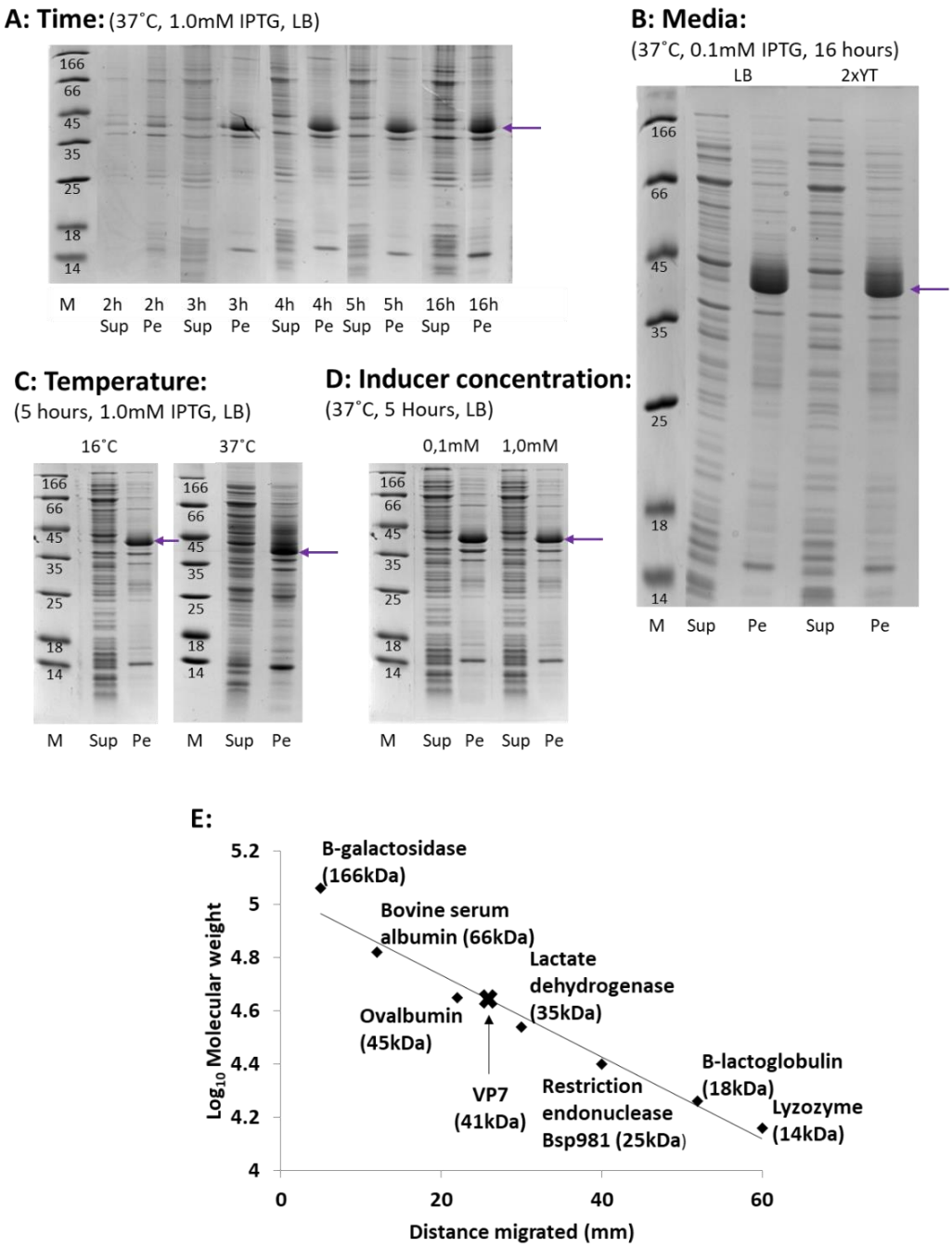

Figure 3.1. Bluetongue virus VP7 expression in BL21(DE3) cells.

SDS-PAGE showing expression of Bluetongue virus VP7 (marked with a purple arrow) in BL21(DE3) cells when varying four different expression conditions namely ***(A)*** *post induction time,* ***(B)*** *cell growth media,* ***(C)*** *post induction temperature and* ***(D)*** *inducer concentration. Expression conditions kept constant are indicated above each gel. "Sup" represents supernatant and "Pe" represents pellet samples.* ***(E)*** *A calibration curve showing Bluetongue virus VP7 migrating a distance that corresponds to the size of 41 kDa with the position of Bluetongue virus VP7 marked with an (****x****) and size and names of proteins found within protein marker indicated. Selected data used in this Figure was published in Russell and Gildenhuys (2018).*

SDS-PAGE analysis showed little difference in protein expression in either the soluble (supernatant) or insoluble (pellet) fractions, with the predominance of expression being seen again in the insoluble fraction (pellet) for both mediums (Figure 3.1B). Therefore, as 2xYT has a greater cost due to the increased percentage of tryptone and yeast, the logical choice would be to use LB medium as a similar yield is obtained at a lower cost.

When post induction temperature was assessed, cells were grown after induction at 16 ˚C and 37 ˚C (Figure 3.1C). SDS-PAGE showed an increase in Bluetongue virus VP7 expression at 37 ˚C compared to 16 ˚C, however, there is also an increase in other bacterial proteins expressed, and therefore at least part of the increase at 37 ˚C could be due to increased cell numbers after five hours at the higher temperature. This is supported by Farewell and Neidhardt (1998) and Noor *et al*. (2013) who reported increased *Escherichia coli* cell growth at higher temperatures compared to lower temperatures. Growing cells as 16 ˚C has been known to produce soluble expression of proteins that are insolubly expressed at higher temperatures (Hockney, 1994; Makrides, 1996). However, growing BL21(DE3) cells containing the Bluetongue virus VP7 insert at 16 ˚C still resulted in a larger quantity of expression being in the insoluble fraction (pellet).

And lastly, two inducer concentrations were tested, namely 0.1 mM and 1.0 mM (Figure 3.1D). Little expression difference was seen between the two inducer concentrations, with both resulting in Bluetongue virus VP7 expression occurring predominantly in the insoluble fraction (pellet).

The chosen conditions for protein expression in BL21(DE3) cells were five hour post-induction growth, at 37 ˚C with 0.1 mM IPTG in LB medium. This was to help prevent the stress placed on bacterial cells that are grown for long periods of time, but still allowing for adequate time for the expression of Bluetongue virus VP7 in a higher proportion to other cellular proteins (Bentley and Kompala, 1990).

3.1.2 Solubilisation.

The lack of soluble expression of Bluetongue virus VP7 in BL21(DE3) cells resulted in the need to solubilize the protein found in inclusion bodies in the bacterial cell pellet. Cellular debris, including bacterial cell wall, membrane components, proteins, and residual soluble proteins, accumulate in the insoluble fraction (pellet) after sonication and centrifugation. These contaminating components can be removed with the use of detergents (such as Triton X-100) and a low concentration of urea or guanidinium chloride, resulting in ‘washed pellets’ (Palmer and Wingfield, 2004). As seen in Figure 3.2A SDS-PAGE analysis depicts several wash steps that were undertaken to remove the contaminating bacterial components, and therefore isolate the inclusion bodies.

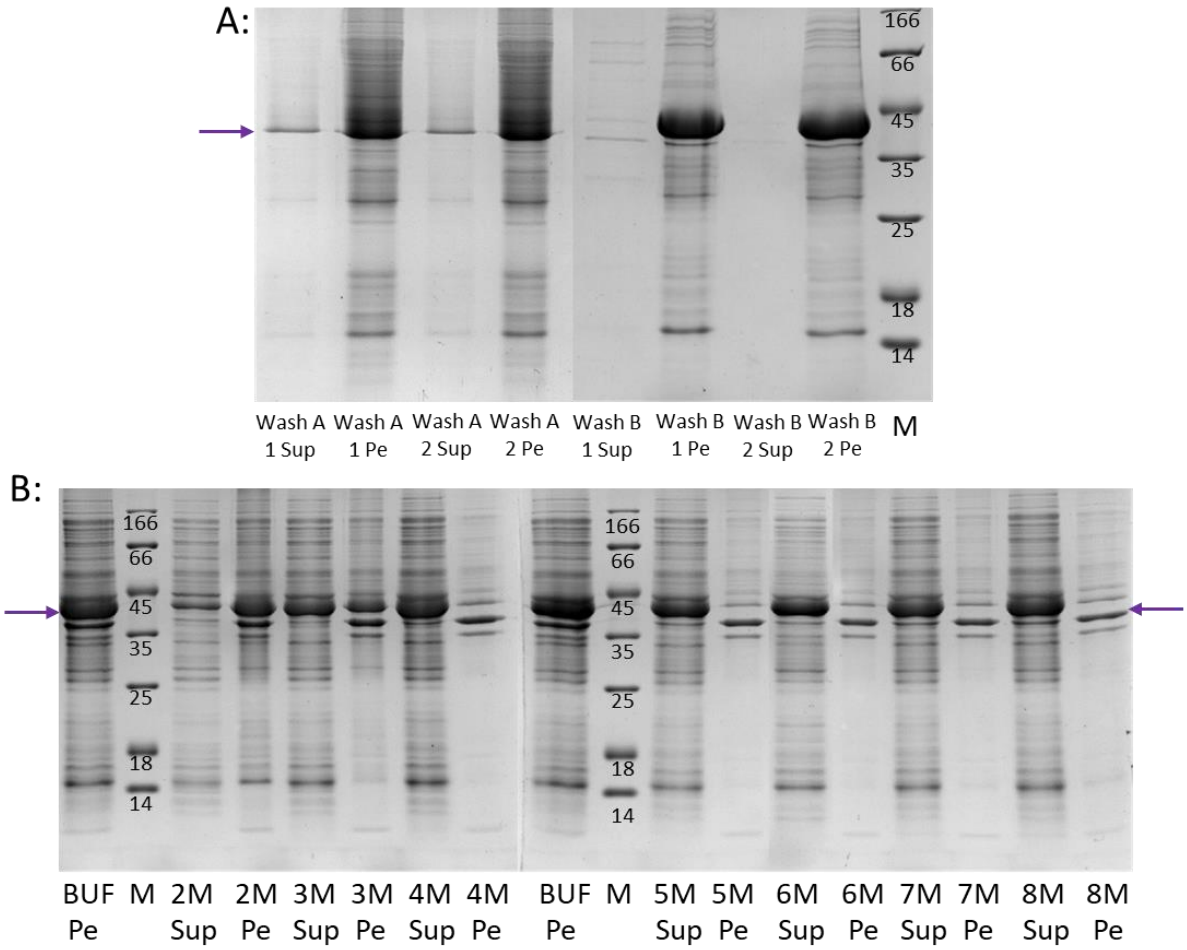

***Figure 3.2. Solubilisation of BL21(DE3) inclusion bodies**.*

*SDS-PAGE analysis of results obtained from the protocol for solubilizing BL21(DE3) inclusion bodies. (**A**) Supernatant and pellet fractions of numbered wash steps, Wash A is with Wash buffer A (containing Triton X-100) and Wash B is with Wash buffer B (buffer components in List of Buffers on page xiv). (**B**) Shows supernatant and pellet samples after centrifugation of the defrosted inclusion bodies in different urea concentrations, depicted as 'x'M, where 'x' is the urea concentration that the sample was frozen in. "Sup" is the supernatant, "Pe" is the resuspended pellet. BUF is the samples before being frozen in urea. Molecular mass marker (marked as "M") has sizes in kDa, marked on the gel. The position of Bluetongue virus VP7 is marked with purple arrows. Selected data used in this Figure was published in Russell and Gildenhuys (2018).*

Triton X-100 causes disruption in SDS-PAGE and thus is the cause of the smudging and apparent lower concentrations seen for samples that contain it (Figure 3.2A). Bluetongue virus VP7 was solubilised from bacterial inclusion bodies using urea and a freeze-thaw step modified from the protocol presented by Qi *et al*. (2015). The Wash buffer B step was repeated so that all of the Triton X-100 was removed before solubilisation. As seen in Figure 3.2B less than half of the pellet is solubilized with urea concentrations of 3 M and below, with a similar high level of solubilisation for urea concentrations of 4 M and above. There appears to be a slight increase between 4 M and 5 M, and then no further increase after that. The urea concentration for solubilisation of at least 95 % of the proteins within the bacterial inclusion bodies including Bluetongue virus VP7 was 5 M urea for BL21(DE3) cells (Figure 3.2B).

3.1.3 Purification.

Solubilized proteins from BL21(DE3) cell inclusion bodies were loaded onto a pre-equilibrated DEAE-Sepharose column using two different buffers as explained in methods. The two buffers were tested as ion-exchange chromatography is sensitive to the ionic strength and type of buffer compound used, as an increase in ionic strength decreases protein binding to the column as competing ions are increased. Sodium phosphate buffers are said to have a higher ionic strength than Tris-HCl buffers at a given concentration (Good and Izawa, 1972). When the solubilized protein mixture containing Bluetongue virus VP7 was loaded onto columns equilibrated with both Equilibration buffer A (containing sodium phosphate) (Figure 3.3A) and Equilibration buffer B (containing Tris-HCl) (Figure 3.3B), Bluetongue virus VP7 bound the column and was eluted off at approximately 250-300 mM sodium chloride and not during pH elution step.

The pH elution step is indicated in Figure 3.3A and B with no visible peaks occurring. With both buffers, multiple other bacterial cellular proteins bound and were eluted from the column under the same conditions as Bluetongue virus VP7, despite a salt gradient being used. Therefore, further purification would be needed. For Equilibration buffer A, solubilized protein from 250 ml of LB culture was used and for Equilibration buffer B, 1000 ml of LB culture was used, explaining discrepancies in the 280 nm absorbance seen. Changes in elution profiles such as peak positioning and values between Figure 3.3 A and B could potentially be due to changes in ionic strength of the different buffers used.

Next, solubilized protein from BL21(DE3) cell inclusion bodies were loaded onto a pre-equilibrated nickel affinity column. Two different nickel cross linked agarose resins were tested, namely Macherey-Nagel Protino® Ni-NTA agarose and GE Healthcare Histrap high performance Ni Sepharose.

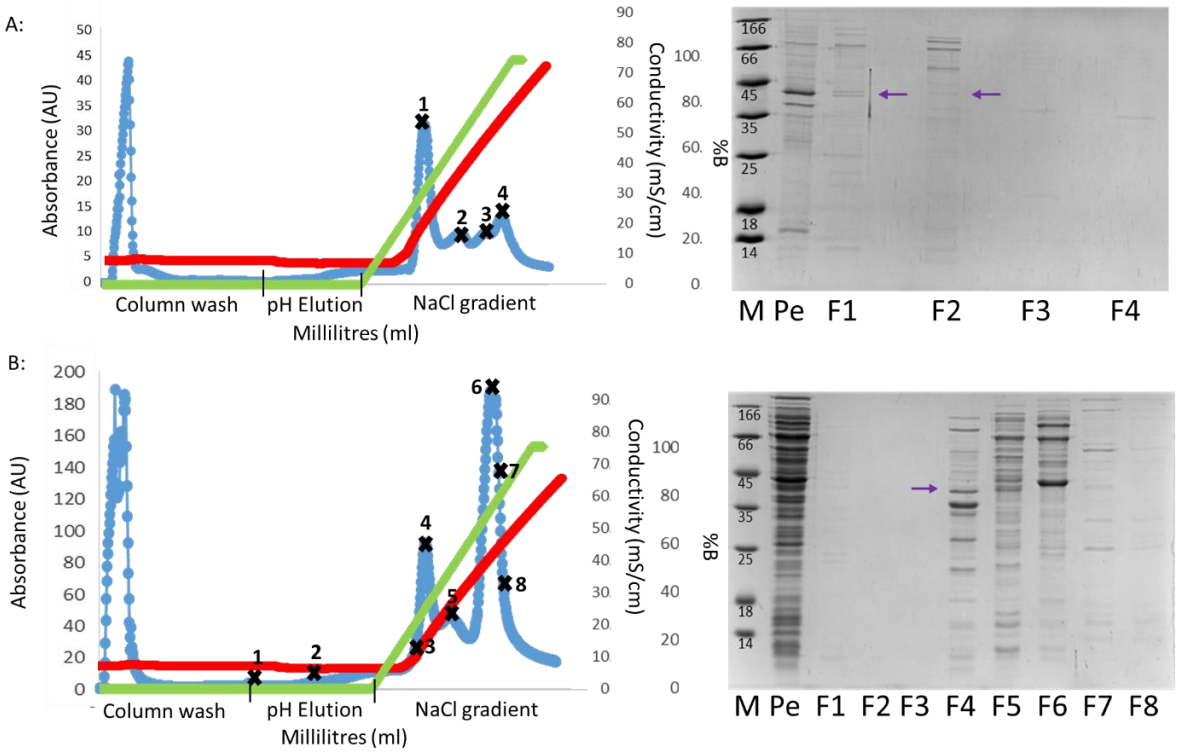

Figure 3.3. Ion-exchange chromatography purification of solubilised Bluetongue virus VP7 from BL21(DE3) cells.

*A DEAE-Sepharose ion-exchange chromatography purification of solubilised protein from inclusion bodies produced by BL21 (DE3) cells for (**A**) Equilibration and Elution buffer A (**B**) Equilibration and Elution buffer B. Chromatograms are shown where the A_{280} effluent (blue), sodium chloride gradient (green), conductivity (red) and fractions collected (numbered and marked with '**x**') are depicted. As well as SDS-PAGE analysis of certain fractions depicted as "FX" on SDS-PAGE, where 'X' represents the fraction number. "Pe" is the sample loaded onto the column. Molecular mass marker (marked as "M") has sizes in kDa, marked on the gel. The position of Bluetongue virus VP7 is marked with purple arrows. Purification performed using and ÄKTAprime system with PrimeView 5.31 software.*

Firstly the Macherey-Nagel Protino® Ni-NTA agarose was tested (Figure 3.4A) which resulted in solubilized Bluetongue virus VP7 binding the column pre-equilibrated and washed with Equilibration buffer C. However, multiple other bacterial proteins bound under the same conditions, and were eluted along with Bluetongue virus VP7 from approximately 150 mM imidazole (approximately 60 % through gradient). This is seen in the chromatogram (Figure 3.4A) which shows an elongated elution peak containing Bluetongue virus VP7 (fractions 4 to 11) with at least two peaks within it (fractions 5 and 6).

Some Bluetongue virus VP7 was also seen to not bind the column, and instead came through in the buffer wash before elution, this may be due to the Macherey-Nagel Protino® Ni-NTA column reaching binding capacity due to a large amount of non-specific bacterial cell protein binding seen, both eluted before and with Bluetongue virus VP7 elution.

The GE Healthcare Histrap high performance purification of Bluetongue virus VP7 from BL21(DE3) cells required two chromatographic steps, as the initial step without imidazole in Equilibration buffer D (Figure 3.4B) resulted in other bacterial proteins binding and eluting with Bluetongue virus VP7, the same is seen with the Macherey-Nagel Protino® Ni-NTA agarose. However, the chromatogram showed more defined peaks at fraction 4 and 6-7 with elution of Bluetongue virus VP7 occurring over fraction 4 to 12.

The decrease in non-specific binding of bacterial proteins seen for the GE Healthcare Histrap high performance columns resulted in them being used for further studies. Bluetongue virus VP7 was eluted from a concentration of approximately 300 mM imidazole (approximately 60 % through the gradient). The fractions collected that contained Bluetongue virus VP7 were loaded onto the same column pre-equilibrated with Equilibration buffer D, with 50 mM imidazole, after being diluted 8-fold with the same Equilibration buffer D to obtain a concentration of approximately 50 mM imidazole in the sample as well. When imidazole was added to the Equilibration buffer D (Figure 3.4C), Bluetongue virus VP7 was found to still bind the column and be eluted off at an imidazole concentration between 300-500 mM, with the chromatogram (Figure 3.4C) showing a double peak over fractions 2 to 4 and 6 to 9. For Figure 3.4C the smudging of samples in SDS-PAGE is caused by the presence of urea and high sodium chloride concentrations in the samples.

For proteins that have a polyhistidine tag on both the C and N terminals, it has been seen that they bind the column resin more tightly, requiring a higher imidazole concentration to elute the protein off the column (Khan *et al*., 2006). This is seen for Bluetongue virus VP7, as an imidazole concentration of up to 500 nm is required to elute it off the column.

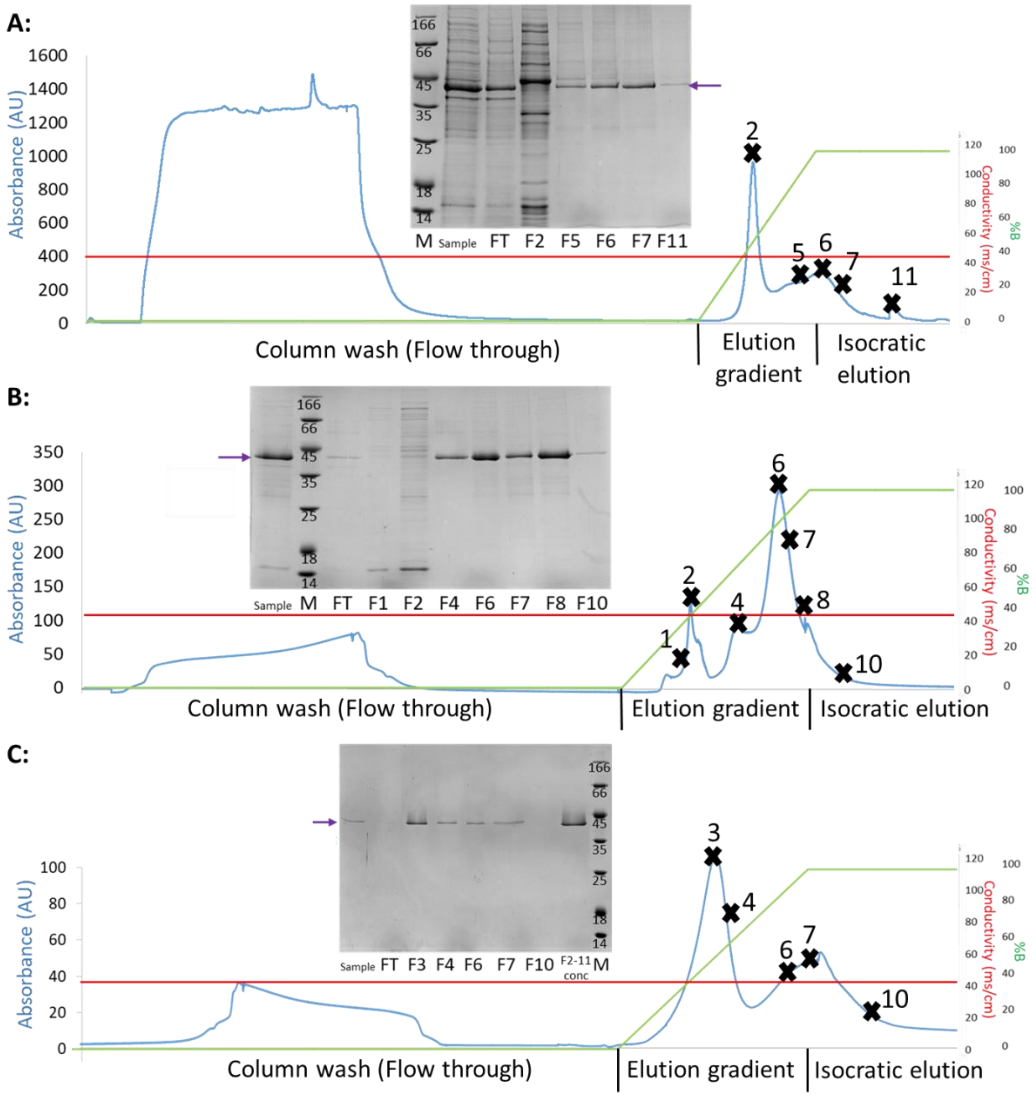

Figure 3.4. Nickel-affinity purification of Bluetongue virus VP7 solubilised from BL21(DE3) cells.

*Nickel-affinity purification for proteins, including Bluetongue virus VP7, solubilised from BL21(DE3) cell inclusion bodies using (**A**)* Macherey-Nagel Protino® Ni-NTA agarose *column (**B**) GE Healthcare Histrap High performance column (**C**) GE Healthcare Histrap High performance column with imidazole in Equilibration buffer D. Each showing chromatogram where the A_{280} effluent (blue), imidazole gradient (green) and conductivity (red) and fractions collected (numbered and marked with '**x**') were recorded. For SDS-PAGE analysis certain fractions were visualised (depicted as "FX", where X is the fraction number) and fractions that were combined and concentrated are labelled "FX-FX conc". The sample loaded is indicated and FT is the flow through. The molecular mass marker (marked as "M") has sizes in kDa, marked on the gel. The position of Bluetongue virus VP7 is marked with purple arrows. Purification performed using and BioRad NGC™ Chromatography system with a computer loaded with ChromLab software (Hercules, USA). Selected data used in this Figure was published in Russell and Gildenhuys (2018).*

It has also been seen that the proteins containing a polyhistidine tag on both the C and N terminal caused multiple elution peaks of the same protein due to slightly different binding contributions from both tags (Khan *et al*., 2006). This double peak elution is seen for Bluetongue virus VP7 in Figure 3.4 and again later in section 3.2.3 Figure 3.8, and is presumably due to Bluetongue virus VP7 containing both a C and N terminal polyhistidine tag. This is advantageous as the requirement of the higher imidazole concentration for Bluetongue virus VP7 elution allows for a level of high purity from purification.

The differences seen in non-specific bacterial protein binding between Macherey-Nagel Protino® Ni-NTA column and GE Healthcare Histrap high performance column were seen for NiCo21(DE3) cells as well (section 3.2.3), despite these cells being genetically modified to decrease non-specific binding of bacterial cells during IMAC purification.

Different structural matrices between the two column types or the different pH conditions required by the two columns could be the cause of the differences seen. Both columns are meant to provide low metal ion leaching and therefore higher protein purity, however, it has been seen that matrices that have a lower specificity often require a lower imidazole concentration to elute the protein of interest than matrices with higher specificity (Bornhorst and Falke, 2000; Block *et al*., 2009). Macherey-Nagel Protino® NI-NTA columns explain that they have NTA matrix, however GE Healthcare Histrap high performance resin does not give details on their structure, but Bluetongue virus VP7 elutes off the Macherey-Nagel Protino® Ni-NTA column at a much lower imidazole concentration (150-250 mM) compared to the GE Healthcare Histrap high performance column (350-500 mM).

That being said, another potentially significant difference between the two columns is the buffer conditions used, and more specifically the pH at which the purification needs to occur. Macherey-Nagel Protino® Ni-NTA column needs a higher pH of 8 compared to GE Healthcare Histrap high performance column requiring a pH of 7.4. As proteins are sensitive to changes in pH and more specifically Rotavirus VP6, the equivalent protein in a related *Reoviridae* virus (Lepault *et al*., 2001), pH differences could alter protein binding. The lower efficacy of the Macherey-Nagel Protino® Ni-NTA column, even with the NiCo21(DE3) cells that have been genetically modified to reduce non-specific binding during IMAC purification, resulted in the GE Healthcare Histrap high performance columns being used for further studies.

For all purifications, Bluetongue virus VP7 bound the column and was eluted within the imidazole gradient. Fractions with high A_{280} absorbance readings were analysed with SDS-PAGE.

Fractions that were found to contain Bluetongue virus VP7 were then combined and concentrated (Figure 3.4). Buffers used during purification contained 500 mM sodium chloride as well as imidazole for certain purifications to help prevent non-specific binding. This did not prevent binding of non-specific bacterial proteins but instead caused them to bind less tightly and thus be eluted first at lower imidazole concentrations (Figure 3.4A, SDS-PAGE lane F2 and Figure 3.4B, SDS-PAGE lane F1 and F2).

Affinity chromatography resulted in polyhistidine tagged Bluetongue virus VP7 being eluted with approximate 95 % purity as estimated using BioRad Image Lab™ software version 6.0.1 (Hercules, USA) "Relative Quantity" tool. The absorbance spectrum of purified Bluetongue virus VP7 was recorded (Figure 3.5) and A_{280} value used to obtain protein concentration using equation 1. Due to the noise present in the absorbance spectrum produced (Figure 3.5), the protein concentration was further confirmed using Bradford assay as described in section 2.8.1.2. The stock concentration was determined to be 13 µM, and therefore approximately 5 mg/250ml cell culture of purified Bluetongue virus VP7 was obtained from BL21(DE3) cells.

3.2 NiCo21(DE3) cells.

Non-specific binding of bacterial cellular proteins occurred for BL21(DE3) cells, both before Bluetongue virus VP7 was eluted and with Bluetongue virus VP7 when no imidazole was added to the Equilibration buffer C and D. It is therefore evident that numerous bacterial cellular proteins bind the nickel histidine affinity resin. NiCo21(DE3) *Escherichia coli* cells were tested as they are derived from modified BL21(DE3) cells to help reduce *Escherichia coli* protein binding during IMAC purification for polyhistidine-tagged proteins. The proteins GlmS, SlyD, Can and ArnA have been modified to either not bind or be easily eluted off during purification, aiding in an improved purity of target proteins isolated using IMAC (Robichon *et al*., 2011).

3.2.1 Expression.

As with BL21(DE3) cells, protein expression in NiCo21(DE3) cells were evaluated using four variables, namely (1) post induction time (Figure 3.6A), (2) cell growth media (Figure 3.6B), (3) post induction temperature (Figure 3.6C) and (4) inducer concentration (Figure 3.6D).

Similar to section 3.1.1 through SDS-PAGE analysis and construction of calibration curves, a size of 41 kDa was obtained for the overexpressed protein, consistent with a size of 38 kDa for Bluetongue virus VP7 protein (Basak *et al*., 1992; Grimes *et al*., 1995) with both a C and N terminal polyhistidine tag and a thrombin cleavage site. This would place the protein in between ovalbumin (45 kDa) and lactate dehydrogenase (35 kDa) in the protein marker.

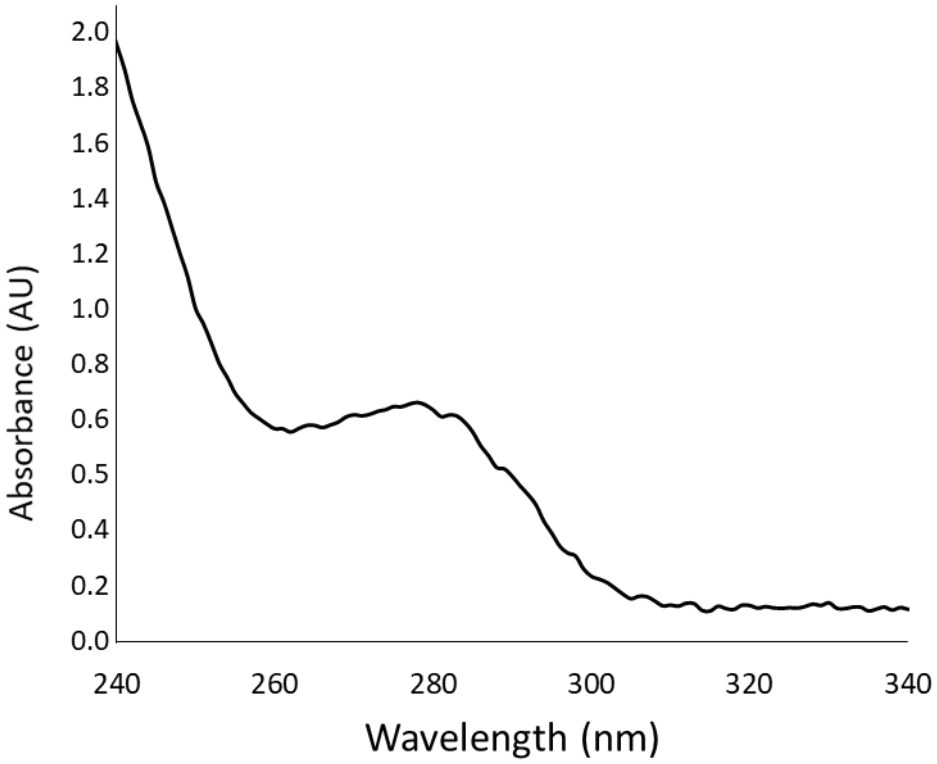

Figure 3.5. Absorbance spectrum of purified Bluetongue virus VP7 from BL21(DE3) cells.

Stock Bluetongue virus VP7 was scanned from 240-340 nm, yielding the above absorbance spectrum. The spectrum was recorded in Primary buffer with 5 M urea using an Applied Photophysics Chirascan Plus (Leatherhead, United Kingdom) at 20 °C.

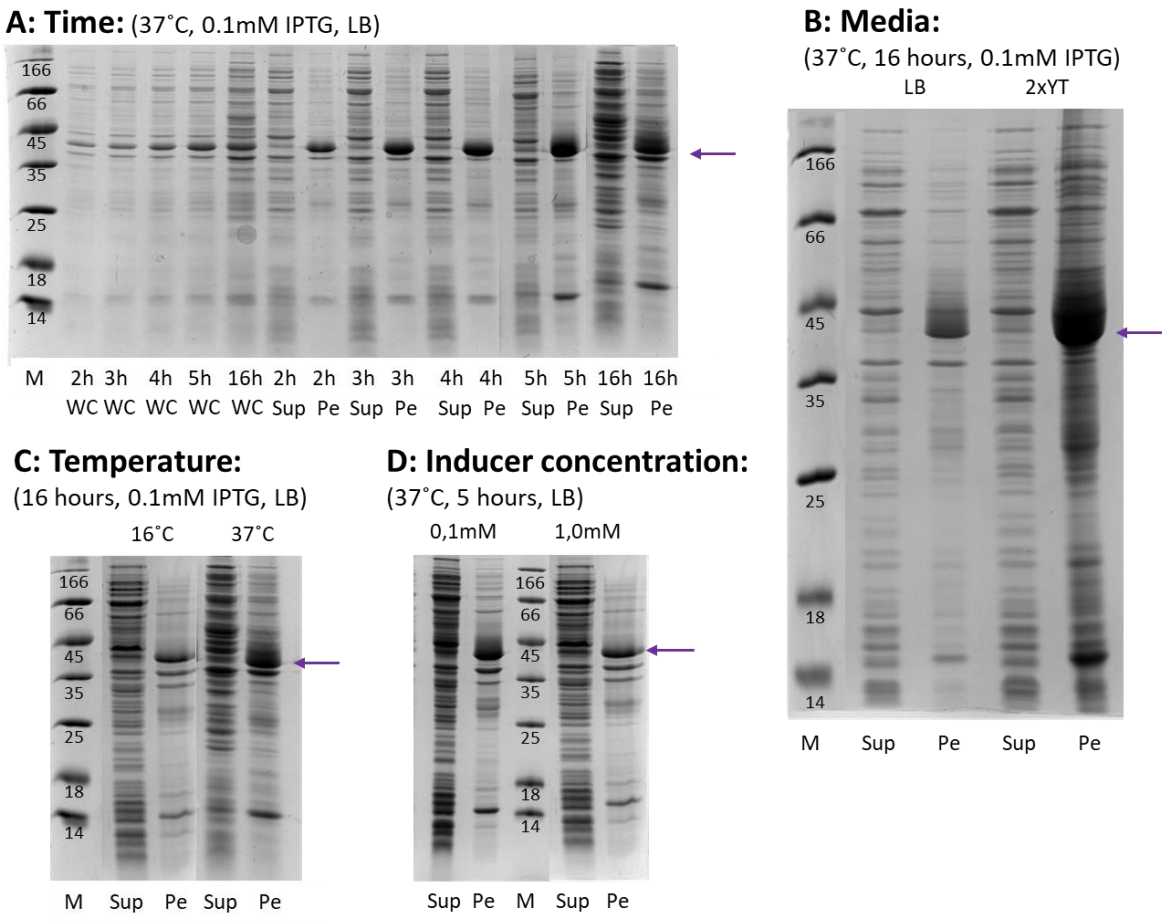

Figure 3.6. Expression of Bluetongue virus VP7 in NiCo21(DE3) cells.

*SDS-PAGE analysis of Bluetongue virus VP7 expression when varying four different expression conditions namely **(A)** post induction time, **(B)** cell growth media, **(C)** post induction temperature and **(D)** inducer concentration. Expression conditions kept constant are indicated above each gel. "WC" is whole cell, "Sup" is supernatant and "Pe" is pellet samples that were obtained and visualised. Bluetongue virus VP7 migrated a distance that corresponds to the size of 41 kDa with the position of Bluetongue virus VP7 marked on the gels with purple arrows. Selected data used in this Figure was published in Russell and Gildenhuys (2018).*

Expression of Bluetongue virus VP7 at different post induction times (Figure 3.6A) revealed a steady increase in expression in whole cell samples over the time period of two to 16 hours post induction. However, as the expression of all bacterial proteins found in the sample also increased over time, at least part of the increase in Bluetongue virus VP7 expression can be attributed to an increase in cell number over an increasing growth period. This increase was again seen in the supernatant and pellet samples taken, however, these revealed that the expression of Bluetongue virus VP7 occurred predominantly in the insoluble (pellet) fraction, with very little increase in soluble expression of Bluetongue virus VP7 over time. As with BL21(DE3) cells (section 3.1.1) there is a large increase between two and three hours, with a small increase between three and four hours, however in NICo21(DE3) cells there is a larger increase between four and five hours and the largest increase in protein expression is seen between five and 16 hours. The large increase between five and 16 hours is predominantly due to the increase in cell density due to the longer growth time as explained in section 3.1.1, again supported by the large increase in expression of bacterial cellular proteins.

When NiCo21(DE3) cells were grown in two cell growth mediums, namely Luria-Bertani (LB) medium and 2xYT medium, (Figure 3.6B), there was a marked increase in protein expression in the cells grown in 2xYT compared to LB, however there is a marked increase in all bacterial protein expression, so again this could be due to an increase in cell numbers, in other words, cell yield, due to the increase in nutrients in the media as 2xYT medium has been known to increase bacterial cell yield (Miller, 1972; Lessard, 2013).

Post induction temperature (Figure 3.6C) resulted in increased Bluetongue virus VP7 expression occurring when cells were grown at 37 ˚C post induction compared to 16 ˚C post induction, with predominant expression occurring in the insoluble fraction (pellet). Lowering post induction temperature, therefore, did not increase soluble (supernatant) expression in NiCo21(DE3) cells. Two inducer concentrations were tested (Figure 3.6D), namely 0.1 mM and 1.0 mM IPTG with little difference between the expression of Bluetongue virus VP7 at the lower and higher IPTG concentration. At both inducer concentrations, the expression of Bluetongue virus VP7 occurred predominantly in the insoluble fraction (pellet).

As with BL21(DE3) cells, five hour post-induction growth, at 37 ˚C with 0.1 mM IPTG in LB medium were the chosen conditions for protein expression in NiCo21(DE3) cells. This was to help prevent the stress placed on bacterial cells that are grown for long periods of time, but still allowing for adequate time for the expression of Bluetongue virus VP7 in a higher proportion to other cellular proteins (Bentley and Kompala, 1990).

Although expression in 2xYT created a much larger yield than LB media, studies have reported that inclusion body formation under more stressed conditions such as higher temperatures, higher inducer concentration and longer times can result in poorer quality protein within the inclusion bodies (Bentley *et al*., 1990; Sanchez de Groot and Ventura, 2006; Jürgen *et al*., 2010). The increased cell yield could potentially cause cell stress and result in a different quality of protein from BL21(DE3) cells grown in LB, therefore LB was chosen for further studies for a more direct comparison between the cell lines.

3.2.2 Solubilisation.

As with BL21(DE3) cells, the lack of soluble expression of Bluetongue virus VP7 resulted in the need to solubilize the protein found in the bacterial cell pellet. As seen in Figure 3.7A SDS-PAGE was used to depict several wash steps that were undertaken as mentioned in section 3.1.2, the 'washing' process used the detergent Triton X-100 and urea to remove cellular debris, including bacterial cell walls, bacterial membrane components, proteins and residual soluble proteins that accumulate in the insoluble fraction (pellet) after sonication and centrifugation (Palmer and Wingfield, 2004) and thus isolates the inclusion bodies.

Triton X-100 causes disruption in SDS-PAGE and thus is the cause of the smudging and apparent lower concentrations seen for samples that contain it (Figure 3.7B). Bluetongue virus VP7 was solubilised from bacterial inclusion bodies using urea and a freeze-thaw step modified from the protocol presented by Qi *et al.* (2015). The Wash buffer B's wash step was repeated so that all of the Triton X-100 was removed before solubilisation. As seen in Figure 3.7B, less than half of the pellet is solubilized with urea concentrations of 3 M and below, with a large increase between 3 M and 4 M. There is a slight increase seen between 4 M and 5 M urea, and then a decrease in the amount of Bluetongue virus VP7 found in the solubilized supernatant for 6 M, 7 M and 8 M. This could be due to the inclusion body pellet precipitating in the higher urea concentrations and therefore not allowing solubilisation to occur. The urea concentration for solubilisation of at least 95 % of the inclusion body proteins, including Bluetongue virus VP7, was 5 M Urea for NiCo21(DE3) cells, and this was used for all further work (Figure 3.7B).

3.2.3 Purification.

Protein solubilized from the NiCo21(DE3) cell inclusion bodies were loaded onto a pre-equilibrated metal affinity column. As with BL21(DE3) cells, two different nickel cross-linked agarose resins were tested, namely Macherey-Nagel Protino® Ni-NTA agarose and GE Healthcare Histrap high performance.

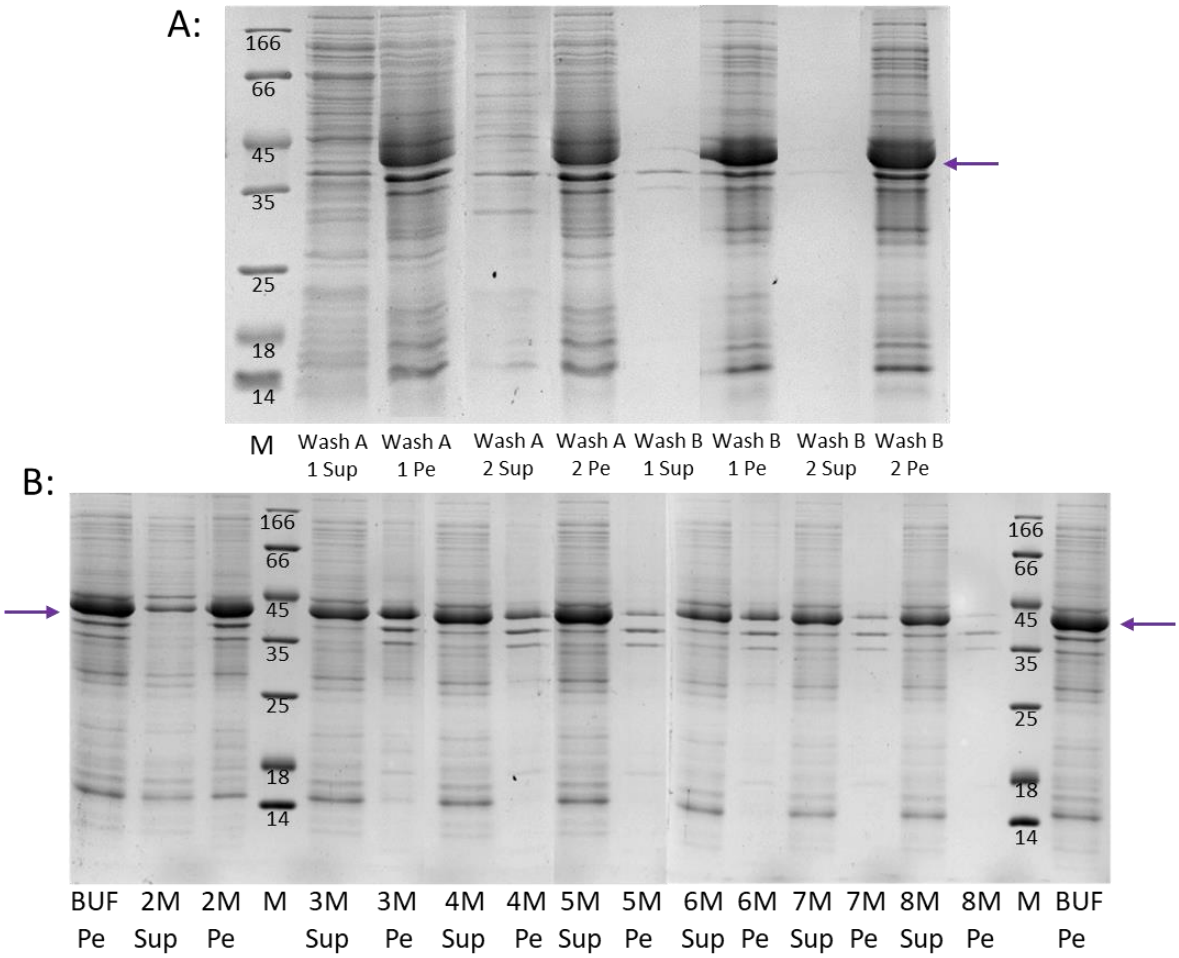

Figure 3.7. Solubilisation of NiCo21(DE3) inclusion bodies.

*SDS-PAGE analysis of results obtained from the protocol for solubilizing NiCo21(DE3) inclusion bodies. (**A**) Supernatant and pellet fractions of numbered wash steps, Wash A is with Wash buffer A (containing Triton X-100) and Wash B is with Wash buffer B (buffer components in List of Buffers on page xiv). (**B**) Shows supernatant and pellet samples after centrifugation of the defrosted inclusion bodies in different urea concentrations, depicted as 'x'M, where 'x' is the urea concentration that the sample was frozen in. "Sup" is the supernatant, "Pe" is the resuspended pellet. BUF is the samples before being frozen in urea. Molecular mass marker (marked as "M") has sizes in kDa, marked on the gel. The position of Bluetongue virus VP7 is marked with purple arrows. Selected data used in this Figure was published in Russell and Gildenhuys (2018).*

Firstly, the Macherey-Nagel Protino® Ni-NTA column was tested (Figure 3.8A) which resulted in solubilized Bluetongue virus VP7 binding the column under the chosen conditions, however, other bacterial proteins bound under the same conditions, and were eluted along with Bluetongue virus VP7 from approximately 150 mM imidazole (Figure 3.8A, SDS-PAGE lane F5), but was predominantly eluted at 250 mM imidazole (Figure 3.8A, SDS-PAGE lane F8). The chromatogram (Figure 3.8A) shows a broad elution peak containing Bluetongue virus VP7 (fractions 5 to 13), with at least three separate peaks within it (fraction 5, 8 and 9). Some Bluetongue virus VP7 was also seen to not bind the column, and instead came through in the buffer wash before elution (Figure 3.8A, SDS-PAGE lane FT1), this could potentially be due to Macherey-Nagel Protino® Ni-NTA reaching its capacity, due to the large quantity of non-specific bacterial protein binding seen.

In comparison to the purification of solubilized proteins from BL21(DE3) cells on the Macherey-Nagel Protino® Ni-NTA agarose, there appears to be less bacterial cell proteins bound and eluted with Bluetongue virus VP7, seen with the chromatogram and SDS-PAGE analysis of fractions (Figure 3.4A and 3.8A). More significantly there is a large decrease in the number of bacterial proteins that bound and were eluted with a lower imidazole concentration of approximately 100 mM.

In fact, approximately a third of the amount of protein bound and was eluted at 100 mM imidazole from NiCo21(DE3) cells, compared to BL21(DE3) cells, as seen through absorbance readings in Figure 3.4A and 3.8A as well as corresponding SDS-PAGE analysis of the appropriate fractions. This is consistent with NiCo21(DE3) cells being genetically modified to decrease non-specific binding of bacterial proteins during purification.

Secondly, the GE Healthcare Histrap high performance resin Bluetongue virus VP7 binding and elution was tested without imidazole in the Equilibration buffer D and sample (Figure 3.8B). Bluetongue virus VP7 bound the column and was eluted from an imidazole concentration of approximately 300-500 mM. This result is comparable to the solubilised protein from BL21(DE3) cells that were purified using the GE Healthcare Histrap high performance with 50 mM imidazole in the Equilibration buffer D and sample. This is consistent with the fact that NiCo21(DE3) cells have been genetically modified to contain less bacterial proteins that are capable of binding to an IMAC column.

That being said, the chromatogram in Figure 3.8B shows a higher degree of similarity to Figure 3.4B of BL21(DE3) cells on the GE Healthcare Histrap high performance column without imidazole in the Equilibration buffer D. However, the absorbance reading of the first peak which occurs at an imidazole concentration of approximately 180 mM is less for BL21(DE3) cells compared to NiCo21(DE3) cells.

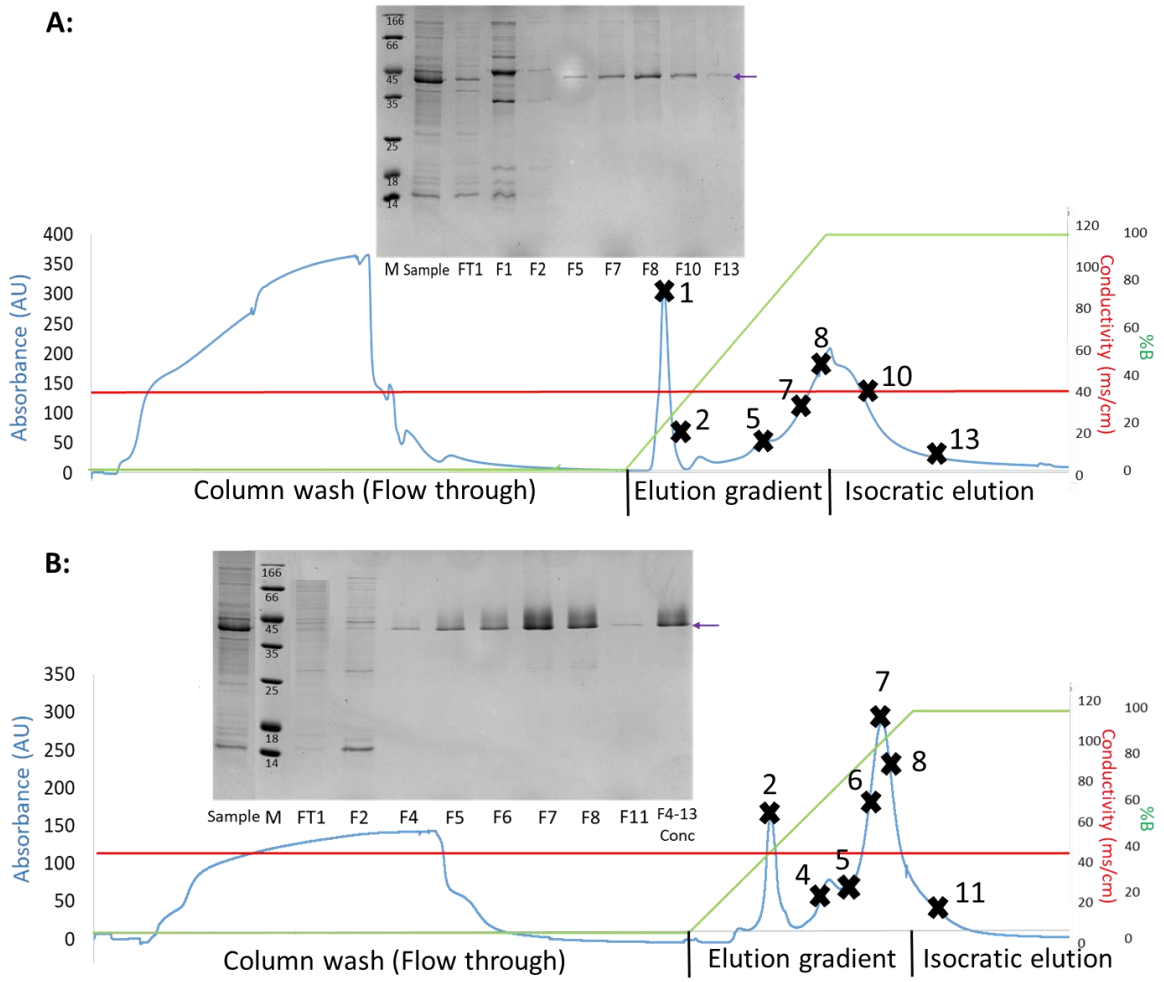

Figure 3.8. Nickel-affinity purification of Bluetongue virus VP7 from NiCo21(DE3) cells.

*Nickel-affinity purification of protein solubilised from NiCo21(DE3) cell inclusion bodies using (**A**) Macherey-Nagel Protino® Ni-NTA agarose column and (**B**) GE healthcare Histrap high performance column. Each showing chromatogram where the A_{280} effluent (blue), imidazole gradient (green) and conductivity (red) and fractions collected (numbered and marked with an '**x**') were recorded. For SDS-PAGE analysis certain fractions were visualised (depicted as "FX", where X is the fraction number). Fractions that contained Bluetongue virus VP7 were combined and concentrated and are labelled "FX-FX conc". The sample loaded is labelled and FT is the flow through of protein that did not bind the column. The molecular mass marker (marked as "M") has sizes in kDa, marked on the gel. The position of Bluetongue virus VP7 is marked with purple arrows. Purification performed using and BioRad NGC™ Chromatography system with ChromLab software (Hercules, USA). Selected data used in this Figure was published in Russell and Gildenhuys (2018).*

Whereas the absorbance reading of the second peak containing the majority of Bluetongue virus VP7 is less for NiCo21(DE3) cells which is consistent with the decrease it non-specific bacterial cell proteins being eluted along with Bluetongue virus VP7, suggesting that instead of preventing binding of non-specific bacterial cell protein completely, the proteins bound less tightly for NiCo21(DE3) cells than for BL21(DE3) cells and were thus eluted at a lower imidazole concentration, thus explaining the higher absorbance seen for NiCo21(DE3) in the first peak. This can also be seen in the difference between Figure 3.4B SDS-PAGE lane F2 and Figure 3.8 B SDS-PAGE lane F2, that shows darker bands in Figure 3.8 B SDS-PAGE lane F2 for NiCo21(DE3) cells over BL21(DE3) cells that correspond to the sized proteins that have bound along with Bluetongue virus VP7 seen in lanes F4 to F8 in Figure 3.4B.

Less Bluetongue virus VP7 was seen to come through in the buffer wash before elution (flow through) for the GE Healthcare Histrap high performance column compared to the Macherey-Nagel Protino® Ni-NTA column (Figure 3.8A and B, SDS-PAGE lane FT1), this is consistent with the fact that the columns are meeting their binding capacity, as the Macherey-Nagel Protino® Ni-NTA column has a much greater amount of non-specific binding.

This is also seen for BL21(DE3) cells on the two columns (Figure 3.4A and B, SDS-PAGE lane FT1). As with BL21(DE3) cells, there was a drastic decrease in non-specific binding of bacterial cell proteins on the GE Healthcare Histrap high performance column compared to the Macherey-Nagel Protino® Ni-NTA column and therefore the GE Healthcare Histrap high performance columns were used for further studies.

For all purifications, Bluetongue virus VP7 bound the column and was eluted within the imidazole gradient. Fractions with high A_{280} absorbance readings were analysed with SDS-PAGE and fractions that were found to contain Bluetongue virus VP7 were then combined and concentrated (Figure 3.8). Buffers used during purification contained 500 mM sodium chloride to help prevent non-specific binding. This did not prevent binding but caused the other bacterial cellular proteins to bind less tightly and be eluted first at lower imidazole concentrations. Affinity chromatography resulted in polyhistidine tagged Bluetongue virus VP7 being eluted with approximate 95 % purity as estimated using BioRad Image Lab™ software version 6.0.1 (Hercules, USA) Relative Quantity tool. The absorbance spectrum of the purified Bluetongue virus VP7 was recorded (Figure 3.9) and A_{280} values were used to obtain protein concentration using equation 1.

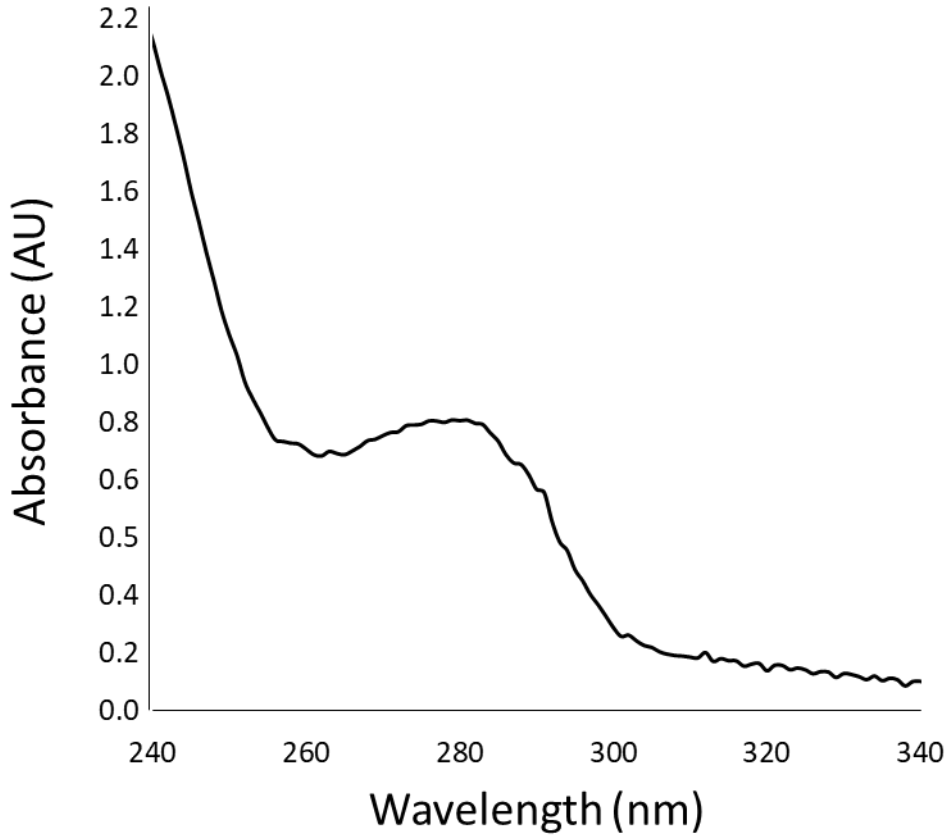

Figure 3.9. Absorbance spectrum of purified Bluetongue virus VP7 from NiCo21(DE3) cells.

Stock Bluetongue virus VP7 was scanned from 240-340 nm, yielding the above absorbance spectrum. The spectrum was recorded in Primary buffer with 5 M urea, using an Applied Photophysics Chirascan Plus (Leatherhead, United Kingdom) at 20 °C.

Due to the noise present in the absorbance spectrum produced (Figure 3.9) the protein concentration was further confirmed using Bradford assay as described in section 2.8.1.2. The concentration was determined to be 16 µM, and therefore approximately 12 mg/250ml cell culture of purified Bluetongue virus VP7 was obtained from NiCo21(DE3) cells.

3.3 C43(DE3) pLysS cells.

OverExpress™ C43(DE3) pLysS cells were tested, as they are known to be a strain of *Escherichia coli* created by Lucigen, that are efficient at tolerating toxic and membrane proteins from a number of different organisms (Miraux and Walker, 1996). Toxic in this sense is any protein that causes damage to the cell after expression, which may or may not lead to cell death or a decrease in cell growth. C43(DE3) pLysS cells contain genetic mutations that allow a tolerance of and higher expression of said proteins. The C43(DE3) pLysS cells carry a chromosomal copy of the T7 RNA polymerase gene (Duman-Seignovert *et al*., 2004). pLysS is a plasmid that contains the T7 lysozyme gene (LysS) which is able to interact with T7 RNA polymerase causing the inhibition of protein expression until cells are induced by the addition of IPTG. This, combined with delayed expression of LacY and T7 RNA polymerase, results in slower induction rates and expression (Wanger *et al*., 2008), which can result in a greater production of soluble protein (Weickert *et al*., 1996). Therefore, C43(DE3) pLysS cells were tested because even though Bluetongue virus VP7 is not known to be toxic, the slower expression could have potentially resulted in a higher level of soluble expression.

3.3.1 Expression.

Protein expression in C43(DE3) pLysS cells were evaluated using three variables, namely (1) post induction time (Figure 3.10A), (2) post induction temperature (Figure 3.10B) and (3) inducer concentration (Figure 3.10C).

When post induction expression in C43(DE3) pLysS cells were tested over a time of two to 16 hours (Figure 3.10A) SDS-PAGE analysis showed an increase in protein expression corresponding to an increase in cell density with increased growth time. Very little expression of Bluetongue virus VP7 was seen in both the soluble (supernatant) and insoluble (pellet) fractions. The lack of expression of Bluetongue virus VP7 was again seen between cells grown at 25 ˚C and 37 ˚C (Figure 3.10B) and with different inducer concentrations of 0.1 mM and 1.0 mM IPTG (Figure 3.10C). The main overexpressed protein band produced by the C43(DE3) pLysS cells, migrated a distance inconsistent with that of Bluetongue virus VP7's molecular mass of 41 kDa (Figure 3.10D). This was further seen when samples from C43(DE3) pLysS, BL21(DE3) and NiCo21(DE3) cells were run on SDS-PAGE (Figure 3.10E) which demonstrated that the overexpressed band migrated a distance relating to a smaller molecular mass in C43(DE3) pLysS cells than in the other two cell lines.

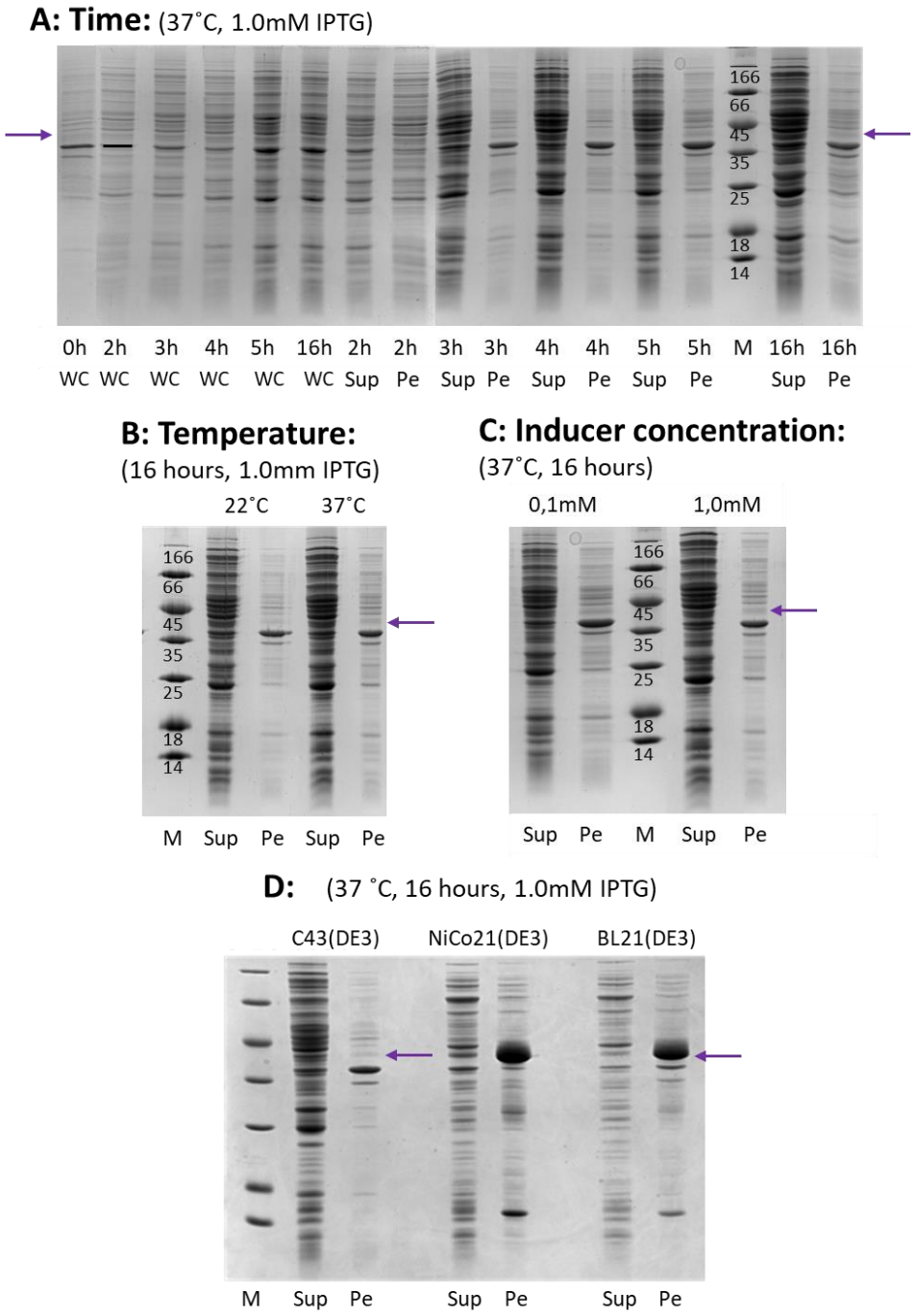

Figure 3.10. Bluetongue virus VP7 expression in C43(DE3) pLysS cells.

*SDS-PAGE of C43(DE3) pLysS cells expression studies depicting whole cell, supernatant and pellet samples under varying conditions namely **(A)** change in post-induction time, **(B)** change in post-induction temperature and **(C)** change in inducer concentration. Expression conditions kept constant are indicated above each gel. "WC" is the whole cell, "Sup" is supernatant and "Pe" is pellet samples that were obtained and visualised. (**D**) SDS-PAGE showing differences in size of overexpressed proteins found in different cells lines containing the pET28a plasmid with Bluetongue virus VP7 insert. The positioning of expressed Bluetongue virus VP7 marked with purple arrows.*

Therefore, we can conclude that very little expression of Bluetongue virus VP7 was seen in either the soluble (supernatant) or insoluble (pellet) fractions under all conditions tested (see Figure 3.10). C43(DE3) pLysS were therefore not used for further studies.

3.4 KRX cells.

Single-Step (KRX) Competent Cells were tested as they are said to provide a tightly controlled expression of proteins using a T7 promoter as they contain a chromosomal copy of the T7 RNA polymerase controlled by a rhamnose promoter ($rhaP_{BAD}$) (Hartnett *et al*., 2006). When rhamnose is added it causes T7 RNA polymerase expression, which then results in the transcription of the gene of interest under control of the T7 promoter. The $rhaP_{BAD}$ promoter is known to ensure less pre-induction basil protein expression than the lac UVS promoter. Lower levels of pre-induction protein expression has been linked to higher levels of soluble protein expression (Hartnett *et al*., 2006; Wegerer *et al*., 2008).

3.4.1 Expression.

KRX cell's protein expression was evaluated using three variables, namely (1) post induction time (Figure 3.11A), (2) post induction temperature (Figure 3.11B) and (3) inducer concentration (Figure 3.11C).

Similarly to section 3.1.1 through SDS-PAGE analysis and construction of calibration curves a size 41 kDa was obtained for the overexpressed protein, consistent with a size of 38 kDa for Bluetongue virus VP7 protein (Basak *et al*., 1992; Grimes *et al*., 1995) with both a C and N terminal polyhistidine tag and a thrombin cleavage site. This would place the protein in between ovalbumin (45 kDa) and lactate dehydrogenase (35 kDa) in the protein marker.

When KRX cells were evaluated over a post-induction time period between two and 16 hours (Figure 3.11A), an increase in protein expression was seen over time with a steady increase between two and three, three and four and four and five hours, but very little increase between five and 16 hours, however as with BL21(DE3) and NiCo21(DE3) expression of Bluetongue virus VP7 occurs largely in the insoluble fraction (pellet) and the increase seen over time results in more protein in the insoluble fraction (pellet) only.

KRX cells were grown, after induction, at three temperatures, namely 16 ˚C, 22 ˚C and 37 ˚C (Figure 3.11B). There was a marked increase in expression of Bluetongue virus VP7 with an increase in temperature. This is seen as there is a large increase in expression between 16 ˚C and 22˚C and a slightly smaller but still significant increase between 22 ˚C and 37 ˚C. At all three temperatures, Bluetongue virus VP7 expression occurred mainly in the insoluble fraction (pellet).

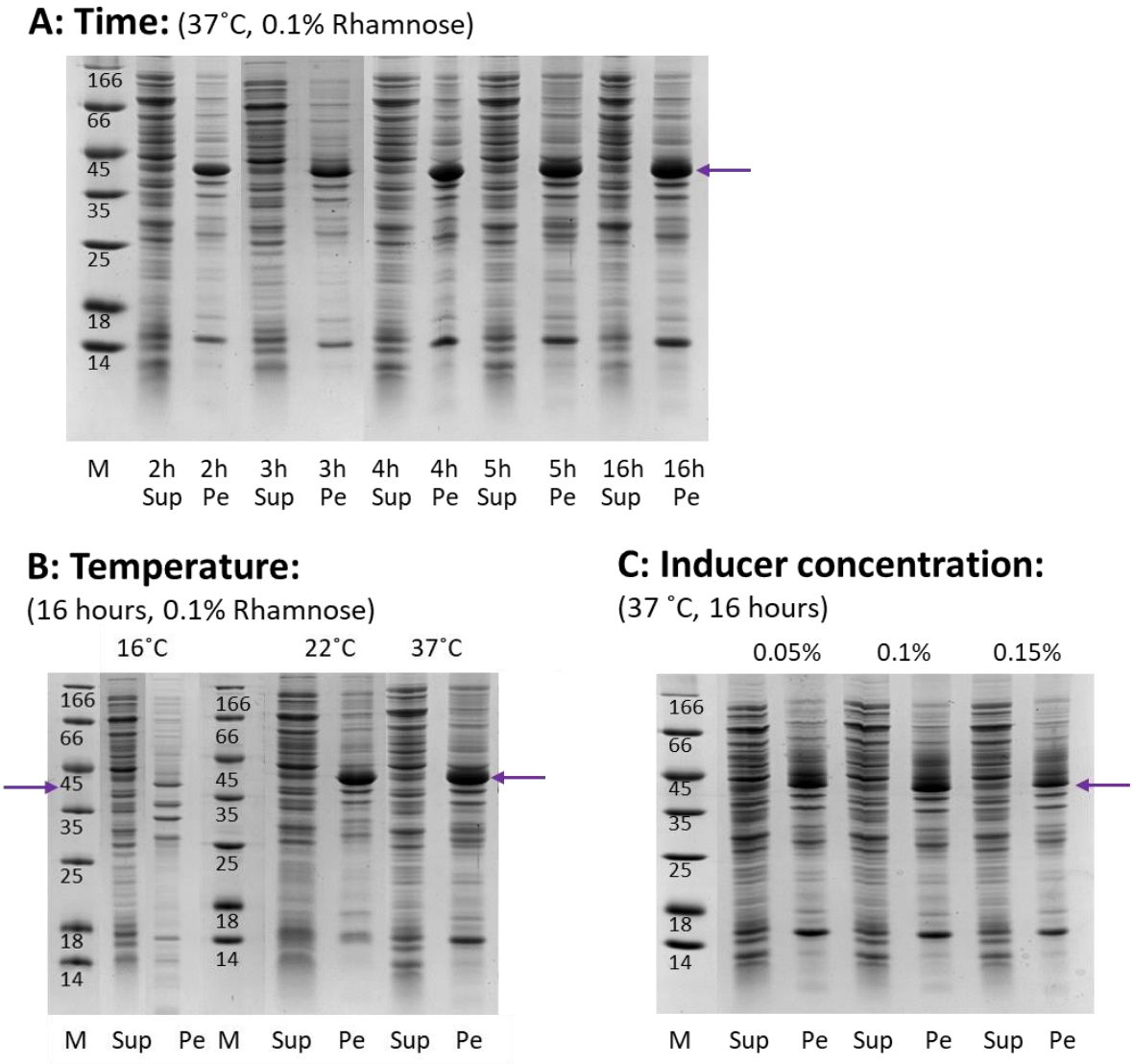

Figure 3.11. Bluetongue virus VP7 expression in KRX cells.

SDS-PAGE of KRX cells expression studies depicting supernatant (Sup) and pellet (Pe) samples for ***(A)*** *change in post-induction time,* ***(B)*** *change in post-induction temperature and* ***(C)*** *change in inducer concentration. Expression conditions kept constant are indicated above each gel. The supernatant (Sup) and pellet (Pe) samples were obtained and visualised. The position of Bluetongue virus VP7 is indicated by purple arrows.*

Lastly, KRX cells were induced with three inducer concentrations, namely 0.05 %, 0.1 % and 0.15 % rhamnose, whilst keeping IPTG concentration constant at 0.1 mM (Figure 3.11C). Bluetongue virus VP7 expression was not seen to increase with an increase in inducer concentration with 0.05 % and 0.1 % concentrations producing similar levels of expression and an apparent decrease in expression at the highest concentration of 0.15 %. For 0.05 %, 0.1 % and 0.15 % rhamnose Bluetongue virus VP7 expression occurred mainly in the insoluble fraction (pellet).

BL21(DE3), NiCo21(DE3) and KRX cells appeared to express similar amounts of insoluble Bluetongue virus VP7 at 37 ˚C, however, both BL21(DE3) cells and NiCo21(DE3) cells expressed less bacterial cell proteins in the insoluble fraction (pellet). The lower concentration of bacterial protein expression in the insoluble fraction with Bluetongue virus VP7 along with the fact that NiCo21(DE3) cells are specifically engineered to help improve purity obtained from IMAC purification, resulted in BL21(DE3) and NiCo21(DE3) cells being used for further studies.

3.5 Buffer exchange of solubilized protein for further studies.

Concentrated fractions of purified protein from BL21(DE3) cells (section 3.1.3) and NiCo21(DE3) cells (section 3.2.3) were in Equilibration buffer D and approximately 400 mM imidazole after purification. In order to study purified Bluetongue virus VP7, changes in buffer conditions were required.

Using dialysis allows for the protein's environment to gradually change from one set of conditions to another. When Bluetongue virus VP7 was dialysed into Primary buffer with 20 mM sodium chloride, visible precipitation was seen. When purified Bluetongue virus VP7 was dialysed into Primary buffer with 20 % glycerol a small amount of visible precipitation occurred, but disappeared with further incubation time. When purified Bluetongue virus VP7 was dialysed into Primary buffer with 5 M ultra-pure urea, no visible precipitation occurred. All three conditions were further tested.

3.6 Protein characterization.

3.6.1 Clear native PAGE.

Clear native PAGE protein samples are placed in a buffer that does not contain any reducing or denaturing agents resulting in the protein maintaining its secondary, tertiary and quaternary structure. Therefore, the protein moves based on its structural conformation as well as its size through the gel (Walker, 1994; Arndt *et al*., 2012). In addition, individual denaturing conditions can, therefore, be evaluated, such as boiling and the addition of denaturants.

The clear native PAGE results confirm that purified Bluetongue virus VP7 protein occurs in at least three forms (lane 1, 7 and 9) however when in the presence of 5 M urea, Bluetongue virus VP7 is primarily in a single form (lane 3) (Figure 3.12). Samples in 5 M urea that have been boiled (lane 2) and had 2 % SDS added (lane 8) are predominantly in a single form as well. Samples in 8 M urea (lane 4) have a similar single form as samples in 5 M urea. Samples in 2 M urea (lane 9) appear to have at least three forms, suggestive that 2 M urea is not sufficient to prevent the formation of oligomers or aggregates. The three forms seen on the gel are potentially monomer, trimer and oligomer, with potentially larger aggregates seen in the loading well, having not entered the gel. These potentially larger oligomers are notably greater in samples without urea. However, this may just be well staining. Monomer, trimer and oligomer are predicted based on studies by Rutkowskaa *et al*. (2011); Monastyrskaya et al. (1997) and Limn *et al*. (2000) that found that African horse sickness virus VP7 and Bluetongue virus VP7 still displayed trimer on an SDS-PAGE and the ability of Rotavirus VP6, a structurally related protein to Bluetongue Virus VP7, to form larger macromolecules under certain conditions (Lepault *et al*., 2001).

Bluetongue virus VP7 that was boiled and had 2 % SDS added, still showed at least three forms (lane7). In 5 % sodium dodecyl sulfate (SDS) there appears to be predominately only two forms of Bluetongue virus VP7 (lane 6) with the smaller form having a much greater concentration. In 8 % SDS there appears to predominantly be only a single form (lane 5). Bluetongue virus VP7 in the presence of 20 % glycerol were not analysed using clear native PAGE as the glycerol interfered with the protein's movement in the gel (data not shown).

3.6.2 Secondary structural characterization.

Far-UV circular dichroism was used as a probe to study the secondary structure of purified Bluetongue virus VP7 in a number of different buffer conditions. For purified Bluetongue virus VP7 dialysed into Primary buffer and 5 M urea or 20 % glycerol, the presence of urea and glycerol in the buffers used meant that the CD spectra were recorded to approximately 210 nm, as the noise to signal ratio was too high below this wavelength, as detected by the dynode voltage. Resulting in the spectra being recorded from 210 and 250 nm.

Bluetongue virus VP7's published structure contains alpha-helices and beta-strands (Grimes *et al*., 1995). The spectrum was anticipated to contain troughs at approximately 218 nm and a peak at approximately 196 nm for the beta-strands, and troughs at approximately 222 nm and 208 nm and a peak at approximately 190 nm for alpha-helices if the protein still had secondary structure. A positive at 212 nm and trough at 195 nm would be seen if 5 M urea had resulted in Bluetongue virus VP7 becoming a random coil (Ranjbar and Gill, 2009).

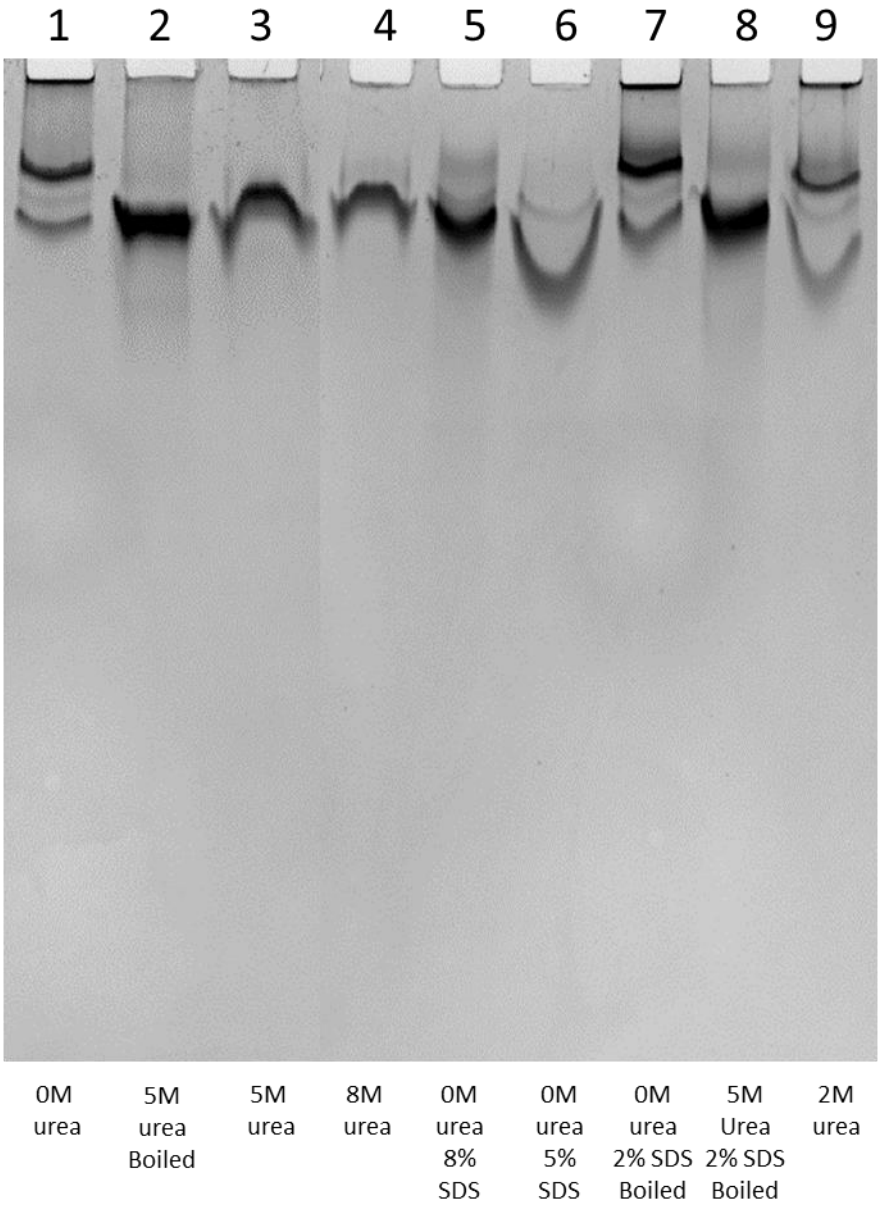

Figure 3.12. Clear native PAGE of purified Bluetongue virus VP7.

Shows clear native PAGE of purified Bluetongue virus VP7 in a BioRad native PAGE sample buffer with specific sample conditions marked on the gel below the respective lane. Selected data used in this Figure was published in Russell and Gildenhuys (2018).

The spectrum produced for Bluetongue virus VP7 in 5 M urea contained negative readings at both 218 nm and 222 nm, with a slight positive movement towards 210nm (Figure 3.13), which is suggestive of a protein that contains both alpha-helices and beta-strands (Ranjbar and Gill, 2009).

Using the data collected from the spectrum for Bluetongue virus VP7 in Primary buffer with 5 M urea, the K2D3 tool of Dichroweb (Louis-Jeune *et al*., 2011) was used to estimate the percentage alpha-helices and beta-strands for Bluetongue virus VP7. The predicted values can be seen in Table 3.1 as well as the percentages of alpha-helices and beta-strands for Bluetongue virus VP7 obtained from a secondary structure server, namely 2Struc (Klose *et al*., 2010), for the PDB file 1BVP generated from crystallography studies by Grimes *et al.* (1995). A similar percentage is seen for both alpha-helices and beta-strands for the predicted values from the spectrum and those predicted from structure produced by Grimes *et al.* (1995), indicative of correctly folded secondary structure in 5 M urea and even in 8 M urea.

When 1.7 µM Bluetongue virus VP7 in Primary buffer with 20 % glycerol was evaluated using far-UV CD, the spectrum collected (Figure 3.13) again showed negative readings at both 218 nm and 222 nm and when studied using K2D3 tool from Dichroweb (Louis-Jeune *et al*., 2011) it was estimated to contain a slightly higher alpha-helical content than Bluetongue virus VP7 in 5 M urea (Table 3.1). However, the increase is within a reasonable percentage for slight structural change.

Far-UV CD spectrum for 1.9 µM Bluetongue virus VP7 in Primary buffer with 6 M guanidinium chloride shows a characteristic spectrum of an unfolded protein with more positive ellipticity leading up to 212 nm, suggesting that secondary structure is unfolded in 6 M guanidinium chloride.

3.6.3 Tertiary structural characterization.

The dominant intrinsic fluorophore is tryptophan, which is extremely sensitive to its environment (Eftink, 1994). The consensus sequence of Bluetongue virus VP7 used contains five tryptophan residues (Trp119, Trp141, Trp188, Trp225 and Trp278) as seen in Figure 2.1 (Grimes *et al*., 1995; Gasteiger *et al*., 2005; Russell *et al*., 2018). The fluorescence spectra obtained for 1.7 µM Bluetongue virus VP7 in Primary buffer with 5 M urea established a single peak (λ_{max}) at 341 nm, indicative that Bluetongue virus VP7 retains a folded tertiary structure (Figure 3.14) as the λ_{max} is in line with the spectra produced by tryptophan in a hydrophobic environment. This peak at 341 nm occurred for purified Bluetongue virus VP7 in Primary buffer with 20 mM sodium chloride without the presence of urea. The scattering of the excitation wavelength can signify the existence of protein precipitation in a protein sample (Lakowicz, 1999). The spectrum for 1.7 µM purified Bluetongue virus VP7 in Primary buffer with 20 mM sodium chloride without the presence of urea, showed significant scattered light at and around 295 nm (Figure 3.14).

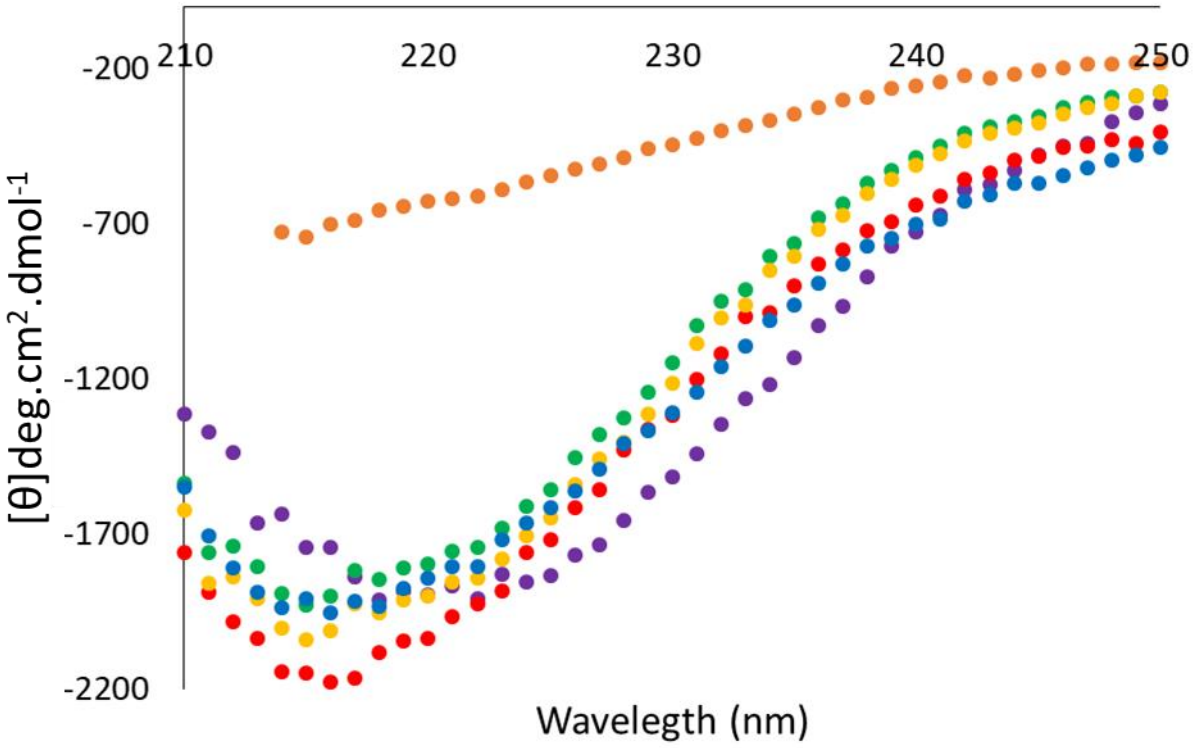

Figure 3.13. Circular dichroism spectra of Bluetongue virus VP7.

Circular dichroism spectra of Bluetongue virus VP7 obtained between 250 and 210 nm for 1.7 µM Bluetongue virus VP7 in Primary buffer with 20 mM sodium chloride (●); 2 M urea (●); 5 M urea (●); 8 M urea (●); 20 % glycerol (●) and 1.9 µM Bluetongue virus VP7 in Primary buffer with 6 M guanidinium chloride (●). Selected data used in this Figure was published in Russell and Gildenhuys (2018).

Table 3.1: Prediction of alpha-helical and beta-strand protein content for Bluetongue virus VP7.

2Struc secondary structure server (Klose et al., 2010) predicated alpha-helical and beta-strand content of Bluetongue virus VP7 monomer and trimer from PDB file 1BVP from Grimes et al. (1995) and K2D2 Dichroweb (Louis-Jeune et al., 2011) predicted alpha-helical and beta-strand values using far-UV CD spectra (Figure 3.13) of Bluetongue virus VP7 in Primary buffer with 0 M, 2 M, 5 M and 8 M urea as well as 20 % glycerol.

Software	Sample	% alpha-helices	% beta strands
2Struc	1BVP Monomer	36.38	17.19
	1BVP Trimer	36.38	18.62
K2D2	0M urea	36.10	18.92
	2M urea	35.90	18.11
	5M urea	36.42	17.70
	8M urea	36.22	17.20
	20% glycerol	38.19	16.21

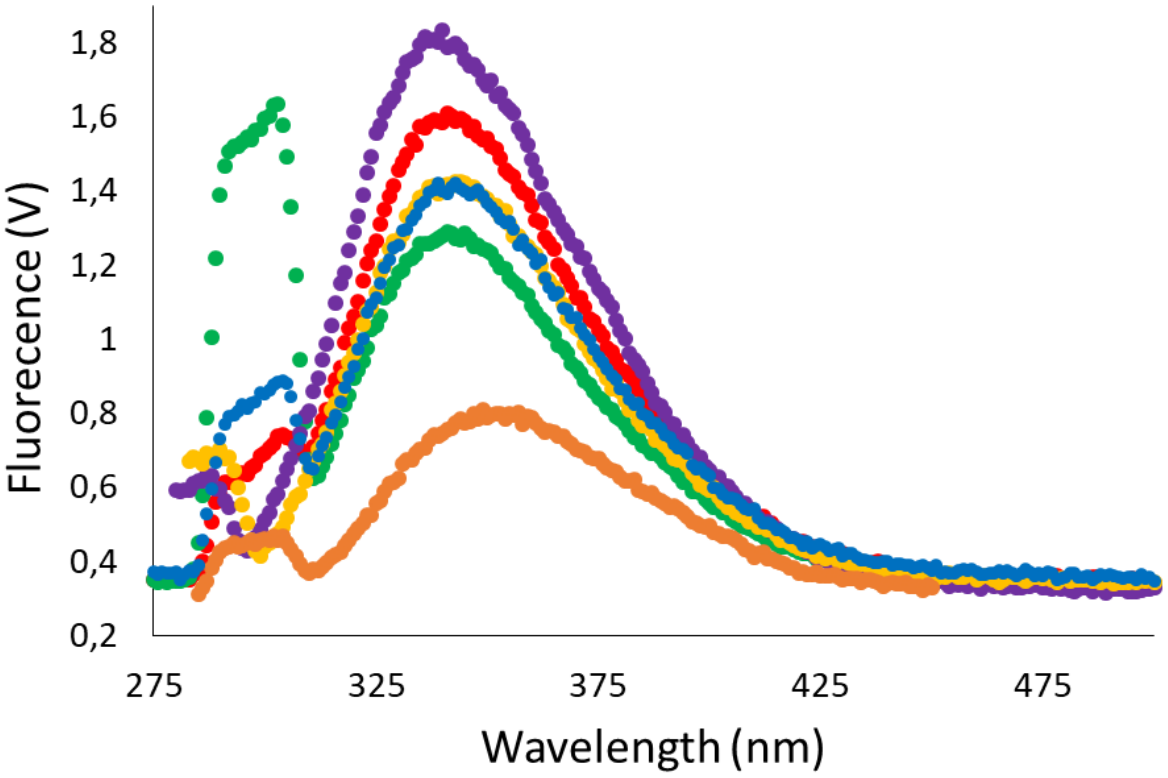

Figure 3.14. Fluorescence emission spectra of Bluetongue virus VP7.

Fluorescence emission spectra obtained between 500 nm and 280 nm for 1.7 µM Bluetongue virus VP7 in Primary buffer with 20 mM sodium chloride (●); 2 M urea (●); 5 M urea (●); (8 M urea (●); 20 % glycerol (●) and 1.9 µM Bluetongue virus VP7 in Primary buffer with 6 M guanidinium chloride (●). Selected data used in this Figure was published in Russell and Gildenhuys (2018).

Therefore, it can be deduced that the exclusion of 5 M urea results in Bluetongue virus VP7 forming protein aggregates (Figure 3.14).

This is in agreement with the clear native PAGE results, where more protein forms and a greater amount of large oligomers were present when urea was absent from the samples (Figure 3.1, lane 1). The 1.7 µM purified Bluetongue virus VP7 in Primary buffer with 20 % glycerol produced a single peak at 339 nm, and a slight increase in fluorescence intensity showing a similar folded tertiary structure as that found in Bluetongue virus VP7 in Primary buffer with 5 M urea (Figure 3.14). This is in agreement with findings that glycerol results in a slightly more compact protein structure (Gekko and Timasheff, 1981a). Bluetongue virus VP7 in Primary buffer with 6 M guanidinium chloride (1.9 µM), shows a decline in fluorescence intensity and a λ_{max} red shift from 341 nm to 355 nm, showing protein unfolding occurring in 6 M guanidinium chloride (Lakowicz, 1999).

3.7 Conformational stability.

3.7.1 Characterization of Bluetongue virus VP7 in the presence of denaturants.

3.7.1.1 Urea.

Bluetongue virus VP7 structure was evaluated in Primary buffer with three different concentrations of urea, namely 2 M, 5 M and 8 M (Figure 3.13 and Figure 3.14).

For far-UV CD spectra collected (Figure 3.13), similar troughs are seen at 218 nm and 222 nm for 2 M, 5 M and 8 M urea, with a decrease in signal seen for 2 M urea presumably due to the protein precipitation caused by it being in a lower urea concentration. This is supported by Dichroweb K2D3 (Louis-Jeune *et al*., 2011) alpha-helical and beta-strand protein content predictions seen in Table 3.1, which shows similar alpha-helical contents for Bluetongue virus VP7 in 2 M, 5 M and 8 M urea. As for Bluetongue virus VP7 without any urea which is close to the 2Struc (Klose *et al*., 2010) prediction using the PDB file 1BVP from Grimes *et al.* (1995) of 36.38 % for both monomer and trimer. For beta-strand content Bluetongue virus VP7 in 5 M and 8 M urea showed a closer value to the 2Struc (Klose *et al*., 2010) predicted monomer value of 17.19 %. Bluetongue virus VP7 without urea and in 2M urea shows a beta-strand percentage closer to the 2Struc (Klose *et al*., 2010) predicted trimer content at 18.62 %.

This is consistent with the clear native PAGE (Figure 3.12, lanes 1 and 9) which showed more than one form present in the Bluetongue virus VP7 samples without urea and in 2 M urea. That being said, even in 8 M urea Bluetongue virus VP7 still has significant secondary structure.

For fluorescence (Figure 3.14) a single peak at 341 nm was seen at all three concentrations although a slight decrease in fluorescence signal was seen at 295 nm for 8 M urea. Significant light scatter was seen in the fluorescence reading for Bluetongue virus VP7 in 2 M urea, consistent with other data collected depicting protein precipitation occurring when urea is removed from the protein sample. Decrease in fluorescence intensity for Bluetongue virus in 2 M urea is due to the increase in protein precipitation, presumably of protein aggregation forming, seen as the scatter around 295 nm (excitation wavelength), depicting that this concentration is not sufficient enough to prevent protein aggregation from occurring. Significant tertiary structure is still seen even when Bluetongue virus VP7 is placed into 8 M urea, showing that even 8 M urea does not significantly alter protein structure.

3.7.1.2 Guanidinium chloride.

Fluorescence and far-UV CD spectra were recorded for purified Bluetongue virus VP7 in Primary buffer with 6 M guanidinium chloride (Figure 3.15). The sample was then diluted down to 1 M guanidinium chloride to check for refolding. For purified Bluetongue virus VP7 the presence of guanidinium chloride resulted in the far-UV CD spectra only being recorded to approximately 214 nm as the noise to signal ratio was too high below this wavelength, as detected by turbidity (dynode voltage). For far-UV CD (Figure 3.15A), there is a substantial loss of secondary structure in 6 M guanidinium chloride.

The ellipticity at 222 nm and 218 nm was used to evaluate the recovery of secondary structure as these are signature troughs in a protein containing both beta-strands and alpha-helices. Refolded Bluetongue virus VP7 (Figure 3.15 A) shows a 94 % recovery at 218 nm and an 89 % recovery at 222 nm. Thus the equilibrium unfolding transition cannot be further analysed to determine thermodynamic parameters.

As seen in Figure 3.15B, at 6 M guanidinium chloride there is a distinct peak at 355 nm, suggesting an unfolded protein. After diluting to 1 M guanidinium chloride the peak returns to 342 nm, suggesting a refolded protein. However, the fluorescence intensity differences due to different protein concentrations caused by dilution for refolding studies prevents percentage recovery values from being obtained as fluorescence intensities cannot be concentration corrected as the signal is not linearly dependent on protein concentration. There is an increase in light scatter at 295 nm, suggesting an increase in protein precipitation that occurs during refolding when not in the presence of urea or glycerol (Figure 3.14).

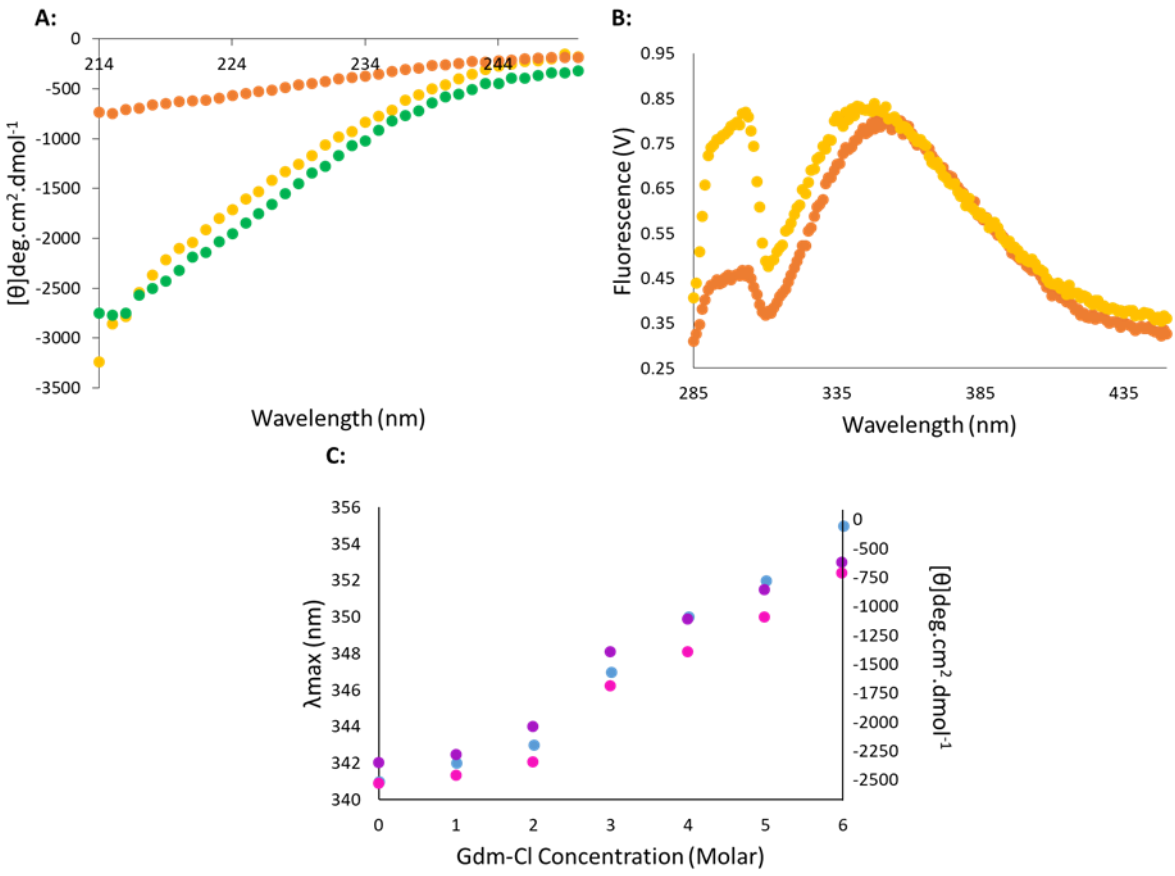

Figure 3.15. Bluetongue virus VP7 in presence of guanidinium chloride.

(A) *Far-UV CD Spectra between 250 nm and 214 nm for Bluetongue virus VP7 in Primary buffer (●) at 1.9 µM, Primary buffer with 6 M guanidinium chloride (●) at 1.9 µM and 1 M guanidinium chloride (●) at 1 µM* ***(B)*** *Fluorescence emission spectrum between 450 nm and 285 nm for purified Bluetongue virus VP7 (not concentration corrected) in Primary buffer with 6 M* guanidinium chloride *(1.9 µM) (●), and when allowed to refold in 1 M* guanidinium chloride *(1.0 µM) (●).* ***(C)*** *Shows λ_{max} fluorescence values (●), far-UV CD 218 nm values (●) and 222 nm values (●) at several guanidinium chloride concentrations.*

Figure 3.15C shows λ_{max} fluorescence values and mean residue ellipticity values at 218 nm and 222 nm for samples from 0 M to 6 M guanidinium chloride, showing cooperative unfolding of the secondary and tertiary structure. The λ_{max} shifting from 341 nm for Bluetongue virus VP7 without the presence of guanidinium chloride to 355 nm in 6 M guanidinium chloride, with significant structural unfolding from 3 M guanidinium chloride. The increase in mean residue ellipticity at both 218 nm and 222 nm indicate similar cooperative unfolding of both alpha-helices and beta-strands, showing significant structural changes occurring from 3 M guanidinium chloride.

3.7.2 Thermal-induced unfolding.

3.7.2.1 Spectroscopic studies.

Far-UV CD was used as a secondary structure stability probe when heating the protein from 20 ˚C to 90 ˚C in two different buffers, namely Primary buffer with 5 M urea and Primary buffer with 20 % glycerol (Figure 3.16). Thermal stability of Bluetongue virus VP7 was tested at three different concentrations, namely 1.0 µM, 1.4 µM and 1.7 µM in the Primary buffer with 5 M urea and at a concentration of 1.0 µM in Primary buffer with 20 % glycerol. A far-UV CD spectrum for the thermal unfolding of protein in Primary buffer with 20 mM sodium chloride, was not obtainable as the noise to signal ratio was too low.

The characteristic troughs for a protein that contains both alpha-helices and beta-strands are 208 nm, 218 nm and 222 nm (Ranjbar and Gill, 2009), however the signal to noise ratio was best at 218 nm and 222 nm due to the presence of urea and glycerol in the samples, and therefore these wavelengths were used as secondary structural probes and not the signal at 208 nm. All the samples demonstrated secondary structural changes consistent with protein unfolding as the 222 nm and 218 nm ellipticity values increased when the temperature was increased (Figure 3.16A, B and D), shifting towards the characteristic far-UV spectrum of a random coil with a positive peak at 212 nm and trough at 195 nm (Ranjbar and Gill, 2009).

The three different concentrations of Bluetongue virus VP7 (1.0 µM, 1.4 µM and 1.7 µM) showed little change in ellipticity for 218 nm and 222 nm between 20 ˚C and 55 ˚C (Figure 3.16A), suggesting minor structural reorganization rather than a major conformational change up until this temperature. Significant secondary structure loss is then seen from approximately 55 ˚C, with some secondary structure still seen to remain even at 90 ˚C, as the spectrum at 90 ˚C is not fully characteristic of a random coil (Figure 3.16B) (Ranjbar and Gill, 2009) and the unfolding curves have not reached a plateau in Figure 3.16A. The spectra for protein refolding after heating (Figure 3.16 B and D) depicts that protein unfolding is irreversible for Bluetongue virus VP7 in Primary buffer with 5 M urea and 20 % glycerol.

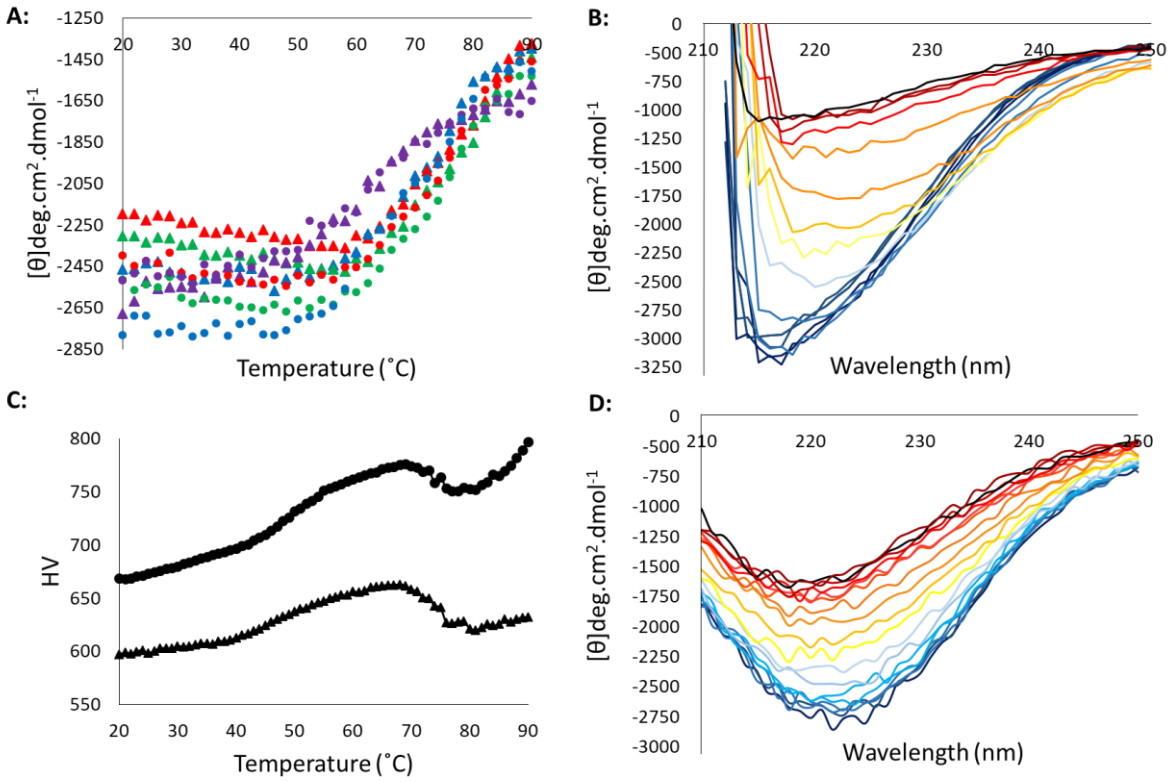

Figure 3.16. Far-UV circular dichroism monitoring of thermal unfolding of Bluetongue virus VP7.

*(**A**) Heat unfolding curves using far-UV CD values at 218 nm and 222 nm wavelengths between 20 ˚C and 90 ˚C, for Bluetongue virus VP7 in Primary buffer with 5 M urea at three different concentrations namely, 1 µM (218 nm●, 222 nm▲), 1.4 µM (218 nm●, 222 nm▲) and 1.7 µM (218 nm●, 222 nm▲) and Bluetongue virus VP7 in Primary buffer with 20 % glycerol (218 nm●, 222 nm ▲) at a concentration of 1 µM. (**B**) Far-UV CD spectrum between 20 ˚C and 90 ˚C (dark blue to dark red) for Bluetongue virus VP7 in Primary buffer with 5 M urea. Protein refolding after heating shown in black. **(C)** Turbidity (dynode voltage) plots Bluetongue virus VP7 in Primary buffer with 5 M urea at 218 nm (●) 222 nm (▲). **(D)** Far-UV CD spectrum between 20 ˚C and 90 ˚C (dark blue to dark red) for Bluetongue virus VP7 in Primary buffer with 20 % glycerol. Protein refolding after heating shown in black. Selected data used in this Figure was published in Russell and Gildenhuys (2018).*

The similar unfolding transitions seen for all three protein concentrations is indicative of a single species of monomeric protein being present in the protein sample. This is because oligomeric protein stability has been seen to increase with an increase in protein concentration, as protein-protein interactions in addition to the protein structure itself, needs to be disrupted (Steif *et al*., 1993; Salminen *et al*., 1996; Shriver and Edmondson, 2009). This finding is consistent with clear native PAGE findings (Figure 3.12) that show that in the presence of 5 M urea, Bluetongue virus VP7 is present predominantly in a single form.

Bluetongue virus VP7 in the presence of 20 % glycerol showed a different unfolding transition with a significant loss in secondary structure from approximately 52 ˚C, suggesting a destabilisation of the structure in comparison to Bluetongue virus VP7 in 5 M urea. That being said, there was significantly more secondary structure remaining at 90 ˚C for Bluetongue virus VP7 in 20 % glycerol when compared to Bluetongue virus VP7 in 5 M urea, showing a less cooperative nature of unfolding in the presence of 20 % glycerol. Limitations of the instrument, being unable to record data from a sample that is being boiled, resulted in the inability to record the full unfolding transition.

Figure 3.16C shows a turbidity (dynode voltage) plot indicating aggregation occurring as protein unfolds with increasing temperature. The drop in readings between 70 ˚C and 80 °C could be due to precipitation of protein aggregates before a further spike in aggregation formation between 80 ˚C and 90 °C.

Intrinsic fluorescence from the aromatic amino acid tryptophan is sensitive to the polarity of the amino acid's immediate environment (Teale, 1960; Longworth, 1971; Lakowicz, 1999), which creates a valuable technique to study protein unfolding, as the fluorescence spectrum changes, the tryptophan residue moves from the hydrophobic environment of a folded protein to the hydrophilic environment of an unfolded protein (Teale, 1960; Gryczynski *et al*., 1988a; Gryczynski *et al*., 1988b; Lakowicz, 1999). The emission of several proteins that contain tryptophan residues caused a reduction in fluorescence intensity and a red shift in λ_{max} when unfolded (Teale, 1960).

Fluorescence monitored unfolding of Bluetongue virus VP7 was undertaken in three different buffers, namely Primary buffer with 5 M urea, Primary buffer with 5 M urea and 300 mM sodium chloride and Primary buffer with 20 % glycerol as seen in Figure 3.17. All samples showed a decline in fluorescence intensity and a slight shift in λ_{max} to a longer wavelength with an increase in temperature (Figure 3.17B and C and D).

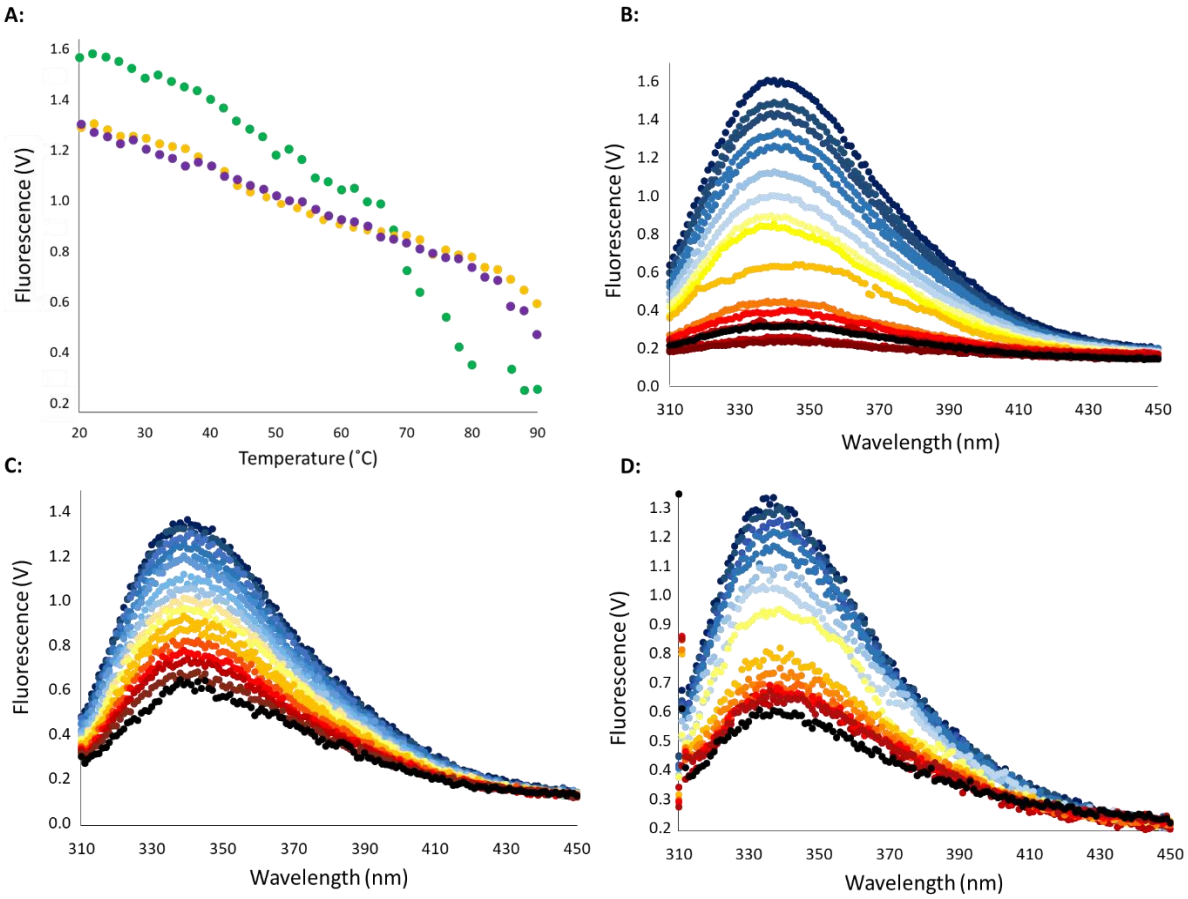

Figure 3.17. Fluorescence monitored thermal unfolding of Bluetongue virus VP7.

(A) *Heat unfolding curve for 341 nm fluorescence readings from 20 ˚C to 90 ˚C for 1.4 µM Bluetongue virus VP7 in Primary buffer with 5 M urea (●), and 1 µM Bluetongue virus VP7 in Primary buffer with 5 M urea, 300 mM sodium chloride (●) and 339 nm for 1.0 µM Bluetongue virus VP7 in Primary buffer with 20 % glycerol (●). The spectrum between 450 nm and 310 nm between 20 ˚C and 90 ˚C (dark blue to dark red) for:* ***(B)*** *1.7 µM Bluetongue virus VP7 in Primary buffer with 5 M urea.* ***(C)*** *1.0 µM Bluetongue virus VP7 in Primary buffer with 5 M urea and 300 mM sodium chloride.* ***(D)*** *1.0 µM Bluetongue virus VP7 in Primary buffer with 20 % glycerol. Protein refolding after heating shown black for each sample. Selected data used in this Figure was published in Russell and Gildenhuys (2018).*

This is consistent with tertiary structure changing in a protein that is unfolding, as the altered emission results from tryptophan residues moving from a hydrophobic to a hydrophilic environment as they become exposed as the protein unfolds (Teale, 1960; Gryczynski *et al*., 1988a; Gryczynski *et al*., 1988b; Lakowicz, 1999). The decline in fluorescence intensity could also partially be due to thermal quenching as the quantum yield of a chromophore is dependent on temperature and is known to decrease with an increase in temperature (Demchenko, 1986).

For Bluetongue virus VP7 in Primary buffer with 5 M urea, a reduction in intensity was seen and a λ_{max} red shift from 341 nm to approximately 348 nm. For Bluetongue virus VP7 in Primary buffer with 20 % glycerol, the λ_{max} shifted from 339 nm to approximately 343 nm and Bluetongue virus VP7 in Primary buffer with 5 M urea with 300 nm sodium chloride showed a λ_{max} shift from 341 nm to 345 nm. The heat unfolding curve for Bluetongue virus VP7 in 5 M urea at 341 nm (Figure 3.17A) shows slight changes in structure until approximately 68 ˚C, after which there are major structural changes occurring until at least 90 ˚C. The heat unfolding curves for Bluetongue virus VP7 in Primary buffer with 20 % glycerol at 339 nm and Primary buffer with 5 M urea with 300 mM sodium chloride at 341 nm (Figure 3.17A) shows that there are only slight structural changes until approximately 85 ˚C, after which there are more prominent structural changes. Limitations of the instrument, being unable to record data from a sample that is being boiled, again resulted in the inability to record the full unfolding transition.

At 90 ˚C the emission maximum for Bluetongue virus VP7 in 5 M urea, 20 % glycerol and 5 M urea with 300 mM sodium chloride was found to be 348 nm, 343 nm and 345 nm respectively, suggesting that complete exposure of tryptophan to an aqueous medium does not occur at this temperature (Lakowicz, 1999). The fluorescence intensity also decreased to a lesser extent for Bluetongue virus VP7 in the presence of 20 % glycerol (without urea) and 300m M sodium chloride (with 5 M urea) when compared to Bluetongue virus VP7 in 5 M urea. Along with smaller λ_{max} shift, this shows an increase in tertiary structure stability when Bluetongue virus VP7 is in sodium chloride or glycerol. Both of which are known substances for increasing protein stability and the preserved structure in these conditions is indicative of their protective function in proteins (von Hippel and Schleich, 1969; Gekko and Timasheff, 1981a; Gekko and Koga, 1983; Cleland and Wang, 1990).

Thermal unfolding was found to be irreversible as the fluorescence and far-UV CD spectra of the cooled protein sample did not return to the same values as those for the protein prior to being heated to 90 ˚C (black line in Figure 3.16B and D and Figure 3.17B, C and D).

The most common cause of irreversible unfolding of heated protein samples is aggregation (Benjwal *et al*., 2006). The turbidity (dynode voltage) recorded during CD experiments can be used as an indicator of the level of aggregate formation as the protein is unfolding via increasing heat. Thermal unfolding of Bluetongue virus VP7 showed an increase in aggregation depicted by an increase in turbidity with the increase in temperature (Figure 3.16C). Therefore the likely cause of the irreversibility of the thermal unfolding of Bluetongue virus VP7 is the heat-induced aggregation during unfolding. The irreversibility of the thermal unfolding of Bluetongue virus VP7 prevents further thermodynamic analysis.

3.7.2.2 Differential scanning calorimetry.

The Bluetongue virus VP7 thermogram (Figure 3.18) that is baseline subtracted and corrected, revealed a single peak with a maxima value at approximately 353 K (80 ˚C). The thermogram shows the start of protein structural alteration after 42 ˚C with the increase in heat capacity, and protein structural changes still occurring until at least 100 ˚C. This is consistent with the spectroscopic analysis of the thermal unfolding of Bluetongue virus VP7 (Figure 3.16 and 3.17), which showed the unfolding transition was not completed at 90 ˚C. Spectroscopic analysis of Bluetongue virus VP7 confirmed the irreversibility of protein unfolding and therefore further thermodynamic analysis could not be undertaken.

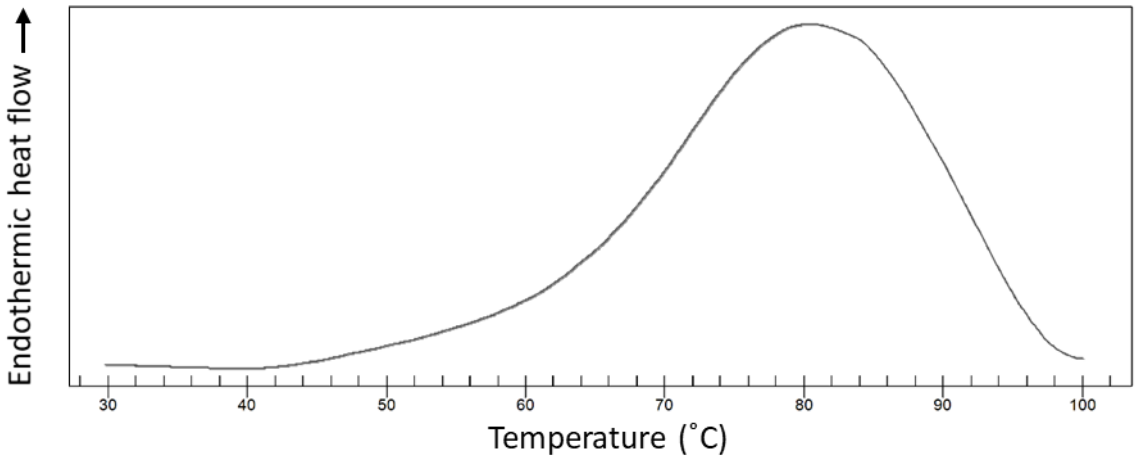

Figure 3.*18*. DSC thermogram of the unfolding of Bluetongue virus VP7.

Thermogram for 1 µM Bluetongue virus VP7 in Primary buffer with 5 M urea, monitored from 10 ˚C to 100 ˚C. TA Instruments Nano Differential scanning calorimeter (New Castle, Delaware), was used with DSCRun software version 4.4.25 and data collected was analysed using NanoAnalyze version 3.7.5.

4. Discussion.

Several recombinant bacterial expression systems were tested under multiple different expression conditions in order to obtain the most appropriate system for optimal protein production in bacterial cells. The recombinant expression systems consisted of the pET28a plasmid with the consensus sequence for Bluetongue virus VP7 gene insert transformed into *Escherichia coli* BL21(DE3), NiCo21(DE3), C43(DE3) pLysS and KRX cells. Bluetongue virus VP7 protein was predominantly expressed in bacterial inclusion bodies, resulting in insoluble protein under all conditions tested (media compositions, post induction temperatures, post induction times and inducer concentrations) in all four *Escherichia coli* strains with little expression occurring in C43(DE3) pLysS at all (Figure 3.1, Figure 3.6, Figure 3.10 and Figure 3.11).

As stated in section 1.7, little is understood about the formation of insoluble inclusion bodies in bacterial cells (Villaverde and Carrio, 2003). However, studies have shown that expression conditions (including inducer concentration, post induction time and temperature) (Chalmers *et al*., 1990; Neubauer *et al*., 1992; Van den Berg *et al*., 1999) as well as the primary sequence of the expressed protein (Chiti *et al*., 2003; Dubay *et al*., 2004) affect the likelihood of the formation of insoluble inclusion bodies. These factors have been linked to the metabolic burden placed on the bacteria cells during expression.

The metabolic burden is the use of the host cells energy and raw materials for the expression of the foreign proteins. The amino acid sequence can affect the metabolic burden placed on the cell as it has been found that tryptophan, phenylalanine, tyrosine, histidine and methionine have the highest energetic costs of all amino acids during their production (Akashi and Gojobori, 2002). Bluetongue virus VP7 has a 1.4 % tryptophan, 3.8 % phenylalanine, 2.4 % tyrosine, 4.6 % histidine and 5.1 % methionine (Russell *et al*., 2018), resulting in close to 20 % of the entire protein being composed of the highest energy costing amino acids.

Lessening metabolic burden on bacterial cells during recombinant protein expression is a complicated exercise, as it is determined by multiple factors including plasmid copy number, promoters used, growth conditions including temperature, aeration and inducer concentrations as well as the protein sequence being expressed (Chalmers *et al*., 1990; Neubauer *et al*., 1992; Van den Berg *et al*., 1999; Chiti *et al*., 2003; Dubay *et al*., 2004). Strategies that have been implemented in the past to try to reduce the metabolic burden have included a number of genetic modifications, including alterations of transport systems and gene knockouts (Chou *et al*., 1994; De Anda *et al*., 2006).

The other approach adopted is the media composition. Media compensation for metabolic burden is not an easy task as different proteins respond very differently to media additives (Lourenco *et al*., 2011). Commonly used tactics include amino acid supplementation (Harcum *et al*., 1992), limiting acetate accumulation and control of the growth rates through feeding strategies and controlling biomass (Gregory and Turner, 1993; Turner *et al*., 1994). However, these often only solve single problems such as limitation of building blocks and toxicity generation, while sufficient energy generation by the bacterial cells still remains an issue (Carneiro *et al*., 2013). All strategies that have been identified have been found to produce temperamental effectiveness that is dependent on the protein itself (Carneiro *et al*., 2013), often requiring extensive trial and error.

This study found that changes in expression conditions and cell lines, did not significantly affect the expression of soluble Bluetongue virus VP7, and instead just influenced the amount of insoluble protein expressed (Figure 3.1, Figure 3.6, Figure 3.10 and Figure 3.11). The fact that Bluetongue virus VP7 is expressed in the soluble fraction in both insect cells and mammalian cells (Oldfield *et al*., 1990; Hosamani *et al*., 2011, Bouet-Cararo *et al*., 2014) suggests that the protein may be adapted to being expressed in these cells as they are the host cells for the virus. A logical suggestion would be that Bluetongue virus VP7 requires post-translational modification, however no evidence has been found of this and the fact that it is still expressed in low concentrations in the soluble fraction in *Escherichia coli*, suggests that it does not require modification (Figure 3.1, Figure 3.6, Figure 3.10 and Figure 3.11). Rotavirus VP6, which is structurally very similar to Bluetongue virus VP7 has been shown to be extremely reactive to buffer conditions such as pH, salts present and ionic strength, with changes in these conditions resulting in changes in protein structure and interactions (Lepault *et al*., 2001). Therefore potentially slight differences in cell conditions could greatly influence expression, affecting soluble and insoluble expression in different cell types.

Another interesting point would be the natural aggregation of viral proteins in viroplasms, which are inclusion bodies that form inside infected cells to house viral proteins during virus replication (Netherton and Wileman, 2011). The viroplasm production occurs to help increase the efficiency of replication as it concentrates components needed such as viral genome, viral proteins and any host proteins in close proximity, that are needed in the replication process (Netherton and Wileman, 2011). Viroplasm formation can help protect the cell from any potentially toxic proteins being expressed during replication, as well as helping to prevent an immune reaction (Wileman, 2007). This suggests that viral proteins are naturally adapted to aggregating together in a small area during replication.

Rotavirus, a related *Reoviridae* virus is known to form viroplasms during replication (Patton *et al*., 2006), therefore potentially, Bluetongue viral proteins may share a similar mechanism, which would help explain the apparent formation of inclusion bodies around correctly folded Bluetongue virus VP7 in bacterial cells.

Bluetongue virus VP7 predominantly being expressed in the bacterial cell inclusion bodies resulted in the need for solubilisation before purification could be undertaken. For Bluetongue virus VP7 solubilisation was achieved using lower urea concentrations with a freeze-thaw step for efficient solubilisation. In Qi *et al.* (2015) it was found that 2 M urea was the optimal urea concentration used to solubilize a number of proteins, as the amount of solubilisation in 2 M urea with a freeze-thaw step was comparable to solubilisation in 8 M urea without a freeze-thaw step (Qi *et al*., 2015). However, for Bluetongue virus VP7 there was a notable decrease in solubilisation with 2 M urea from 5 M urea, but no notable increase in solubilisation from 5 M urea to 8 M urea as seen in Figure 3.2B and 3.7B.

Walther *et al*. (2013) described solubilisation of inclusion bodies resulting from pore-like structures forming in the amyloid-like fibrous outer layer of the inclusion body vesicle and that the size and number of pores formed is dependent on the solubilisation method used, but that generally there is an increase in the quantity and diameter of pores with an increase denaturant concentration. Therefore, for this method of solubilisation of Bluetongue virus VP7 we would expect the main role of urea at the lower concentrations to be the physical separation of the protein molecules by disturbing hydrophobic interactions, and the main force of solubilisation to come from the stress of the low temperature and the physical ice crystals that form during freezing that cause “punctures” in the inclusion body structure to create the needed pores (Clark, 1998; Qi *et al*., 2015).

The physical separation of the proteins is important for them to fit through the pores, and therefore provide more efficient solubilisation as more protein is able to be released from the inclusion bodies. Urea binding to proteins has been found to be concentration dependent, which often results in the need for high concentrations of urea to ensure sufficient binding to effectively interact with the proteins (Muralidhara and Prakash, 2001). This is in agreement with results seen in Figure 3.14 which show significant protein precipitation, as seen in the light scatter around 295 nm in the fluorescence spectrum of Bluetongue virus VP7 in 2 M urea, similar to the spectrum produced in the sample without any urea, suggesting that 2 M urea is not sufficient to physically separate the Bluetongue virus VP7 molecules from one another. This is supported by the clear native PAGE gel (Figure 3.12) which shows at least three forms present in the samples without urea and predominantly only a single form in samples with 5 M urea.

Furthermore, the fluorescence spectrum of Bluetongue virus VP7 in 5 M urea showed very little light scatter around 295 nm suggesting that 5 M urea is significantly more effective at separating the Bluetongue virus VP7 molecules, and hence why there is the increase in solubilisation seen between 2 M and 5 M urea. There was no further increase in solubilisation from 6 M to 8 M Figure 3.2B and 3.7B and the slight decrease in fluorescence from 5 M urea to 8 M urea (Figure 3.14) resulting from either quenching or slight change in tertiary structure as the λ_{max} doesn't change, suggesting very little structural change has occurred locally around the tryptophans. It has been seen that even at high denaturant concentrations intermolecular and intramolecular interactions have been known to occur (Bhavesh *et al*., 2001).

Using lower denaturant concentrations for solubilisation of bacterial cell inclusion bodies is advantageous because the use of milder solubilisation conditions can help improve the retrieval of native protein when compared to solubilisation using higher concentrations of denaturants (Khan *et al*., 1998; Patra *et al*., 2000; Umetsu *et al*., 2005). This is not an uncommon occurrence as proteins inside bacterial cell inclusion bodies have been shown to still contain native-like secondary structures (Przybycien *et al*., 1994; Ami *et al*., 2006). Furthermore, freezing-induced separation of multimeric proteins has been observed, with said proteins still maintaining native-like secondary structure even in an alkaline pH and low concentrations of urea (Stancel and Deal, 1969; Nema and Avis, 1993; Pikal-Cleland, 2000). Studies have found that inclusion bodies may enclose properly folded proteins stored inside the 'vesicle sacks' (Jevsevar *et al*., 2005; Peternel *et al*., 2008a; Peternel *et al*., 2008b).

This appears to be the case for Bluetongue virus VP7, as recombinant protein characterization after solubilisation and purification reveals a native-like secondary structure and a folded tertiary structure even in the presence of 5 M urea as seen in Figure 3.13 and 3.14. This was supported by the predicted alpha-helical and beta-strand percentages made using the K2D3 tool of Dichroweb (Louis-Jeune *et al*., 2011) that indicated a very similar percentage for alpha-helices and beta-strands that is contained in a natively folded Bluetongue virus VP7 molecule obtained from Grimes *et al.* (1995). This is further supported by the unfolding of Bluetongue virus VP7 in guanidinium chloride, which when diluted from 6 M to 1 M (Figure 3.15), the λ_{max} value shifted from 355 nm to 342 nm, with Bluetongue virus VP7 in 1 M guanidinium chloride showing a λ_{max} very similar to Bluetongue virus VP7 in urea (341 nm). However, displaying significant light scattering at 295nm, like Bluetongue virus VP7 when not in the presence of urea or glycerol. (Figure 3.14 and 3.15 B).

The single peak at 341 nm for Bluetongue virus VP7 in 5 M urea and 339 nm in 20 % glycerol (Figure 3.14) is indicative of a tryptophan residue emission spectra in hydrophobic surroundings, indicating the Bluetongue virus VP7 is folded and contains tertiary structure (Lakowicz, 1999).

Furthermore, the folded structure of Bluetongue virus VP7 in 5 M urea and 20 % glycerol are similar, suggesting that the inclusion bodies formed during expression may contain properly folded protein. Therefore 5 M urea does not significantly alter Bluetongue virus VP7's structure which has been seen in Basak *et al.* (1996), who reported that VP7 in *Orbiviruses* retains its structure in 8 M urea. Urea, therefore, helps avoid the development of larger oligomers or aggregates, this is essential in the solubilisation and subsequent purification but does not significantly denature the protein structure.

The protein's stability is further demonstrated by its ability to maintain significant secondary and tertiary structure to at least 55 ˚C even in the presence of 5 M urea when probed with far-UV CD and intrinsic fluorescence as seen in Figure 3.16 and 3.17. In far-UV circular dichroism, the spectrum shifted from troughs indicating a protein containing beta-strands (218 nm) and alpha-helices (222 nm) to a spectra more characteristic of a random coil as the protein was heated to 90 ˚C (Figure 3.16). A buried tryptophan has a λ_{max} of around 335 nm, whereas a tryptophan in a hydrophilic environment has a λ_{max} around 355 nm, depicting an unfolded protein (Teale, 1960; Gryczynski *et al*., 1988a; Gryczynski *et al*., 1988b; Lakowicz, 1999). Often the fluorescence intensity decreases, and λ_{max} shifts to longer wavelengths when a protein unfolds (Lakowicz, 1999). These shifts are seen with Bluetongue virus VP7 as it is heated from 20 ˚C to 90 ˚C, showing significant stability until approximately 55 ˚C and irreversible unfolding when heated to 90 ˚C.

The λ_{max} values at 90 ˚C are 348 nm, 343 nm and 345 nm for Bluetongue virus VP7 in 5 M urea, 20 % glycerol and 300 mM sodium chloride with 5 M urea respectively, and is suggestive that the protein unfolding transition is not complete at 90 ˚C and that significant tertiary structure remains, especially when compared to Bluetongue virus VP7 unfolding in 6 M guanidinium chloride (Figure 3.15B and C), which shows a shift in λ_{max} to 355 nm, a characteristic of a denatured protein (Teale, 1960; Gryczynski *et al*., 1988a; Gryczynski *et al*., 1988b; Lakowicz, 1999). This is further supported by the thermogram (Figure 3.18) of Bluetongue virus VP7 in 5 M urea when heated between 10 ˚C and 100 ˚C, which showed the unfolding transition occurred until at least 100 ˚C. The smaller shift in λ_{max} and fluorescent intensity decreases caused by temperature increases are indicative of increased tertiary structure stability of Bluetongue virus VP7 when the protein sample is heated to 90 ˚C in glycerol (without urea) or sodium chloride (with 5 M urea) (Figure 3.17).

Glycerol is a viscous osmolyte and is well known for increasing protein stability during both thermal and chemical denaturation, as well as prevention of protein aggregation during protein refolding (Jarabak *et al*., 1966; Jarabak, 1972). The exact molecular mechanism of glycerol increasing protein stability is unknown, however glycerol has been seen to alter the native structure of a protein to a more compacted state (Gekko and Timasheff, 1981a; Gekko and Timasheff, 1981b), this is seen in Figure 3.14, with slight shift in λ_{max} from 341 to 339 nm and a slight increase in fluorescence intensity seen for the same protein concentration between Bluetongue virus VP7 in 5 M urea and 20 % glycerol.

The prevention of protein precipitation when dialysing in a solution containing glycerol is predominantly due to the glycerol changing the viscosity of the protein environment, with the higher viscosity (surface tension) likely blocking protein molecule interactions and thus preventing protein precipitation (Ou *et al*., 2002). The protective nature of glycerol against protein aggregation and denaturation is dependent on the concentration of glycerol in the solution, with an increase in glycerol most often resulting in an increase in protein stability (Ou *et al*., 2002; Ruan *et al*., 2003). Studies have shown that glycerol molecules do not often bind the protein themselves, but instead change water tension around the protein preventing the hydrophobic regions of the protein from becoming exposed and resulting in proteins being preferentially hydrated around their surface, which increases the free energy needed to denature it (Schachman and Lauffer, 1949; Gekko and Timasheff, 1981a; Gekko and Timasheff, 1981b; Timasheff, 1993; Ruan *et al*., 2003).

Similarly, sodium chloride acts as a weak kosmotrope, as it contributes to the stability and structure of water-water interactions, creating favourable interactions that result in the stabilization of intermolecular interactions in proteins (von Hippel and Schleich, 1969). Kosmotropic co-solvents such as sodium chloride, interact with the water molecules instead of the protein molecules themselves, resulting in preferential hydration much like glycerol (Arakawa and Timasheff, 1982). The preferential hydration results in net repulsion between protein and solvent, resulting in protein molecules compacting to reduce total surface area exposure, this then leads to an increase in hydrophobic aggregation, which increases the Gibbs free energy needed to denature the protein (Schachman and Lauffer, 1949; Gekko and Timasheff, 1981a; Gekko and Timasheff, 1981b; Timasheff, 1993). Sodium chloride, much like glycerol, stabilized the protein structure despite not interacting directly with the protein (Galinski *et al*., 1997; Soderlund *et al*., 2003).

In contrast, guanidinium chloride and urea are chaotropes, meaning they can disrupt the network of hydrogen bonds between water molecules, and therefore are able to weaken the stability of the protein's structure by weakening the hydrophobic effect (Salvi *et al*., 2005).

When Bluetongue virus VP7 was studied in the presence of guanidinium chloride, which is well known for being a stronger denaturant then urea (Green and Pace, 1974; Pace, 1986), the fluorescence spectra (Figure 3.15C) revealed a shift in λ_{max} from 341 nm without guanidinium chloride to 355 nm in the presence of 6 M guanidinium chloride, which is the characteristic red shift seen in many proteins when unfolding (Lakowicz, 1999). The unfolding reaction appeared to be reversible by the λ_{max} shifting back to 342 nm when the sample was diluted back to 1 M guanidinium chloride. The far-UV CD spectrum of Bluetongue virus VP7 in guanidinium chloride (Figure 3.15C) supported the unfolding of the protein's secondary structure at 6 M guanidinium chloride. As the spectra takes on the characteristics of a random coil, the ellipticity becomes more positive and again displayed characteristics of reversibility as ellipticity decreased as the protein solution was diluted back to 1 M guanidinium chloride, however, the percentage reversibility was not high enough to do further analysis. When Bluetongue virus VP7 was studied in the presence of urea very little structural (either secondary or tertiary) change was seen for Bluetongue virus VP7 between samples without urea and samples containing up to 8 M urea (Figure 3.13 and 3.14).

This is not the first time where one denaturant is more efficient than another at unfolding a protein. The mechanism of denaturation becomes very important here, however it must be noted that the exact molecular mechanism for protein denaturation by either guanidinium chloride or urea is still not fully understood, but rather deductions have been made from experimental data and denaturant simulations (Camilloni *et al*., 2008). Two proposed mechanisms involve the direct interaction of the denaturant with the protein and the indirect alteration of the solvent environment with resultant interruption of hydrophobic interactions as urea or guanidinium chloride in water causes the surface tension of the solution to increase (Schellman, 1955; Frank and Franks, 1968; Bennion and Daggett, 2003; Camilloni *et al*., 2008).

The dissimilarities seen in the capacity of urea and guanidinium chloride to denature proteins has been largely attributed to their differential interactions with the protein (Robinson and Jencks, 1965; Tanford, 1970; Makhatadze and Privalov, 1992). Two of the most important differences found between urea and guanidinium chloride is that urea is known to readily form hydrogen bonds to polarized areas of charge, such as the peptide backbone, disrupting native intermolecular bonds and interactions (Schellman, 1955; Frank and Franks, 1968; Prakash *et al*., 1981), whereas guanidinium chloride does not. Guanidinium chloride instead is attracted to the peptide backbone and aromatic protein side chains where it causes disruption of hydrophobic interactions, including shielding the unfavourable increase of interaction with water molecules as the protein unfolds (Parui *et al*., 2016).

Also significant is the ionic nature of guanidinium chloride, as the charge that the chloride and guanidinium ions carry enables it to screen for favourable intermolecular and intramolecular electrostatic interactions that may help stabilize or destabilize the protein's structure and therefore, reduction or elimination of these electrostatic interactions can promote the unfolded protein form (Tanford, 1970; Greene and Pace, 1974; Pace, 1986; Monera *et al*., 1994). Interestingly, low concentrations of urea and guanidinium chloride are capable of stabilizing certain proteins. Urea acts as a weak kosmotrope is some cases, that is it increases the stability of water-water interactions, creating favourable interactions for protein stability (von Hippel and Schleich, 1969; Vanzi *et al*., 1998), whereas guanidinium chloride is able to neutralise destabilizing electrostatic interactions (Monera *et al*., 1994; Bhuyan, 2002; Povarova *et al*., 2010). However, at higher concentrations, the binding of guanidinium ions favours and therefore promotes destabilization of the protein structure (Tanford, 1970; Greene and Pace, 1974; Pace, 1986). Similarly, the preferential interaction of urea with the protein increases with concentration increases, resulting in destabilisation of the protein structure (Prakash *et al*., 1981).

Once the process of destabilization of the protein has begun, it then increases exponentially if the unfolding is cooperative, this is believed to occur as urea and guanidinium chloride display preferential interaction with proteins, meaning that the denaturant molecules have an attraction to the protein surface and therefore bind or interact with the protein surface, including peptide bonds (Robinson and Jencks, 1965; Tanford, 1970; Prakash *et al*., 1981). As the protein then unfolds more protein surface area becomes exposed, and therefore the ability of the denaturant to bind to and interact with the protein increases (Pace, 1986).

Another important difference seen is that urea appears to destabilize beta-strand structures first, whereas guanidinium chloride appears to destabilize alpha-helical structures first (Camilloni *et al*., 2008). The extent to which guanidinium chloride is able to be more efficient than urea at unfolding a protein has been found to be dependent on the protein's primary sequence as well as the protein's secondary and tertiary structure. It has been shown that guanidinium chloride is most efficient at destabilizing proteins in which electrostatic interactions are important in protein structure (Monera *et al*., 1994) and the planar amino acid side chains within the protein of interest play a large role in alpha-helical stability (Dempsey *et al*., 2005).

This is further verified through the fact that guanidinium chloride shows the same efficiency of destabilization as urea with sodium chloride in proteins that rely on salt bridges for their stability (Smith and Scholtz, 1996).

This is significant as Bluetongue virus VP7 contains more than double the alpha-helical content as beta-strand content (Grimes *et al*., 1995). It would appear, based on findings, that Bluetongue virus VP7's stability is largely reliant on the stability of alpha-helical components found within the proteins as well as the intermolecular and intramolecular electrostatic interactions within the protein structure, which can then explain how guanidinium chloride, which is known to be able to interact with these components, is able to unfold the protein, whereas urea is unable to.

Protein stability is particularly important in vaccine design as the conformation stability of a protein plays a large role in the immunogenic effectiveness of the antigens that the protein is presenting. This is significant for both conformational B cell epitopes and linear T and B cell epitopes as proteases can access the peptide backbone easily when the protein is unfolded (Scheiblhofer *et al*., 2017).

5. Conclusion.

Full-length Bluetongue virus VP7 was expressed, using a pET28a plasmid and *Escherichia coli* expression system. It was then solubilized using a lower urea concentration with a freeze-thaw step, and purified using nickel-affinity chromatography to at least 95 % homogeneity. Bacterial expression resulted in predominantly insoluble Bluetongue virus VP7 expression under all conditions tested. Once solubilized from bacterial inclusion bodies, purified Bluetongue virus VP7 was characterised and stability tested under a number of different conditions. Bluetongue virus VP7, when probed with far-UV CD and intrinsic fluorescence, was found to be stable until at least 55 ˚C even when in 5 M urea, and its tertiary structure stability was increased with the addition of sodium chloride and a less cooperative unfolding was seen in the presence of glycerol, with a higher preservation of secondary and tertiary structure when heated to at least 90 ˚C.

In the presence of 5 M urea, Bluetongue virus VP7 was seen to be predominantly a single monomeric form that has native-like secondary and a folded tertiary structure. There was little secondary or tertiary structure change seen even in 8 M urea. When urea was removed, protein precipitation was seen as the protein molecules grouped to form larger oligomers or aggregates. It can, therefore, be seen that urea is able to prevent protein molecules from forming oligomers or aggregates, but is ineffective at unfolding the structure of the protein.

Guanidinium chloride's ability to unfold Bluetongue virus VP7 where urea was unable to, suggests that the alpha-helical structures found within Bluetongue virus VP7, as well as intermolecular and intramolecular electrostatic forces, play a large role in maintaining the stability of the Bluetongue virus VP7's structure.

Glycerol and sodium chloride were able to increase preservation of protein structure by preferential hydration, which results in a more compact protected protein structure. Significantly, for further studies, the secondary and tertiary structure of Bluetongue virus VP7 in urea and glycerol appeared to be similar when probed with far-UV CD and fluorescence.

Currently, the vaccines beings used have several downfalls, including non-cross neutralisation between serotypes, the inability to distinguish vaccinated animals from infected animals and genomic re-assortment occurring in cocktail attenuated vaccine administration. As there are no antivirals currently available and vaccines are expensive and often ineffective, an economically viable and fully protective vaccine is needed. The significance of Bluetongue virus VP7's stability and high conservation across serotypes, along with its ability to induce a T-cell immune response, and the fact that regions on Bluetongue virus VP7 have been found to be accessible to host antibodies, makes it a viable candidate to be part of a recombinant protein vaccine against Bluetongue virus.

6. References.

Adams, B and Holmes, E. 1935. Adsorptive properties of synthetic resins. *J Soc Chem Ind.* **54**: 1-6.

Afshar, A, Thomas, F, Wright, P, Shapiro, I, Shettigara, P and Anderson, I. 1987. Comparison of competitive and indirect enzyme-linked immunosorbent assays for detection of bluetongue virus antibodies in serum and whole blood. *J Clin Microbiol*. **25**(9): 1705-1710.

Ahern, T and Klibanov, A. 1988. Analysis of processes causing thermal inactivation of enzymes. *Methods Biochem Anal*. **33**: 91-127.

Akashi, H and Gojobori, T. 2002. Metabolic efficiency and amino acid composition in the proteomes of *Escherichia coli* and Bacillus subtilis. *Proc Natl Acad Sci USA*. **99**(6): 3695-3700.

Akov, S. 1972. Protein digestion in haematophagous insects. In Rodriques, J (Ed*), Insect and mite nutrition.* Amsterdam. North-Holland: 531-540.

Alexander, G, Alexander, M and St. George, T. 1996. Bluetongue: its impact on international trade in meat and livestock. In St Geoge, T and Kegao, P (Eds.), *Proceedings of the First South East Asia and Pacific Regional Bluetongue Symposium*. Kunming, Canberra: Australia Center for International Agricultural Research. August 22-24th, 1995: 254-258.

Alexander, K, MacLachlan, N, Kat, P, House, C, O'Brien, S, Lerche, N, Sawyer, M, Frank, L, Holekamp, K, Smale, L, McNutt, W, Laurenson, K, Mills, M and Osburn, B. 1994. Evidence of natural bluetongue virus infection among African carnivores. *Am J Trop Med Hyg.* **51**(5): 568-576.

Alexander, R, Haig, D, Alexander, R, Clark, R, Sterne, R, Louw, J, Van der Reyden, D and De Kock, V. 1951. The use of egg attenuated bluetongue virus in the production of a polyvalent vaccine for sheep: a propagation of the virus in sheep. *Onderstepoort J Vet Sci Anim Ind*. **25**(1): 3-15.

Ami, D, Natalello, A, Taylor, G, Tonon, G, and Maria Doglia, S. 2006. Structural analysis of protein inclusion bodies by Fourier transform infrared microspectroscopy. *Biochim Biophys Acta.* **1764**(4): 793-799.

Amin, B, Mohammed, A and Jilo, K. 2016. Diagnosis, Prevention and Control of Blue Tongue in Sheep: Review. *Global Veterinaria.* **17**(1): 63-77.

Appleton, J and Letchworth, G. 1983. Monoclonal antibody analysis of serotype-restricted and unrestricted bluetongue viral antigenic determinants. *Virology*. **124**(2): 286-299.

Arakawa, T and Timasheff, S. 1982. Preferential interactions of proteins with salts in concentrated solutions. *Biochemistry*. **21**(25): 6545-6552.

Arndt, C, Koristka, S, Bartsch, H and Bachmann, M. 2012. Native Polyacrylamide Gels. *Methods in Mol Biol*. **869**: 49-53.

Atkins, J and de Paula, J. 2006*. Physical Chemistry for the Life Sciences*. United Kingdom. Oxford.

Bailey, J. 1993. Host-vector interactions in *Escherichia coli*. *Adv Biochem Eng Biotechnol*. **48**: 29-52.

Barratt-Boyes, S and MacLachlan, N. 1994. Dynamics of viral spread in Bluetongue virus infected calves. *Vet Microbiol.* **40**: 361-371.

Barzilai, E and Tadmor, A. 1971. Multiplication of bluetongue virus in goats following experimental infection. *Refu Vet.* **28**: 11-20.

Basak, A, Gouet, P, Grimes, J, Roy, P and Stuart, D. 1996. Crystal Structure of the Top Domain of African Horse Sickness Virus VP7: Comparisons with Bluetongue Virus VP7. *J Virol*. **70**(6): 3797-3806.

Basak, A, Stuart, D and Roy, P. 1992. Preliminary Crystallographic Study of Bluetongue Virus Capsid Protein, VP7. *Mol Biol*. **228**(2): 687-689.

Batten, C, Maan, S, Shaw, A, Maan, N and Mertens, P. 2008. A European field strain of bluetongue virus derived from two parental vaccine strains by genome segment reassortment. *Virus Res*. **137**(1): 56-63.

Bekker, J, Dekock, G and Quinlan, J. 1934. The occurrence and isolation of bluetongue in cattle-the so-called pseudo foot and mouth disease in South Africa. *Onderst J Vet Sci*. **2**: 393-507.

Benjwal, S, Verma, S, Röhm, K and Gursky, O. 2006. Monitoring protein aggregation during thermal unfolding in circular dichroism experiments. *Protein Sci*. **15**(3): 635-639.

Bennion, B and Daggett, V. 2003. The molecular basis for the chemical denaturation of proteins by urea. *Proc Natl Acad Sci USA*. **100**(9): 5142-5147.

Bentley, W and Kompala, D. 1990. Optimal induction of protein synthesis in recombinant bacterial cultures. *Ann N Y Acad Sci.* **589**: 121-138.

Bertani, G. 1951. Studies on lysogenesis. I. The mode of phage liberation by lysogenic *Escherichia coli*. *J Bacteriol*. **62**: 293-300.

Bhavesh, N, Panchal, S, Mittal, R and Hosur, R. 2001. NMR identification of local structure preferences I HIV protease tethered heterodimer in 6M guanidine hydrochloride. *FEBS Lett*. **509**(2): 218-224.

Bhuyan, A. 2002. Protein stabilization by urea and guanidine hydrochloride. *Biochemistry*. **41**(45): 13386-13394.

Birley, M and Boorman, J. 1982. Estimating the survival and biting rates of haematophagous insect with particular reference to Culicoides obsoletus group in Southern England. *J Anim Ecol.* **51**(1): 135-148.

Block, H, Maertens, B, Spriestersbach, A, Brinker, N, Kubicek, J, Fabis, R, Labahn, J and Schäfer, F. 2009. Immobilized-metal affinity chromatography (IMAC): a review. *Methods Enzymol*. **463**: 439-473.

Bornhorst, J and Falke, J. 2000. Purification of Proteins Using Polyhistidine Affinity Tags. *Methods Enzymol*. **326**: 245-254.

Bouet-Cararo, C, Contreras, V, Caruso, A, Top, S, Szelechowski, M, Bergeron, C, Viarouge, C, Desprat, A, Relmy, A, Guibert, J, Dubois, E, Thiery, R, Bréard, E, Bertagnoli, S, Richardson, J, Foucras, G, Meyer, G, Schwartz-Cornil, I, Zientara, S and Klonjkowski, B. 2014. Expression of VP7, a bluetongue virus group specific antigen by viral vectors: analysis of the induced immune responses and evaluation of protective potential in sheep. *PLoS ONE*. **9**:e111605.

Bowen, R and Howard, T. 1984. Transmission of bluetongue virus by intrauterine inoculation or insemination of virus-containing bovine semen. *Am J Vet Res.* **45**(7): 1386-1388.

Bowne, J and Jones, R. 1966. Observations on bluetongue virus in the salivary glands of an insect vector, Culicoides variipennis. *Virology*. **30**(1): 127-133.

Boyd, G, Adamson, A and Myers Jr, L. 1947. The exchange adsorption of ions from aqueous solutions by organic zeolites; kinetics. *J Am Chem Soc*. **69**(11): 2836-2848.

Bradford, M. 1976. A rapid and sensitive method for the quantification of microgram quantities of protein utilizing the principle of protein-dye binding. *Anal Biochem*. **72**: 248-254.

Briegel, H and Lea, A. 1975. Relationships between protein and proteolytic activity in the mid-gut of mosquitoes. *J Insect Physiol.* **21**: 1597-1604.

Brooks, J, Long, H, Tierney, R, Shannon-Lowe, C, Leese, A, Fitzpatrick, M, Taylor, G and Rickinson, A. 2016. Early T cell recognition of B cells following Epstein-Barr virus infection: identifying potential targets for prophylactic vaccination. *PLoS Path*. **12**(4): e100.

Bruylants, G, Wouters, J and Michaux, C. 2005. Differential scanning Calorimetry in Life Science: Thermodyamics, Stability, Molecular Recognition and Application in Drug Design. *Cur Med Chem*. **12**(17): 2011-2020.

Calamai, M, Canale, C, Relini, A, Stefani, M, Chiti, F and Dobson, C. 2005. Reversal of protein aggregation provides evidence for multiple aggregated States. *J Mol Biol*. **346**: 603-616.

Camilloni, C, Guerini Rocco, A, Eberini, I, Gianazza, E, Broglia, R and Tiana, G. 2008. Urea and Guanidinium Chloride Denature Protein L in Different Ways in Molecular Dynamics Simulations. *Biophys J*. **94**(12): 4654-4661.

Campbell, C. 1985. Immunogenicity of bluetongue virus inactivated by gamma irradiation. *Vaccine*. **3**(5): 401-406.

Carneiro, S, Ferreira, E and Rocha, I. 2013. Metabolic responses to recombinant bioprocesses in *Escherichia coli*. *J Biotechnol*. **164**: 396-408.

Carrio, M, Gonzalez-Montalban, N, Vera, A, Villaverde, A and Ventura, S. 2005. Amyloid-like properties of bacterial inclusion bodies. *J Mol Biol.* **347**(5): 1025-1037.

Caspar, D and Klug, A. 1962. Physical principles in the construction of regular viruses. *Cold Spring Harb Symp Quant Biol.* **27**: 1-24.

Chaga, G, Hopp, J and Nelson, P. 1999. Immobilized metal ion affinity chromatography on Co^{2+}-carboxymethylaspartate-agarose Superflow, as demonstrated by one-step purification of lactate dehydrogenase from chicken breast muscle. *Biotechnol Appl Biochem*. **29**: 19-24.

Chaignat, V, Worwa, G, Scherrer, N, Hilbe, M, Ehrensberger, F, Batten, C, Cortyen, M, Hofmann, M and Thuer, B. 2009. Toggenberg Orbivirus, a new bluetongue virus: initial detection, first observation in the field and experimental infection of sheep and goats. *Vet Microbio*. **138**: 11-19.

Chalmers, J, Kim, E, Telford, J, Wong, E, Tacon, W, Shuler, M and Wilson, D. 1990. Effects of temperature on *Escherichia coli* overproducing β-lactamase or human epidermal growth factor. *Appl Environ Microbiol*. **56**: 104-111.

Chamberlain, R and Sudia, W. 1961. Mechanism of transmission of viruses by mosquitoes. *Ann Rev Entomol*. **6**: 371-390.

Chandler, L, Ballinger, M, Jones, R and Beaty, B. 1985. The virogenesis of bluetongue virus in Culicoides variipennis. *Prog Clin Biol Res.* **178**: 245-253.

Chang, S, Noel, R and Regnier, F. 1976. High Speed ion Exchange Chromatography of Proteins. *Anal Chem*. **48**(13): 1839-1845.

Chiang, E, Persaud-Sawin, D, Kulkarni, S, Garcia, J and Imani, F. 2006. Bluetongue virus and double-stranded RNA increase human vascular permeability: role of p38 MAPK. *J Clini Immuno*. **26**(4): 406-416.

Chiti, F, Stefani, M, Taddei, N, Ramponi, G and Dobson, C. 2003. Rationalization of the effects of mutations on peptide and protein aggregation rates. *Nature*. **424**(6950): 805-808.

Chou, C, Bennett, G and San, K. 1994. Effect of modified glucose uptake using genetic engineering techniques on high-level recombinant protein production in *Escherichia coli* dense cultures. *Biotechnol Bioeng*. **44**(8): 952-960.

Clark, E. 1998. Refolding of recombinant proteins. *Curr Opin Biotechnol*. **9**(2): 157-163.

Cleland, J and Wang, D. 1990. Cosolvent assisted protein refolding. *Biotechnology (NY)*. **8**(12): 1274-1278.

Coetzee, P, Stokstad, M, Venter, E, Myrmel, M and Van Vuuren, M. 2012. Bluetongue: a historical and epidemiological perspective with the emphasis on South Africa. *Virol J.* **9**(198).

Cowley, J and Gorman, B. 1989. Cross-neutralization of genetic reassortants of bluetongue virus serotypes 20 and 21. *Vet Microbiol*. **19**(1): 37-51.

Crowe, J, Döbeli, H, Gentz, R, Hochuli, E, Stüber, D and Henco, K. 1994. 6xHis-Ni-NTA chromatography as a superior technique in recombinant protein expression/purification. *Methods Mol Biol*. **31**: 371-387.

Datar, R, Cartwright, T and Rosen, C. 1993. Process economics of animal cell and bacterial fermentations: a case study analysis of tissue plasminogen activator. *Biotechnology (N Y).* **11**(3): 349-357.

De Anda, R, Lara, A, Hernandez, V, Hernandez-Montalvo, V, Gosset, G, Bolivar, F and Ramirez, O. 2006. Replacement of the glucose phosphotransferase transport system by galactose permease reduces acetate accumulation and improves process performance of *Escherichia coli* for recombinant protein production without impairment of growth rate. *Meta Eng*. **8**(3): 281-290.

De Bernardez, C. 1998. Refolding of recombinant proteins. *Curr Opin Biotechnol*. **9**(2): 157-163.

DeMaula, C, Jutila, M, Wilson, D and MacLachlan, N. 2001. Infection kinetics, prostacyclin release and cytokine-mediated modulation of the mechanism of cell death during bluetongue virus infection of cultured ovine and bovine pulmonary artery and lung microvascular endothelial cells. *J Gen Virol*. **82**(4): 787-794.

Demchenko, P. 1986. *Ultraviolet Spectroscopy of Proteins*. Berlin Heidelberg. Springer.

Dempsey, C, Piggott, T and Mason, P. 2005. Dissecting contributions to the denaturant sensitivities of proteins. *Biochemistry.* **44**(2): 775-781.

Dobson, C. 2003. Protein folding and misfolding. *Nature.* **426**(6968): 884-890.

Doglia, S, Ami, D, Natalello, A, Gatti-Lafranconi, P and Lotti, M. 2008. Fourier transform infrared spectroscopy analysis of the conformational quality of recombinant proteins within inclusion bodies. *Biotechnol J*. **3**(2): 193-201.

Drew, C, Gardner, I, Mayo, C, Matsuo, E, Roy, P and MacLachlan, N. 2010a. Bluetongue virus infection alters the impedance of monolayers of bovine endothelial cells as a result of cell death. *Vet Immunol Immunopathol*. **136**: 108-115.

Drew, C, Heller, M, Mayo, C, Watson, J and MacLachlan, N. 2010b. Bluetongue virus infection activates bovine monocyte-derived macrophages and pulmonary artery endothelial cells. *Vet Immunol Immunopathol.* **136**: 292-296.

Drolet, B, Mills, K, Belden, E and Mecham, J. 1990. Enzyme-linked immunosorbent assay for efficient detection of antibody to bluetongue virus in pronghorn (*Antilocapra americana*). *J Wildl Dis*. **26**(1): 34-40.

Du, J, Bhattacharya, B, Ward, T and Roy, P. 2014. Trafficking of bluetongue virus visualized by recovery of tetracysteine-tagged virion particles. *J Virol*. **88**(21): 12656-12668.

Dubay, K, Pawar, A, Chiti, F, Zurdo, J, Dobson, C and Vendruscolo, M. 2004. Prediction of the absolute aggregation rates of amyloidogenic polypeptide chains. *J Mol Biol*. **341**(5): 1317-1326.

Dumon-Seignovert, L, Cariot, G, Vuillard, L. 2004. The toxicity of recombinant proteins in *Escherichia coli*: a comparison of overexpression in BL21(DE3), C41(DE3), and C43(DE3). *Protein Expr Purif*. **37**(1): 203-206.

Dungu, B, Gerdes, T and Smit, T. 2004. The use of vaccination in the control of bluetongue in southern Africa. *Vet Ital*. **40**(4): 616-622.

Du Toit, R. 1944. The transmission of Blue-tongue and Horse-sickness by Culicoides. *Onderstepoort J Vet Sci Anita Indust.* **19**: 7-16.

Eaton, B and Crameri, G. 1989. The site of bluetongue virus attachment to glycophorins from a number of animal erythrocytes. *J Gen Virol*. **70**(12): 3347-3353.

Eaton, B, Hyatt, A and White, J. 1987. Association of bluetongue virus with the cytoskeleton. *Virology* **157**(1): 107-116.

Eckweiler, H, Noyes, H and Falk, K. 1921. The amphoteric properties of some amino-acids and peptides. *J Gen Physiol*. **3**(3): 291-308.

Edsall, J. 1935. Apparent molal heat capacities of amino acids and other organic compounds. *J Am Chem Soc*. **57**(8): 1506-1507.

Eftink, M. 1994. The Use of Fluorescence Methods to Monitor Unfolding Transitions in Proteins. *Biophys J.* **66**: 482-501.

Eftink, M and Ghiron, C. 1981. Fluorescence quenching studies with proteins. *Anal Biochem.* **14**(2): 199-227.

Enserink, M. 2006. Emerging infectious diseases. During a hot summer, bluetongue virus invades northern Europe. *Science*. **313**(5791): 1218-1219.

Erasmus, B. 1975. Bluetongue in sheep and goats. *Aust Vet J*. **51**(4): 165-170.

Farewell, A and Neidhardt, F. 1998. Effect of Temperature on In Vivo Protein Synthetic Capacity in Escherichia coli. *J Bacteriol*. **180**(17): 4704-4710.

Forzan, M, Marsh, M and Roy, P. 2007. Bluetongue virus entry into cells. *J Virol.* **81**(9): 4819-4827.

Foster, N and Jones, R. 1979. Multiplication rate of bluetongue virus in the vector Culicoides variipennis (Diptera: Ceratopogonidae) infected orally. *J Med Entomol*. **15**(3): 302-303.

Frank, H and Franks, F. 1968. Structural approach to the solvent power of water for hydrocarbons; urea as a structure breaker. *J Chem Phys*. **48**(10): 4746-4757.

French, T, Marshall, J and Roy, P. 1990. Assembly of double-shelled, virus like particles of bluetongue virus by the simultaneous expression of four structural proteins. *J Virol*. **64**(12): 5695-5700.

French, T and Roy, P. 1990. Synthesis of Bluetongue Virus (BTV) Corelike Particles by a Recombinant Baculovirus Expressing the Two Major Structural Core Proteins of BTV. *J Virol*. **64**(4):1530-1530.

Galinski, E, Stein, M, Amendt, B and Kinder, M. 1997. The kosmotropic (structure-forming) effect of compensatory solutes. *Comp Biochem Physiol*. **117A**(3): 357-365.

Gambles, R. 1949. Bluetongue of sheep in Cyprus. *J comp Pathol*. **59**: 176-190.

Gard, G. 1984. Studies of bluetongue virulence and pathogenesis in sheep. Technical Bulletin No. 103, Department of Industries and Development, Darwin, Australia.

Gasteiger, E, Hoogland, C, Gattiker, A, Duvaud, S, Wilkins, M, Appel, R and Bairoch, A. 2005. Protein Identification and Analysis Tools on the ExPASy Server. In *Walker, J (ed), The Proteomics Protocols Handbook*. Humana Press: 571-607.

Gekko, K and Timasheff, S. 1981a. Mechanism of protein stabilization by glycerol: preferential hydration in glycerol-water mixtures. *Biochemistry*. **20**(16): 4667-4676.

Gekko, K, and Timasheff, S. 1981b. Thermodynamic and kinetic examination of protein stabilization by glycerol. *Biochemistry*. **20**(16): 4677-4686.

Gekko, K and Koga, S. 1983. Increased thermal stability of collagen in the presence of sugars and polyols. *J Biochem*. **94**(1): 199-208.

Georgiou, G and Valax, P. 1999. Isolating inclusion bodies from bacteria. *Methods Enzymol.* **309**: 48-58.

Gibbs, E, Lawman, M and Herniman, K. 1979. Preliminary observations on transplacental infection of bluetongue virus in sheep. A possible overwintering mechanism. *Res Vet Sci.* **27**(1): 118-120.

Giddings, J. 1965. *Dynamics of Chromatography: Principles and Theory*. New York. CRC Press.

Gitlin, I, Carbeck, J, Whitesides, G. 2006. Why are proteins charged? Networks of charge-charge interactions in proteins measured by charge ladders and capillary electrophoresis. *Angew Chem Int Ed Engl*. **45**(19): 3022-60.

Gogarten, J, and Townsend, J. 2005. Horizontal gene transfer, genome innovation and evolution. *Nat Rev Microbiol*. **3**(9): 679-687.

Good, N and Izawa, S. 1972. Hydrogen ion buffers. *Methods Enzymol*. **24**: 53-68.

Gorman, B. 1990. The bluetongue viruses. *Curr Top Microbiol Immunol*. **162**: 1-19.

Greene, R and Pace, C. 1974. Urea and guanidine hydrochloride denaturation of ribonuclease, lysozyme, a-chymotrypsin, and 0-lactoglobulin. *J Biol Chem*. **249**(17): 5388-5393.

Gregory, M and Turner, C. 1993. Open-loop control of specific growth rate in fed-batch cultures of recombinant E. coli. *Biotechnol Tech*. **7**(12): 889-894.

Grimes, J, Basak, A, Roy, P and Stuart, D. 1995. The crystal structure of bluetongue virus VP7. *Nature* **373**(6510): 167-170.

Grimes, J, Burroughs, J, Gouet, P, Diprose, J, Malby, R, Zientara, S, Mertens, P and Stuart, D. 1998. The atomic structure of the bluetongue virus core. *Nature*. **395**(6701): 470-478.

Grimes, J, Jakana, M, Ghosh, A, Basak, P, Roy, W, Chiu, D and Stuart, B. 1997. An atomic model of the outer layer of the bluetongue virus core derived from X-ray crystallography and electron cryomicroscopy. *Structure.* **5**(7): 885-893.

Gryczynski, I, Lakowicz, J and Steiner, R. 1988a. Frequency-domain measurements of the rotational dynamics of the tyrosine groups of calmodulin. *Biophys Chem.* **30**(1): 49-59.

Gryczynski, I, Wiczk, W, Johnson, M and Lakowicz, J. 1988b. Lifetime distributions and anisotropy decays of indole fluorescence in cyclohexane/ethanol mixtures by frequency-domain fluorometry. *Biophys. Chem*. **32**: 173-185.

Gumm, I and Newman, J. 1982. The preparation of purified bluetongue virus group antigen for use as a diagnostic reagent. *Arch Virol.* **72**: 83-93.

Gupta, P, Hall, C and Voegler, A. 1998. Effect of denaturant and protein concentrations upon protein refolding and aggregation: a simple lattice model. *Protein Sci*. **7**(12): 2642-2652.

Hager, D and Burgess, R. 1980. Elution of proteins from sodium dodecyl sulfate-polyacrylamide gels, removal of sodium dodecyl sulfate, and renaturation of enzymatic activity: results with sigma subunit of Escherichia colt RNA polymerase, wheat germ DNA topoisomerase, and other enzymes. *Anal Biochem*. **109**(1): 76-86.

Harcum, S, Ramirez, D and Bentley, W. 1992. Optimal nutrient feed policies for heterologous protein production. *Appl Biochem Biotechnol*. **34**(5): 161-173.

Hartnett, J, Gracyalny, J and Slater, M. 2006. The single step (KRX) competent cells: efficient cloning and high protein yields, Promega Notes **94**: 27-30.

Hassan, S. 1999. Functional analysis of the outer capsid proteins VP2 and VP5 of BTV. D. Phil. dissertation. University of Oxford, Oxford, United Kingdom.

Hassan, S, Wirblich, C, Forzan, M and Roy, P. 2001. Expression and functional characterization of bluetongue virus vp5 protein: Role in cellular permeabilization. *J Virol.* **75**(18): 8356-8367.

Himmelhoch, S. 1971.Chromatography of proteins on ion-exchange adsorbents. *Methods Enzymol*. **22**: 273-286.

Hitzeman, R, Hagie, F, Levine, H, Goeddel, D, Ammerer, G and Hall, B. 1981. Expression of: a human gene for interferon in yeast. *Nature*. **293**(5835): 717-722.

Hjerten, S. 1964. The Preparation of Agarose Spheres for Chromatography of Molecules and Particles. *Biochim Biophys Acta*. **79**(2): 393-398.

Hochuli, E, Döbeli, H and Schacher, A. 1987. New metal chelate adsorbent selective for proteins and peptides containing neighbouring histidine residues. *J Chromatogr*. **411**: 177-184.

Hockney, R. 1994. Recent developments in heterologous protein production in *Escherichia coli*. *Trends Biotechnol*. **12**(11): 456-463.

Hoffmann, F and Rinas, U. 2004. Stress induced by recombinant protein production in *Escherichia coli*. *Adv Biochem Eng Biotechnol*. **89**: 73-92.

Hosamani, M. Shimizu, S, Hirota, J, Kokuho, T, Kubota, T, Watanabe, S, Ohta, M, Muneta, Y and Inumaru, S. 2011. Expression and Characterization of Bluetongue Virus Serotype 21 VP7 Antigen: C Terminal Truncated Protein has Significantly Reduced Antigenicity. *J Vet Med Sci*. **73**(5): 609-613.

Hourrigan, J and Klingsporn, A. 1975. Bluetongue: the disease in cattle. *Aust Vet J.* **51**(4): 170-174.

Howard, T, Bowen, R and Pickett, B. 1985. Isolation of bluetongue virus from bull semen. *Prog Clin Biol Res.* **178**: 127-134.

Howell, P. 1966. Some aspects of the epizootiology of bluetongue. *Bull Off Inst Epiz*. **66**: 341-352.

Howerth, E, Greene, C and Prestwood, A. 1988. Experimental induced bluetongue virus infection in the white-tailed deer: coagulation, clinical pathologic and gross pathologic changes. *Am J Vet Res*. **49**(11): 1906-1913.

Huismans, H. 1979. Protein synthesis in bluetongue virus-infected cells. *Virology* .**92**(2): 385-396.

Huismans, H, Cloete, M and Le Roux, A. 1987a. The genetic relatedness of a number of individual cognate genes of viruses in the bluetongue and closely related serogroups. *Virology*. **161**(2): 421-428.

Huismans, H and Erasmus, B. 1981. Identification of the serotype-specific and group-specific antigens of bluetongue virus. *Onderstepoort J Vet Res.* **48**(2): 51-58.

Huismans, H, van der Walt, N, Cloete, M, and Erasmus, B. 1987b. Isolation of a capsid protein of bluetongue virus that induces a protective immune response in sheep. *Virology*. **157**(1): 172-179.

Huismans, H, Van Duk, A and Els, H. 1987c. Uncoating of parental bluetongue virus to core and subcore particles in infected 1 cells. *Virology.* **157**(1): 180-188.

Hulo, C, de Castro, E, Masson, P, Bougueleret, L, Bairoch, A, Xenarios, I and Le Mercier, P. 2011. ViralZone: a knowledge resource to understand virus diversity. *Nucleic Acids Res*. **39**(Database issue): D576-582.

Hunter, P and Modumo, J. 2001. A monovalent attenuated serotype 2 bluetongue virus vaccine confers homologous protection in sheep*. Onderstepoort J Vet Res.* **68**(4): 331-333.

Hutcheon, D. 1902. Malarial catarrhal fever of sheep. *Vet Res*. **14**: 629-633.

Hutchens, T and Yip, T. 1990. Differential interaction of peptides and protein surface structures with free metal ions and surface-immobilized metal ions. *J Chromatogr*. **500**: 531-542.

Hyatt, A and Eaton, B. 1988. Ultra structural distribution of the major capsid proteins within bluetongue virus and infected cells*. J Gen Virol*. **69**(4): 805-815.

Hyatt, A, Eaton, B and Brookes, S. 1989. The release of bluetongue virus from infected cells and their superinfection by progeny virus. *Virology.* **173**(1): 21-34.

Itakura, K, Hirose, T, Crea, R, Riggs, A, Heyneker, H, Bolivar, F and Boyer, H. 1977. Expression in *Escherichia coli* of a chemically synthesized gene for the hormone somatostatin. *Science*. **198**(4321): 1056-1063.

Iwakura, M, Obara, K, Kokubu, T, Ohashi, S and Izutsu, H. 1992. Expression and purification of growth hormone-releasing factor with the aid of dihydrofolate reductase handle. *J Biochem*. **112**(1): 57-62.

Iwata, H, Yamagawa, M and Roy, P. 1992. Evolutionary relationships among the gnat-transmitted orbiviruses that cause African horse sickness, bluetongue, and epizootic hemorrhagic disease as evidenced by their capsid protein sequences. *Virology*. **191**(1): 251-261.

Jarabak, J. 1972. Human Placental 15-Hydroxyprostaglandin Dehydrogenase*. Proc Natl Acad Sci U S A*. **69**(3): 533-534.

Jarabak, J, Seeds, E and Talalay, P. 1966. Reversible Cold Inactivation of a 17β-Hydroxysteroid Dehydrogenase of Human Placenta: Protective Effect of Glycerol. *Biochemistry*. **5**(4): 1269-1279.

Jenckel, M, Bréard, E, Schulz, C, Sailleau, C, Viarouge, C, Hoffmann, B, Höper, D, Beer, M and Zientara, S. 2015. Complete Coding Genome Sequence of Putative Novel Bluetongue Virus Serotype 27*. Genome Announcements.* **3**(2).

Jennings, D and Mellor, P. 1988. The vector potential of British Culicoides species for bluetongue virus. *Vet Microbiol*. **17**(1): 1-10.

Jevsevar, S, Gaberc-Porekar, V, Fonda, I, Podobnik, B, Grdadolnik, J and Menart, V. 2005. Production of nonclassical inclusion bodies from which correctly folded protein can be extracted. *Biotechnol Prog*. **21**(2): 632-639.

Jones, R and Foster, N. 1978. Heterogeneity of *Culicoides variipennis* field populations to oral infection with bluetongue virus. *Am J Trop Med Hyg*. **27**: 178-183.

Joseph, B, Pichaimuthu, S, Srimeenakshi, S, Murthy, M, Selvakumar, K, Ganesan, M and Manjunath, S. 2015. An Overview of the Parameters for Recombinant Protein Expression in *Escherichia coli*. *J Cell Sci Ther*. **6**(5): 221.

Jürgen, B, Breitenstein, A, Urlacher, V, Büttner, K, Lin, H, Hecker, M, Schweder, T and Neubauer, P. 2010. Quality control of inclusion bodies in *Escherichia coli*. *Microb Cell Fact*. **9**(41).

Kar, A, Bhattacharya, B and Roy, P. 2007. Bluetongue virus RNA binding protein NS2 is a modulator of viral replication and assembly. *BMC Mol Biol.* **8**(4).

Karlsson, E, Ryden, L and Brewer, J. 1998. Ion exchange chromatography. In Janson, J and Ryden, L (Eds), *Protein purification. Principles, High Resolution Methods, and Applications. Ion exchange chromatography*. (2nd Ed). New York. Wiley: 145-206.

Kaur, J, Kumar, A, Kaur, J. 2017. Strategies for optimization of heterologous protein expression in *E. coli*: Roadblocks and reinforcements*. Int J Bio Macromol.* **106**: 803-822.

Kauzmann, W. 1959. Some factors in the interpretation of protein denaturation. *Adv Protein Chem.* **14**: 1-63.

Kelly, S and Price, N. 2000. The use of circular dichroism in the investigation of protein structure and function. *Curr Prot Pept Sci*. **1**(4): 349-384.

Khan, F, He, M and Taussig, M. 2006. Double-Hexahistidine Tag with High-Affinity Binding for Protein Immobilization, Purification, and Detection on Ni-Nitrilotriacetic Acid Surfaces. *Anal Chem.* **78**(9): 3072-3079.

Khan, R, Rao, K, Eshwari, A, Totey, S and Panda, A. 1998. Solubilization of recombinant ovine growth hormone with retention of native-like secondary structure and its refolding from the inclusion bodies of *Escherichia coli*. *Biotechnol Prog*. **14**(5): 722-728.

Kimple, M, Brill, A and Pasker, R. 2015. Overview of Affinity Tags for Protein Purification. *Curr Protoc Protein Sci*. **73**.

Klose, D, Wallace, B and Janes, R. 2010. 2Struc: the secondary structure server. *Bioinformatics*. **26**(20): 2624-2625.

Koshiyama, I, Hamano, M and Fukushima, D. 1981. A heat denaturation study of the 11S globulin in soybean seeds. *Food Chem*. **6**(4): 309-322.

Koumbati, M, Mangana, O, Nomikou, K, Mellor, P and Papadopoulos, O. 1999. Duration of bluetongue viremia and serological responses in experimentally infected European breeds of sheep and goats. *Vet Microbiol.* **64**(4): 277-285.

Kowalik, T and Li, J. 1991. Bluetongue virus evolution: sequence analyses of the genomic S1 segments and major core protein VP7. *Virology.* **181**(2): 749-755.

Kurucz, I, Titus, J, Jost, C and Segal, D. 1995. Correct disulfide pairing and efficient refolding of detergent-solubilized single-chain Fv proteins from bacterial inclusion bodies. *Mol Immunol*. **32**: 1443-1452.

Ladokhin, A, Jayasinghe, S and White, S. 2000. How to measure and analyze tryptophan fluorescence in membranes properly, and why bother? *Anal Biochem*. **285**(2): 235-245.

Laemmli, U. 1970. Cleavage of structural proteins during the assembly of the head of bacteriophage T4. *Nature.* **227**(5259): 680-685.

Lakowicz, J. 1999. *Principles of fluorescence spectroscopy*. (2nd Ed). USA. Plenum Press: 445-465.

Lampson, G and Tytell, A. 1965. A simple method for estimating isoelectric points. *Anal Biochem*. **11**(2): 374-377.

Lathe, G and Ruthven, C. 1956. The Separation of Substances on the Basis of Their Molecular Weights, Using Columns of Starch and Water. *Biochem J*. **60**(4): 665-674.

Lederberg, J. 1952. Cell genetics and hereditary symbiosis. *Physiol Rev*. **32**(4): 403-430.

Lepault, J, Petitpas, I, Erk, I, Navaza, J, Bigot, D, Dona, M, Vachette, P, Cohen, J and Rey F. 2001. Structural polymorphism of the major capsid protein of rotavirus. *EMBO J*. **20**(7):1498-1507.

Lessard, J. 2013. Growth media for E. coli. *Methods Enzymol.* **533**: 181-189.

Lewis, S and Grubman, M. 1990. Bluetongue virus: surface exposure of VP7. *Virus Res.* **16**(1): 17-26.

Li, Q, Maddox, C, Rasmussen, L, Hobrath, J and White, L. 2009. Assay development and high throughput antiviral drug screening against Bluetongue virus. *Antiviral Res*. **83**(3): 267-273.

Lichty, J, Malecki, J, Agnew, H, Michelson-Horowitz, D, and Tan, S. 2005. Comparison of affinity tags for protein purification. *Protein Expr Purif*. **41**(1): 98-105.

Lilie, H, Schwarz, E and Rudolph, R. 1998. Advances in refolding of proteins produced in E. coli. *Curr Opin Biotechnol*. **9**(5): 497-501.

Limn, C, Staeuber, N, Monastyrskaya, K, Gouet, P and Roy, P. 2000. Functional Dissection of the Major Structural Protein of Bluetongue Virus: Identification of Key Residues within VP7 Essential for Capsid Assembly. *J Viro*. **74**(18): 8658-8669.

Linterman, M and Hill, D. 2016. Can follicular helper T cells be targeted to improve vaccine efficacy? F1000 Res. **5**.

Longworth, J. 1971. Luminescence of polypeptides and proteins. In Steiner, R and Weinryb, I (ed), *Excited States of Proteins and Nucleic Acids*. Boston. Springer: 319-484.

Loudon, P, Hirasawaa, T, Oldfield, S, Murphy, M and Roy, P. 1991. Expression of the outer capsid protein VP5 of two bluetongue viruses, and synthesis of chimeric double shelled virus-like particles using combinations of recombinant baculoviruses. *Virology*. **182**(2): 793-801.

Louis-Jeune, C, Andrade-Navarro, M and Perez-Iratxeta, C. 2012. Prediction of protein secondary structure from circular dichroism using theoretically derived spectra. *Proteins*. **80**(2):374-81.

Lourenco, A, Carneiro, S, Pinto, J, Rocha, M, Ferreira, E and Rocha, I. 2011. A study of the short and long-term regulation of E. coli metabolic pathways. *J Integr Bioinform.* **8**(3): 183.

Maan, S, Maan, N, Nomikou, K, Veronesi, E, Bachanek-Bankowska, K, Belaganahalli, M, Attoui, H and Mertens, P. 2011. Complete Genome Characterization of a Novel 26th Bluetongue Virus Serotype from Kuwait. *PLoS ONE*. **6**(10): 1-11.

MacLachlan, N. 1994. The Pathogenesis and Immunology of Bluetongue Virus infection in ruminants. *Comp Immun Microbiol Infect Dis*. **17**(314): 197-206.

MacLachlan, N, Drew, C, Darpel, K and Worwa, G. 2009. The Pathology and Pathogenesis of Bluetongue. *J Comp Pathol*. **141**(1): 1-16.

MacLachlan, N and Thompson, J. 1985. Bluetongue virus-induced interferon in cattle. *Am J Vet Res*. **46**(6): 1238-1241.

Makhatadze, G and Privalov, P. 1992. Protein interactions with urea and guanidinium chloride. A calorimetric study. *J Mol Biol*. **226**(2): 491-505.

Makrides, S. 1996. Strategies for achieving high-level expression of genes in *Escherichia coli*. *Microbiol Rev.* **60**(3): 512-538.

Margreiter, G, Messner, P, Caldwell, K and Bayer, K. 2008. Size characterization of inclusion bodies by sedimentation field-flow fractionation. *J Biotechnol*. **138**: 67-73.

Marin-Lopez, A and Ortego, J. 2016. Generation of Recombinant Modified Vaccinia Virus Ankara Encoding VP2, NS1, and VP7 Proteins of Bluetongue Virus. *Methods Mol Biol*. **1349**: 137-50.

Marino, M. 1989. Expression systems for heterologous protein transduction. *BioPharm*. **2**(7): 1833.

Marston, F. 1986. The purification of eukaryotic polypeptides synthesized in Escherichia coli. *Biochem J*. **240**(1): 1-12.

Martin, V, Pascual, E, Avia, M, Peña, L, Valcárcel, F and Sevilla, N. 2015. Protective efficacy in sheep of adenovirus-vectored vaccines against bluetongue virus is associated with specific T cell responses. *PLoS ONE*. **10**:e0143273.

Martyn, J, Gould, A and Eaton, B. 1991. High-level expression of the VP7 and the non-structural protein NS3 of BTV by yeast expression vector: use of expressed VP7 as a group reactive antigen in blocking ELISA. *Virus Res.* **18**: 165-178.

Megahed, M. 1956. A culture method for Culicoides nubeculosus (Meigen) (Diptera Ceratopogonidae) in the laboratory, with notes on the biology. *Bull Entomol Res*. **47**(1): 107-114.

Mellor, P. 1990. The replication of bluetongue virus in Culicoides vectors. *Curr Top Microbiol Immunol*. **162**: 143-161.

Mellor, P and Wittmann, E. 2002. Bluetongue virus in the Mediterranean Basin 1998-2001. *The Vet J*. **164**(1): 20-37.

Mertens, P, Brown, F and Sangar, D. 1984. Assignment of the genome segments of bluetongue virus type 1 to the proteins which they encode. *Virology*. **135**(1): 207-217.

Mertens, P, Burroughs, J and Anderson J. 1987. Purification and properties of virus particles, infectious subviral particles, and cores of bluetongue virus serotypes 1 and 4. *Virology*. **157**(2): 375-386.

Mertens, P, Diprose, J, Maan, S, Singh, K, Attoui, H and Samuel, A. 2004. Bluetongue virus replication, molecular and structural biology. *Vet Ital*. **40**(4): 426-437.

Miller, J. 1972. *Experiments in molecular genetics*. New York. Cold Spring Harbor.

Miroux, B and Walker, J. 1996. Over-production of proteins in *Escherichia coli*: mutant hosts that allow synthesis of some membrane proteins and globular proteins at high levels. *J Mol Biol*. **260**(3): 289-298.

Mohl, B and Roy, P. 2014. Bluetongue Virus Capsid Assembly and Maturation. *Viruses.* **6**(8): 3250-3270.

Monastyrskaya, K, Staeuber, N, Sutton, G and Roy, P. 1997. Effects of Domain-Switching and Site-Directed Mutagenesis on the Properties and Functions of the VP7 Proteins of Two Orbiviruses. *Virology*. **237**: 217-227.

Monera, O, Kay, C and Hodges, R. 1994. Protein denaturation with guanidine hydrochloride or urea provides a different estimate of stability depending on the contributions of electrostatic interactions. *Protein Sci*. **3**(11): 1984-1991.

Morell, M, Bravo, R, Espargaró, A, Sisquella, X, Avilés, F, Fernàndez-Busquets, X and Ventura, S. 2008. Inclusion bodies: Specificity in their aggregation process and amyloid-like structure. *Biochim Biophys Acta*. **1783**(10): 1815-1825.

Moulton, J. 1961. Pathology of bluetongue of sheep in California. *J Am Vet Med Assoc.* **138**: 493-498.

Muralidhara, B and Prakash, V. 2001. Molten globule state of human serum albumin. *Curr Sci*. **72**: 831-834.

Myers, R, Eastes, J and Urquhart, D. 1941. Adsorption Isotherms of Synthetic Resin Ion-Exchange Adsorbents. *Ind Eng Chem*. **33**(10): 1270-1275.

Nema, S and Avis, K. 1993. Freeze-thaw studies of a model protein, lactate dehydrogenase, in the presence of cryoprotectants. *J Parenter Sci Technol*. **47**(2): 76-83.

Netherton, C and Wileman, T. 2011. Virus factories, double membrane vesicles and viroplasm generated in animal cells. *Curr Opin Virol*. **1**(5): 381-387.

Neubauer, P, Hofmann, K, Holst, O, Mattiasson, B and Kruschke, P. 1992. Maximizing the expression of a recombinant gene in *Escherichia coli* by manipulation of induction time using lactose as inducer. *Appl Microbiol Biotechnol.* **36**(6): 739-744.

Noad, R and Ray, P. 2009. Bluetongue vaccines. *Vaccines.* **27**: 86-89.

Noor, R, Islam, Z, Munshi, S and Rahman, F. 2013. Influence of Temperature on Escherichia coli Growth in Different Culture Media. *J Pure and Appi Micro*. **7**(2): 899-904.

Nozaki, Y. 1972.The preparation of guanidine hydrochloride. *Methods Enzymol*. **26**: 43-50.

Oldfield, S, Adachi, A, Urakawa, T, Hirasawa, T and Roy, P. 1990. Purification and characterization of the major group-specific core antigen VP7 of bluetongue virus synthesized by a recombinant baculovirus. *J Gen Virol.* **71**(11): 2649-2656.

Ou, W, Park, Y, Meng, F and Zhou, H. 2002. Effects of Glycerol in the Refolding and Unfolding of Creatine Kinase. *Isinghua Sci technol.* **7**(4): 352-362.

Pace, C. 1986. Determination and analysis of urea and guanidine hydrochloride denaturation curves. *Methods Enzymol*. **131**: 266-80.

Palmer, I and Wingfield, P. 2004. Preparation and Extraction of Insoluble (Inclusion-Body) Proteins from *Escherichia coli*. *Curr Protoc Protein Sci*. **6**(3).

Parker, J, Herniman, K, Gibbs, E and Sellers, R. 1975. An experimental inactivated vaccine against bluetongue. *Vet Rec*. **96**(13): 284-287.

Parui, S, Manna, R and Jana, B. 2016. Destabilization of Hydrophobic Core of Chicken Villin Headpiece in Guanidinium Chloride Induced Denaturation: Hint of π-Cation Interaction. *J Phys Chem B*. **120**(36): 9599-9607.

Patel, A and Roy, P. 2014. The molecular biology of Bluetongue virus replication. *Virus Res*. **182**: 5-20.

Pathak, K, Biswas, S, Tembhurne, P, Hosamani, M, Bhanuprakash, V, Prasad, G, Singh, R, Rasool, T and Mondal, B. 2008. Prokaryotic expression of truncated VP7 Bluetongue virus (BTV) and reactivity of the purified recombinant protein with all BTV-type-specific sera. *J Viro Methods*. **152**: 6-12.

Patra, A, Mukhopadhyay, R, Mukhija, R, Krishnan, A, Garg, L and Panda, A. 2000. Optimization of inclusion body solubilization and renaturation of recombinant human growth hormone from *Escherichia coli*. Protein *Expr Purif*. **18**(2): 182-192.

Patton, J, Silvestri, L, Tortorici, M, Vasquez-Del Carpio, R and Taraporewala, Z. 2006. Rotavirus genome replication and morphogenesis: role of the viroplasm. *Curr Top Microbiol Immunol*. **309**: 169-187.

Perkins, S. J .1986. Protein volumes and hydration effects. *Eur J Biochem*. **157**(1): 169-180.

Peternel, S, Grdadolnik, J, Gaberc-Porekar, V and Komel, R. 2008a. Engineering inclusion bodies for non-denaturing extraction of functional proteins. *Microb Cell Fact*. **7**: 34.

Peternel, S, Jevsevar, S, Bele, M, Gaberc-Porekar, V and Menart, V. 2008b. New properties of inclusion bodies with implications for biotechnology. *Biotechnol Appl Biochem.* **49**(4): 239-246.

Peterson, E and Sober, H. 1956. Chromatography of Proteins. I. Cellulose Jon-exchange Adsorbents. *J Am Chem Soc*. **78** (4): 751-755.

Pikal-Cleland, K, Rodriguez-Hornedo, N, Amidon, G and Carpenter, J. 2000. Protein denaturation during freezing and thawing in phosphate buffer systems: monomeric and tetrameric beta-galactosidase. *Arch Biochem Biophys.* **384**(2): 398-406.

Porath, J, Carlsson, J, Olsson, I, and Belfrage, G. 1975. Metal chelate affinity chromatography, a new approach to protein fractionation. *Nature*. **258**(5536): 598-599.

Porath, J and Flodin, P. 1959. Gel filtration: a method for desalting and group separation. *Nature*. **183**: 1657-1659.

Povarova, O, Kuznetsova, I and Turoverov, K. 2010. Differences in the Pathways of Proteins Unfolding Induced by Urea and Guanidine Hydrochloride: Molten Globule State and Aggregates. *PLoS ONE.* **5**(11): e15035.

Prakash, V, Loucheux, C, Scheuffle, S, Gorbunoff, J and Timasheff, S. 1981. Interactions of proteins with solvent components in 8 M urea. *Arch Biochem Biophys*. **210**(2): 455-464.

Prasad, B, Yamaguchi, S and Roy, P. 1992. Three-dimensional structure of single-shelled bluetongue virus. *J Virol.* **66**(4): 2135-2142.

Privalov, P. 1979. Stability of proteins: small globular proteins. *Adv Protein Chem*. **33**: 167-241.

Privalov, P. 1980. Scanning microcalorimeters for studying macromolecules. *Pure and Appi Chem*. **52**: 479-497.

Privalov, P. 1982. Stability of proteins. Proteins which do not present a single cooperative system. *Adv Prot Chem*. **35**: 1-104.

Privalov, P and Gill, S. 1988. Stability of Protein Structure and Hydrophobic Interaction. *Adv Protein Chem.* **39**: 191-234.

Przybycien, T, Dunn, J, Valax, P and Georgiou, G. 1994. Secondary structure characterization of beta-lactamase inclusion bodies. *Protein Eng.* **7**(1): 131-136.

Puri, N, Crivelli, E, Cardamone, M, Fiddes, R, Bertolini, J, Ninham, B and Brandon, M. 1992. Solubilization of growth hormone and other recombinant proteins from *Escherichia coli* by using a cationic surfactant. *Biochem J*. **285**(3): 871-879.

Qi, X, Sun, Y and Xiong, S. 2015. A single freeze-thawing cycle for highly efficient solubilization of inclusion body proteins and its refolding into bioactive form. *Microb Cell Fact*. **14**: 24.

Rahmen, N, Fulton, A, Ihling, N, Magni, M, Jaeger, K and Büchs, J. 2015. Exchange of single amino acids at different positions of a recombinant protein affects metabolic burden in *Escherichia coli*. *Microbial Cell Factories*. **14**: 10.

Ranjbar, B and Gill, P. 2009. Circular Dichroism Techniques: Biomolecular and Nanostructural Analyses-A Review. *Chem Biol Drug Des*. **74**(2): 101-120.

Ratinier, M, Caporale, M, Golder, M, Franzoni, G, Allan, K, Nunes, S, Armezzani, A, Bayoumy, A, Rixon, F, Shaw, A and Massimo, P. 2011. Identification and characterization of a novel non-structural protein of bluetongue virus. *PLoS Pathog.* **7**(12): e1002477.

Righetti, P and Verzola, B. 2001. Folding/unfolding/refolding of proteins: Present methodologies in comparison with capillary zone electrophoresis. *Electrophoresis*. **22**(12): 2359-2379.

Robertson, A and Murphy, K. 1997. Protein Structure and the Energetics of Protein Stability. *Chem Rev*. **97**(5): 1251-1268.

Robinson, D and Jencks, W. 1965. The Effect of Compounds of the Urea-Guanidinium Class on the Activity Coefficient of Acetyl tetraglycine Ethyl Ester and Related Compounds. *J Am Chem Soc*. **87**(11): 2462-2470.

Robichon, C, Luo, J, Causey, T, Benner, J and Samuelson, J. 2011. Engineering *Escherichia coli* BL21(DE3) Derivative Strains To Minimize E. coli Protein Contamination after Purification by Immobilized Metal Affinity Chromatography . *Appl Environ Microbiol*. **77**(13): 4634-4646.

Rojas, J, Rodriguez-Calvo, T, Peña, L and Sevilla, N. 2011. T cell responses to bluetongue virus are directed against multiple and identical CD4+ and CD8+ T cell epitopes from the VP7 core protein in mouse and sheep. *Vaccine*. **29**(40): 6848-6857.

Roy, P. 1990. Use of baculovirus expression vectors: development of diagnostic reagents, vaccines and morphological counterparts of bluetongue virus. *FEMS Microbiol. Immunol*. **2**(4): 223-234.

Roy, P, French, T and Erasmus, B. 1992. Protective efficacy of virus-like particles for bluetongue disease. *Vaccine*. **10**(1): 28-32.

Ruan, K, Xu, C, Li, T, Li, J, Lange, R and Balny, C. 2003. The thermodynamic analysis of protein stabilization by sucrose and glycerol against pressure-induced unfolding: The typical example of the 33-kDa protein from spinach photosystem II. *Eur J Biochem*. **270**(8): 1654-1661.

Russell, B and Gildenhuys, S. 2018. Solubilisation and purification of recombinant bluetongue virus VP7 expressed in a bacterial system. *Protein Expr Purif*. **147**: 85-93.

Russell, B, Gildenhuys, S and Parbhoo, N. 2018. Analysis of Conserved, Computationally Predicted Epitope Regions for VP5 and VP7 across 3 Orbiviruses. *Bioinform Biol Insights.* **12**: 1-12.

Rutkowskaa, D, Meyera, Q, Mareeb, F, Vosloob, W, Ficka, W and Huismansa, H. 2011. The use of soluble African horse sickness viral protein 7 as an antigen delivery and presentation system. *Virus Res*. **156**: 35-48.

Salminen, T, Teplyakov, A, Kankare, J, Cooperman, B, Lahti, R and Goldman, A. 1996. An unusual route to thermostability disclosed by the comparison of Thermus thermophilus and Escherichia m coli inorganic pyrophosphatase. *Protein Sci*. **5**(6): 1014-1025.

Salvi, G, De Los Rios, P and Vendruscolo, M. 2005. Effective interactions between chaotropic agents and proteins. *Proteins*. **61**(3): 492-499.

Sanchez-Cordon, P, Rodriguez-Sanchez, B, Risalde, M, Molina, V, Pedrera, M, Sanchez-Vizcaino, J and Gomez-Villamandos, J. 2010. Immunohistochemical detection of bluetongue virus in fixed tissue. *J Comp Pathol.* **143**(1): 20-28.

Sanchez de Groot, N and Ventura, S. 2006. Effect of temperature on protein quality in bacterial inclusion bodies. *FEBS Letters*. **580**(27): 6471-6476.

Savini, G, MacLachlan, N, Sanchez-Vizcaino, J and Zientara, S. 2008. Vaccines against bluetongue in Europe. *Comp Immunol Microbiol Infect Dis.* **31**: 101-120.

Schachman, J and Lauffer, M. 1949. The hydration, size and shape of tobacco mosaic virus. *J Am Chem Soc.* **71**(2): 536-554.

Scheiblhofer, S, Laimer, J, Machado, Y, Weiss, R and Thalhamer, J. 2017. Influence of protein fold stability on immunogenicity and its implications for vaccine design. *Expert Rev Vaccines*. **16**(5): 479-489.

Schellman, J. 1955. The thermodynamics of urea solutions and the heat of formation of the peptide hydrogen bond. *C R Trav Lab Carlsberg*. **29**: 223-229.

Schellman, J. 1987. The thermodynamic stability of proteins. *Annu Rev Biophys Chem*. **16**: 115-137.

Schmid, F. 2001. Biological Macromolecules: UV-visible Spectrophotometry. In *Encyclopedia of Life Sciences*. London. Macmillan: 1-4.

Schmitt, J, Hess H, Stunnenberg HG. 1993. Affinity purification of histidine-tagged proteins. *Mol Biol Rep*. **18**(3): 223-230.

Sellers, R and Taylor, W. 1980. Epidemiology of bluetongue and the import and export of livestock, semen and embryos. *Bull Off int Epiz*. **92**: 587-592.

Shriver, J and Edmondson, S. 2009. Defining the Stability of Multimeric Proteins. *Methods Mol Biol*. **490**: 57-82.

Smith, A and Hall, C. 2001. Protein refolding versus aggregation: computer simulations on an intermediate-resolution protein model. *J Mol Biol*. **312**(1): 187-202.

Smith, J and Scholtz, J. 1996. Guanidine hydrochloride unfolding of peptide helices: Separation of denaturant and salt effects. *Biochemistry.* **35**(22): 7292-7297.

Söderlund, T, Zhu, K, Jutila, A and Kinnunen, P. 2003. Effects of betaine on the structural dynamics of Thermomyces (Humicola) lanuginosa lipase. *Coll Surf B: Biointerfaces*. **26**: 75-83.

Sørenson, H and Mortensen, K. 2005. Advanced genetic strategies for recombinant protein expression in *Escherichia coli. J Biotechnol.* **115**(2): 113-128.

Spink, C. 2008. Differential Scanning Calorimetry. *Methods Cell Biol*. **84**: 115-141.

Spreull, J .1905. Malarial catarrhal fever (bluetongue) of sheep in South Africa. *J Comp Pathol Ther*. **18**: 321-337.

Stancel, G and Deal Jr, W. 1969. Reversible dissociation of yeast glyceraldehyde 3-phosphate dehydrogenase by adenosine triphosphate. *Biochemistry*. **8**(10): 4005-4011.

Stanisich, V. 1988. Identification and analysis of plasmids at the genetic level In: Grinsted, J, Bennett, P (Eds), *Methods in Microbiology* (Vol. 21). London. Academic Press: 11–47.

Steif, C, Weber, P, Hinz, H, Flossdorf, J, Cesareni, G and Kokkinidis, M. 1993. Subunit interactions provide a significant contribution to the stability of the dimeric four-alpha-helical-bundle protein ROP *Biochemistry*. **32**(15): 3867-3876.

Stewart, M, Dubois, E, Sailleau, C, Breard, E, Viarouge, C, Desprat, A, Thiery, R, Zientara, S and Roy, P. 2013. Bluetongue virus serotype 8 virus-like particles protect sheep against virulent virus infection as a single or multi-serotype cocktail immunogen. *Vaccine*. **31**(3): 553-355.

Studier, F and Moffatt, B. 1986. Use of bacteriophage T7 RNA polymerase to direct selective high-level expression of cloned genes. *J Mol Biol*. **189**(1): 113-130.

Sturtevant, J. 1987. Biochemical applications of differential scanning calorimetry. *Annu Rev Phys Chem*. **38**: 463-488.

Sudheerbabu, G, Narasimha reddy, Y and Dhanalaxmi, K. 2016. Cloning and expression of bluetongue virus vp7 protein upper domain in prokaryotic system. *Int J Micro Biochem Mol Bio*. **2**(2): 4-6.

Tan, B, Nason, E, Staeuber, N, Jiang, W, Monastryrskaya, K and Roy, P. 2001. RGD Tripeptide of Bluetongue Virus VP7 Protein Is Responsible for Core Attachment to Culicoides Cells. *J Virol*. **75**(8): 3937-3947.

Tanford, C. 1961. *Physical chemistry of macromolecules*. New York. Wiley.

Tanford, C. 1962. The interpretation of hydrogen ion titration curves of proteins. *Adv Protein Chem*. **17**: 69-165.

Tanford, C. 1970. Protein denaturation. Part C. Theoretical models for the mechanism of denaturation. *Adv Protein Chem* **24**: 1-95.

Teale, F. 1960. The ultraviolet fluorescence of proteins in neutral solution. *Biochem J.* **76**(2): 381-388.

Terpe, K. 2003. Overview of tag protein fusions: from molecular and biochemical fundamentals to commercial systems. *Appl Microbiol Biotechnol.* **60**(5): 523-533.

Terpe, K. 2006. Overview of bacterial expression systems for heterologous protein production: from molecular and biochemical fundamentals to commercial systems. *Appl Microbiol Biotechnol*. **72**(2): 211-222.

Thuenemann, E, Meyers, A, Verwey, J, Rybicki, E and Lomonossoff, G. 2013. A method for rapid production of heteromultimeric protein complexes in plants: assembly of protective bluetongue virus-like particles. *Plant Biotechnol J.* **11**(7): 839-846.

Timasheff, S. 1993. The control of protein stability and association by weak interactions with water: how do solvent affect these processes? *Annu Rev Biophys Biomol Struct*. **22**: 67-97.

Tsumoto, K, Ejima, D, Kumagai, I and Arakawa, T. 2003. Practical considerations in refolding proteins from inclusion bodies. *Protein Expr Purif*. **28**(1): 1-8.

Tsumoto, K, Umetsu, M, Kumagai, I, Ejima, D, Philo, S and Arakawa, T. 2004. Role of Arginine in Protein Refolding, Solubilization, and Purification. *Biotechnol prog.* **20**(5): 1301-1308.

Turner, C, Gregory, M and Turner, M. 1994. A study of the effect of specific growth rate and acetate on recombinant protein production of *Escherichia coli* JM107. *Biotechnol Lett*. **16**(9): 891-896.

Umetsu, M, Tsumoto, K, Nitta, S, Adschiri, T, Ejima, D, Arakawa, T and Kumagai, I. 2005. Nondenaturing solubilization of beta2 microglobulin from inclusion bodies by L-arginine. *Biochem Biophys Res Commun*. **328**(1): 189-197.

Van den Berg, B, Ellis, R and Dobson, C. 1999. Effects of macromolecular crowding on protein folding and aggregation. *EMBO J*. **18**(24):6927-6933.

Van den Berg, B, Wain, R, Dobson, C and Ellis, R. 2000. Macromolecular crowding perturbs protein refolding kinetics: implications for folding inside the cell. *EMBO J*. **19**(15): 3870-3875.

Vandenbussche, F, Vanbinst, T, Verheyden, B, Van Dessel, W, Demeestere, L, Houdart, P, Bertels, G, Praet, N, Berkvens, D, Mintiens, K, Goris, N and De Clercq, K. 2008. Evaluation of antibody ELISA and real-time RT-PCR for the diagnosis and profiling of Bluetongue virus serotype 8 during the epidemic in Belgium in 2006. *Vet Micro*. **129**: 15-27.

Van Dijk, A and Huismans, H. 1982. The effect of temperature on the in vitro transcriptase reaction of bluetongue virus, epizootic haemorrhagic disease virus and African horsesickness virus. *Onderstepoort J Vet Res*. **49**(4): 227-232.

Vanzi, F, Madan, B and Sharp, K. 1998. Effect of the Protein Denaturants Urea and Guanidinium on Water Structure: A Structural and Thermodynamic Study. *J Am Chem Soc*. **120**(41):10748-10753.

Verwoerd, D, Els, H, De Villiers, E and Huismans, H .1972. Structure of the bluetongue virus capsid. *J Virol.* **10**(4): 783-794.

Verwoerd, D and Erasmus, B. 2004. Bluetongue. In Coetzer, J and Tustin, R (Eds.), *Infectious diseases of livestock* (2nd Ed). Cape Town. Oxford: 1201–1220.

Verwoerd, D and Huismans, H. 1972. Studies on the *in vitro* and the *in vivo* transcription of the bluetongue virus genome. *Onderstepoort J Vet Res.* **39**(4)**:** 185-191.

Verwoerd, D, Huismans, H and Erasmus, B. 1979. Orbiviruses. In Fraenkel-Conrat, H and Wagner, R (Eds), *Comprehensive Virology*. (Vol 14). New York. Plenum Press: 285-345.

Villaverde, A and Carrio, M. 2003. Protein aggregation in recombinant bacteria: biological role of inclusion bodies. *Biotechnol Lett*. **25**(17): 1385-1395.

von Hippel, P and Schleich, T .1969. Ion effects on the solution structure of biological macromolecules. *Acc Chem Res.* **2**(9): 257-265.

Waage, J and Mumford, J. 2008. Agricultural biosecurity. *Philos Trans R Soc Lond B Biol Sci*. **363**(1492): 863-876.

Wagner, S, Klepsch, M, Schlegel, S, Appel, A, Draheim, R, Tarry, M, Högbom, M, van Wijk, K, Slotboom, D, Persson, J and de Gier, J. 2008. Tuning *Escherichia coli* for membrane protein overexpression. *PNAS*. **105** (38): 14371-14376.

Walker, J. 1994. Nondenaturing Polyacrylamide Gel Electrophoresis of Proteins. *Methods Mol Biol*. **32**: 17-22.

Walther, C, Mayer, S, Sekot, G, Antos, D, Hahn, R, Jungbauer, A and Dürauer, A. 2013. Mechanism and model for solubilisation of inclusion bodies. *Chem Eng Sci*. **101**: 631-641.

Wang, L. 2009. Towards revealing the structure of bacterial inclusion bodies. *Prion*. **3**(3): 139-145.

Wang, L, Scanlon, D, Kattenbelt, J, Mecham, J and Eaton, B. 1994. Fine mapping of a surface-accessible, immunodominant site on the bluetongue virus major core protein VP7. *Virology*. **204**(2): 811-814.

Ward, M. 1994. The epidemiology of bluetongue virus in Australia-a review. *Aust Vet J.* **71**(1): 3-7.

Watson, E, O'Neil, M, Justin, J and Brenner, N. 1964. A differential scanning calorimeter for quantitative DTA. *Anal Chem*. **36**(7): 1233-1238.

Wegerer, A, Sun, T and Altenbuchner, J. 2008. Optimization of an E. coli L-rhamnose-inducible expression vector: test of various genetic module combinations. *BMC Biotechnol.* **8**(2).

Weickert, M, Doherty, D, Best, E and Olins, P. 1996. Optimization of heterologous protein production in *Escherichia coli*. *Curr Opin Biotechnol*. **7**(5): 494-499.

Wileman, T. 2007. Aggresomes and pericentriolar sites of virus assembly: cellular defense or viral design? *Annu Rev Microbiol*. **61**: 149-167.

Wirblich, C, Bhattacharya, B and Roy, P. 2006. Nonstructural protein 3 of bluetongue virus assists virus release by recruiting ESCRT-I protein Tsg101. *J Virol.* **80**(1): 460-473.

Wirth, M, Bode, J, Zettlmeissl, G, and Hauser, H. 1988. Isolation of overproducing recombinant mammalian cell lines by a fast and simple selection procedure. *Gene* **73**(2)**:** 419-426.

Woody, R. 1995. Circular Dichroism. *Methods Enzymol.* **246**: 34-71.

Wu, X, Liu, Q, He, J, Zang, M, Wang, H, Li, Y and Tang, L. 2015. Preparation and Characterization of a Monoclonal Antibody against the Core Protein VP7 of the 25th Serotype of Bluetongue Virus. Monoclon antib immunodiagn immunother. **34**(2): 116-121.

Xu, G, Wilson, W, Mecham, J, Murphy, K, Zhou, E and Tabachnick, W. 1997. VP7: an attachment protein of bluetongue virus for cellular receptors in Culicoides variipennis. *J Gen Virol*. **78**(7): 1617-1623.

Yip, T, Nakagawa, Y, Porath, J. 1989. Evaluation of the interaction of peptides with Cu(II), Ni(II), and Zn(II) by high-performance immobilized metal ion affinity chromatography. *Anal Biochem*. **183**(1): 159-171.

Zhang, X, Patel, A, Celma, C, Yu, X, Roy, P and Zhou, Z. 2016. Atomic model of a nonenveloped virus reveals pH sensors for a coordinated process of cell entry. *Nat Struct Mol Biol*. **23**(1): 74-80.